APDA-150

METHODS FOR DETERMINING THE ENERGY RELEASE IN HYPOTHETICAL REACTOR MELTDOWN ACCIDENTS

Richard B. Nicholson

DECEMBER 1962

ATOMIC POWER
DEVELOPMENT ASSOCIATES, INC.

APDA-150

METHODS FOR DETERMINING THE ENERGY RELEASE IN HYPOTHETICAL REACTOR MELTDOWN ACCIDENTS

Richard B. Nicholson

DECEMBER 1962

METHODS FOR DETERMINING THE ENERGY RELEASE IN HYPOTHETICAL REACTOR MELTDOWN ACCIDENTS

by

Richard B. Nicholson

A dissertation submitted in partial fulfillment of the requirements for the degree of

Doctor of Philosophy

in the

University of Michigan

December 1962

PREFACE

The present investigation is an outgrowth of several years of study of the safety of fast reactors during my association with the design of the Enrico Fermi Atomic Power Plant. I am indeed grateful to my friends at Atomic Power Development Associates and the Power Reactor Development Company for their constant encouragement throughout the course of this study, and wish especially to express my appreciation to Mr. W. J. McCarthy and Mr. J. B. Nims.

The financial support for this work was furnished by the Atomic Power Development Associates, Inc., and by the Ford Foundation through an Engineering Faculty Development Fellowship, which made it possible to devote my full attention to academic studies and research.

Others who gave material assistance in the preparation of computer programs and provided useful discussions are J. W. Stephenson, Marilyn Friedman, A. Klickman, R. Mueller, Y. J. Shin, and S. Kapil. I also acknowledge the cooperation of the Argonne National Laboratory in providing experimental data for my studies of two-dimensional effects.

My work in the study of the safety of fast reactors has been stimulated by many discussions with Professor H. A. Bethe of Cornell University who has offered invaluable advice, not only in this research

but also in my other recent endeavors.

I am much indebted to Professor Paul F. Zweifel, chairman of my doctoral committee, who has given freely of his time and advice and from whom I have learned much about the physics of nuclear reactors. I also thank the other members of the faculty of the Department of Nuclear Engineering for the sincere interest they have demonstrated in me throughout my studies at the University of Michigan.

TABLE OF CONTENTS

LIST OF TABLES

LIST OF ILLUSTRATIONS

LIST OF APPENDICES

ABSTRACT

A method for estimating the energy release in hypothetical fast reactor meltdown accidents is evaluated. It is hypothesized that the melted core of a reactor is rearranged in such a way that it forms a secondary critical assembly, and that there is a constant rate of reactivity increase. It is assumed that the mechanism for terminating the resulting power excursion is disassembly of the core due to the pressure of vaporized uranium produced by the excursion.

Two basic assumptions are utilized: that the reactivity effects during disassembly can be calculated from perturbation theory; and that the decrease in density during disassembly can be ignored in the equations of hydrodynamics. It is shown that these two assumptions are reasonable, and that an approximate treatment of the motion of material near the core surfaces can be justified.

The Bethe-Tait method for calculating energy release is discussed, and modified to include polynomial approximations to the power distribution and reactivity worth distribution, as well as a different treatment of the movement of material near the core surface. It is shown that the energy release is approximately the same for tamped and untamped cores for rates of reactivity increase up to 6.4 sec^{-1}, the highest rate treated.

An improved method is presented which eliminates some of the approximations of the Bethe-Tait method, and which is programmed for the IBM-7090 digital computer. It is shown that the threshold equation of state generally used in previous energy release calculations tends to cause an overestimate for weak and moderate excursions, and that the saturated vapor pressure must be considered in these cases. The influence of the delayed neutrons is evaluated and shown to be small. The dependence of the energy release upon prompt neutron generation time, initial power level, rate of reactivity insertion, and Doppler effect is investigated. It is shown that in some cases Doppler effect can limit the energy release to a small value even for high rates of reactivity insertion.

A method for calculating the material movement and reactivity reduction in two dimensional cylindrical geometry is presented and applied to a calculation of the energy release for two particular configurations. A simple spherical model is developed which gives good agreement with the two-dimensional calculations.

CHAPTER I

INTRODUCTION

The study of the safety of fast reactors since 1954 has been, to a large extent, dominated by the question of what would happen if for some unspecified reason the core of the reactor should accidentally melt.[1] There are two principle reasons for this emphasis on the study of fast reactor meltdown accidents. First, there is the fundamental point that fast power reactors have a high critical mass of enriched uranium which occupies of the order of 20% to 50% of the volume of the core, the remainder consisting of structural materials and coolant passages.[2] The same amount of uranium or plutonium compacted to full density could produce several individual critical masses, or a slight rearrangement of the core materials induced by melting of the fuel (if the rearrangement resulted in a compaction of the fuel into a smaller volume) could produce a large increase in reactivity.[1] If such a rearrangement should occur rapidly then there would be a high rate of reactivity increase that would produce a severe power excursion.

Another reason for the extensive investigation of fast reactor meltdown accidents is that until recently the only fast power reactor that has been operated extensively is the Argonne National Laboratory's EBR-I reactor,[3] and in November, 1955, the core of that reactor did

accidentally melt down.[4] While melt-down of the EBR-I did not result in an explosion or even a severe power excursion (the rearrangement of fuel upon melting may even have given a substantial reduction in reactivity), the event did nevertheless focus attention upon accidents of this type. The EBR-I reactor was eventually disassembled and rebuilt. Elaborate studies[5] with the rebuilt version have explained the cause of the accidental meltdown and shown that it was due to the particular mechanical design of the reactor and not due to any fundamental characteristic of fast reactors in general.

The overall problem of reactor meltdown can be divided into at least four broad areas. One area is the study of the events that could conceivably lead to meltdown, the stability of the reactor to power oscillation, the ability of the reactor to terminate accidental power excursions by means of the negative temperature coefficient of reactivity and its ability to withstand coolant flow transients without damage. This area of study has been extensively investigated in connection with the design of all of the large power reactors.[6-8]

The second area of study related to reactor meltdown is the study of the behavior of the fuel material as it melts and moves from its normal location under the forces of gravity, forces exerted by the coolant, which may be flowing past the fuel or may be boiling violently, and effects of the cladding material and the fission-product gases contained within the fuel. Considerable work of this type has been

done in connection with the fast reactor program[1, 9-12]. The Argonne National Laboratory has in operation the TREAT reactor,[13] a thermal reactor with a test hole and viewing port, that was designed and built specifically for the purpose of studying the behavior of fast reactor fuels during meltdown. All of the work in this area of study is directed towards determining under what conditions, if any, the melting core of a fast reactor can redistribute itself into a super-critical configuration and, if so, how rapidly it can happen. Studies of this type are inherently difficult to generalize, and most conclusions drawn may always have to be limited to the particular core designs studied in the experiments. It has even been difficult to draw definite conclusions about a particular well-defined accident from the experimental studies. No one has yet been able to prove that a particular fast reactor core meltdown accident definitely would or would not produce a supercritical configuration. For most cases studied it has seemed more likely that the fuel would be dispersed into a sub-critical condition. We expect that a great deal of work will continue to be done on studies of the behavior of the core material during meltdown. It can be a particularly profitable area of study because the solution of this problem can exert a major influence upon the course taken in future designs of the now expensive containment structures.

Since it must still be regarded as conceivable that a fast reactor

might melt into a supercritical configuration, it has been necessary to evaluate the consequences. Thus a third major area of study is that concerned with estimating the magnitude of the energy release for a reactor that is moving into a given supercritical configuration at a given rate, and a fourth area is the study of how to contain the resulting explosion and prevent the fission products from escaping the reactor building. A considerable amount of effort has been expended upon both of these areas of study[1, 14-21].

For this dissertation we have chosen to isolate as much as possible the third area discussed above, methods for estimation of the energy release, given that a reactor is passing into a supercritical configuration at a given rate of reactivity increase. About the only visible connection with a real meltdown accident is that we have in these studies covered the range of rates of reactivity increase from 0.0013 sec^{-1} up to 6.4 sec^{-1} which approximately brackets any reactivity transient of interest that could conceivably result from a reactor meltdown accident.* This isolation of one part of the overall problem is a rather artificial one, because the energy release in a real accident may depend to an important extent upon the detailed

---

*Lower rates of reactivity increase do not produce a power excursion that could be regarded as serious, and it is very difficult to imagine an accident that would involve forces sufficiently great to assemble the critical mass rapidly enough to produce a rate of reactivity increase greater than 6.4 sec^{-1}. For the rates of reactivity increase typically studied in fast reactor meltdown accidents see for example Reference 1.

nature of the fuel distribution. Except in Chapter VI where we investigate possible consequences of two very non-uniform fuel distributions, all of the calculations have been limited to situations that can be approximated by uniform homogeneous spherical reactor cores. The basic method of analysis, however, can be adapted to much more complicated situations if the time comes when one might wish to calculate the energy release for some particular predicted meltdown configuration. The main objective of this dissertation is an evaluation of a basic method of analysis involving certain approximations, and to this end there is no great loss in restricting the calculations to uniform spherical geometry. At the same time we have been able to formulate the method in a slightly more general manner than has been done before and determine the importance of certain effects that others have previously ignored. In some cases these effects are shown to be important.

The general method of analysis that we have pursued is discussed in detail in Chapter II. It is a generalization and extension of a method which has come to be known as the Bethe-Tait analysis because of a joint paper[14] by H. A. Bethe of Cornell University and J. H. Tait of the U.K.A.E.A. However, some of the original work[22] on fast reactor explosion analysis was done before the Bethe-Tait paper and some significant improvements have been made since, the work of V. Z. Jankus[16] being especially noteworthy.

In a reactor meltdown accident which produces a secondary critical assembly, the following sequence of events is visualized. The coolant either drains out, or is boiled out of the core. The fuel then melts and for some reason moves from its normal configuration into one which has a higher reactivity. The reactivity increases above prompt critical at some rate and causes a power excursion to develop, which is ultimately terminated by disassembly of the core.

The forces effecting the disassembly are high pressures produced in the uranium by the power excursion. The high pressures are attained because the energy is generated in a very short time, and the inertia of the core materials resists the disassembly process. Because the time is very short, the movement of material is negligible until the pressures do become quite high. Since there is a certain amount of void space left in the core when the coolant drained or boiled out, the uranium expansion can at first take place internally and the pressure does not become large until there has been sufficient thermal expansion to fill the void spaces or until the temperature becomes high enough to produce a high saturated vapor pressure. Thus there is an initial phase of the power excursion during which the disassembly process can be ignored and the power increase is approximately described by the reactor kinetic equations with the given rate of reactivity increase. By the time the pressure finally begins to rise there has been sufficient reactivity added to produce a very short

exponential period so the pressure rises rapidly from that time on, and disassembly occurs quickly. The disassembly phase occupies a very short period of time and the additional amount of reactivity added during this phase, due to the assumed rate of reactivity insertion, can often be neglected. Bethe and Tait took advantage of these two approximations in order to simplify the calculations.

The maximum reactivity attained before disassembly is normally only ~ 0.01 or less, and therefore only a slight amount of core expansion is required to terminate the excursion. Because of this it is possible to calculate the reactivity changes with sufficient accuracy by first order perturbation theory. Also, it is reasonable in most instances to assume that the pressure at each point in the core is independent of the small expansion* that occurs to terminate the excursion. The Bethe-Tait method utilizes this assumption and the perturbation theory approximation.

In our general method presented in Chapter II we have also used perturbation theory to calculate the reactivity reduction and have assumed that the pressure is independent of the small expansion. These are the two most important assumptions of the method and they are discussed in some detail in the following chapters.

The Argonne National Laboratory in cooperation with the Los

---

*The expansion of course continues after termination of the power excursion and eventually becomes large. Then the pressure decreases.

Alamos Scientific Laboratory has done some work with an explosion model in which the basic approximations of the Bethe-Tait model are abandoned in favor of more nearly rigorous expressions.[18] The changes in pressure due to density changes are included and the reactivity is calculated periodically by a modified S_n calculation rather than by first order perturbation theory. Their more nearly rigorous treatment greatly complicates the problem and required the development of an elaborate computer program, Ax-1, to effect the solution. It should be especially useful for the solution of problems involving high density cores. In Appendices B and C we show that our approximations are less accurate in high density systems, particularly for determination of the pressure. However, the simplicity of our method makes it much easier to check the reliability of the calculations. Furthermore, the extension to two or three dimensions is relatively easy compared to a similar extension of the Ax-1 code, which already requires appreciable computer running time for the present version, limited to spherically symmetric problems.

The Ax-1 code represents an extension of some earlier work by Stratton, et al[17], who studied prompt excursions in small solid uranium assemblies. By adjusting the parameters of their equation of state, they were able to obtain close agreement with the experiments done in Godiva, a small critical assembly at Los Alamos.

Stratton, et al,[17] also analyzed some larger assemblies using the Bethe-Tait model and using a model of a layered core. The latter

model is one of alternate spherical shell layers of high density uranium and very low density uranium. Their layered model gives markedly lower energy release than a Bethe-Tait calculation, in which the materials are all uniformly homogenized.

In Chapter II our basic method of analysis is set down in a quite general form so that it is clear how one could, if he wished, proceed to solve problems involving more complicated fuel distributions than those treated in subsequent chapters. Also, having written the expressions in this general form, we are free to calculate power distributions and reactivity worth distributions in any manner desired, i.e., multi-group diffusion theory, or the S_n method, or even to use distributions measured in a critical experiment as we do in Chapter VI.

In Chapter III we present a modification of the original Bethe-Tait method of analysis, but developed from our general expressions in Chapter II. We show there that some substantial improvements can be made in the treatment of power and reactivity distributions with no great increase in numerical difficulty. We have shown how one can obtain an accurate solution of the equations by iteration with very little numerical effort. We have evaluated the energy release as a function of two dimensionless parameters as Jankus[1] did, and obtain agreement with his results. We have then repeated the same calculation with a different surface boundary condition and show that the

result is not very sensitive to the surface condition, the numerical results being independent of the surface condition for small values of the parameter x and only slightly affected for high values.

Chapter IV treats a more nearly rigorous solution of the basic method of Chapter II. We utilize a digital computer program to solve the system of equations. But the most important difference between the analysis in Chapter IV and that in Chapter III is the form chosen for the relation between pressure and energy. Bethe and Tait, as well as Jankus, always assumed that the pressure is zero until the energy exceeds a given threshold and then is proportional to the energy in excess of threshold. This approximation neglects the vapor pressure that exists (and is not always negligible) for lower energies. We have instead used the sataturated vapor pressure and found that the pressures which actually exist when the energy density is below the threshold, exert a major influence on calculated energy release except for very severe power excursions. It has thus been shown that the threshold equation that has been used in most previous calculations is not a suitable one for the moderate and weaker accidents. For sufficiently high rates of reactivity increase the threshold model is found to be adequate.

Another refinement in Chapter IV is the inclusion of the effects of delayed neutrons. In all previous work on fast reactor explosions the delayed neutrons have been ignored. As expected, the delayed neutrons

are found to be of no importance except for rates of reactivity increase that are lower than those of usual interest in explosion studies. At the lowest rate of reactivity increase treated, .00013 sec^{-1}, the difference in energy release was only 20% when the delayed neutrons were completely ignored and $\sim$ 2% when they were ignored only for times beyond prompt critical.

We show the dependence of the energy release on some parameters of the theory, i.e. the rate of reactivity increase, initial power level and prompt neutron generation time. The results are consistent with the earlier calculations of Jankus[16] for high rates of reactivity increase, although, of course, the differences mentioned above due to the more realistic equation of state cause disagreement for the weaker accidents. We find that the energy release is not very sensitive to the prompt neutron generation time. This is not believed to be a new result, but we stress it because it is sometimes mistakenly stated that there is a great difference between the power excursions for fast reactors and thermal reactors because of the difference in prompt neutron generation times. We find that the difference in total energy release is only about a factor of 2.

Chapter V is a study of the influence of Doppler effect upon the energy release in fast reactor explosion calculations. The magnitude of the Doppler temperature coefficient is varied as a parameter. It is shown that even relatively small coefficients exert an important influence, and that coefficients as large as have been predicted for some

fast reactors can limit the energy release to a level that can hardly be called explosive. The author understands that similar results have been found by D. C. Menzies.[23] This result is as expected, since the importance of Doppler effect in limiting power excursions has long been recognized.[24, 25] However, as explained in Chapter V, the Doppler effect does play a slightly different role in fast reactor explosion studies than it does in the more conventional power transient studies, because the effects on reactivity of thermal expansion are delayed by material inertia.

All of the work of Chapters III, IV, and V of this dissertation was based upon a spherical, uniform, homogeneous model. In a real reactor meltdown accident, some substantial non-uniformities may occur. We have therefore made a study of two particular fuel configurations involving extreme non-uniformities. In Chapter VI we show that the deviation from uniform spheres can be of substantial importance. We also show that the energy release can be estimated fairly well for these two cases by an equivalent spherical model. However, it does not seem possible to generalize this result, and it is better to analyze the extremely non-spherical configurations in a geometry that more nearly approximates the real situation. The work of Chapter VI demonstrates the ease with which such cases can be treated within the framework of our general method.

We have included an Appendix on the question of state of uranium.

Here we have not attempted to improve upon the work of others. We have reviewed the several attempts at determining the equation of state and have chosen to use Brout's[26] estimates, which we have extended to higher densities. We also made some slight alterations of the saturated vapor pressure curve in order to make valid comparisons between the energy release calcuated using an equation of state of the vapor pressure form and that calculated using a threshold equation of state.

Appendices B and C are a study of the validity of two approximations in our basic method of analysis. We show that, if the density is not too high, then it is reasonable to neglect the effect upon pressure of the small expansions that occur prior to termination of the power excursion. We also show that the energy release calculation is not very sensitive to the treatment of the restraint at the core surface. Jankus[16] has also made some studies of the effect of tamping by the reflector, using the Ax-1 code, and concludes that "the density of the blanket has no significant, direct influence for the short lifetimes considered in these calculations." Our Appendix C shows why the tamper is not generally very important.

For the calculations of Chapters IV and V it was necessary to specify a simple reactor model. That model is described in Appendix D. Appendix E sketches a derivation of the temperature dependence of the Doppler effect for use in Chapter V.

Our work is mainly concerned with the techniques for calculating the total energy generated in a reactor meltdown accident. Once the energy is calculated it still remains necessary to determine the effects of that energy release on the surrounding structures. In Appendix F we briefly discuss certain aspects of this problem.

CHAPTER II

THE BASIC METHOD OF ANALYSIS

The foundations of the basic method of analysis employed in this dissertation were laid by H. A. Bethe and J. H. Tait.[14] They developed a simple procedure for estimating the energy release in reactor explosions subject to several simplifying assumptions. In the present work an effort is made to minimize the extent of the approximations while still applying the same basic principles(which are believed to be very well founded) and still keeping the method fairly simple. It is the purpose of this section to formulate what will be called the basic method of analysis, which forms a starting point for all subsequent approximations and calculations.

The geometrical model in this section is quite arbitrary. It is not even necessary that the material properties of the system be position-independent. However, in recognition of the fact that in applying the method it is assumed that the core is uniform and homogeneous (or at least that the core can be subdivided into regions that are individually uniform and homogeneous) the material density is written as a constant. In actual calculations the geometry is treated as either spherically symmetric or cylindrically symmetric. The basic method presented here could be utilized, at least in principle,

in situations having no symmetry at all.

There are two assumptions that are utilized throughout: *

1. The distribution of reactivity worth of core material is assumed independent of time, i.e., perturbation theory is used for calculating the reactivity changes during the explosive disassembly of the core. The basic configuration that is perturbed is then that which is in existence at the beginning of the power excursion.

2. The pressure at each point in the core as a function of time can be calculated from the energy density deposited at that point and the material density that existed at the beginning of the power excursion, i.e., the decrease in density due to core expansion can be ignored.

These two assumptions result in a tremendous simplification of the problem, and for most conceivable situations of interest there is very little error introduced. The reason that these assumptions are usually valid is that the total amount of reactivity to be compensated by material movement during the excursion is very small, and thus the total movement of material is very small until after the power excursion has been terminated. This has been shown explicitly in Appendix B. The greatest reactivity that is ever apt to be enccuntered in the study of hypothetical fast reactor accidents is of the order of 0.01 above prompt

---

*Except in Appendix C

critical.* Now for a typical fast reactor core the average fractional volumetric expansion required to reduce the reactivity by 0.01 is ~ 1.5%. It is quite clear that under such conditions, if the density changes are not terribly non-uniform, assumption 1 is reasonable.

It is possible to find situations in which assumption 2 would not be valid. For example, if a liquid at the density of the normal liquid state is heated at constant volume until the pressure is several atmospheres, and then the liquid is allowed to expand 1% in volume, the pressure will drop radically. Thus, very high density systems require careful consideration, but in Appendix B we show that the procedures can often be justified even for high density. We show that there is definitely no problem for densities of 10 gm/cc and less.

REACTOR KINETICS

The basic equations describing an explosion subject to assumptions 1 and 2 are presented here. First there are the point reactor kinetics equations:[27]

$$\frac{d^2Q}{dt^2} = \frac{(k-1-\beta)}{\ell}\frac{dQ}{dt} + \sum_{i=1}^{6} \lambda_i C_i + S \ , \qquad (1)$$

---

*The maximum reactivity attained above prompt critical is shown in Chapter III to be approximately proportional to the square root of the rate of reactivity increase. The highest reactivity attained in any of our calculations was .0059 for a rate of reactivity increase 6.4 sec^{-1}. This is about as high a rate as is ever considered in fast reactor meltdown studies because it is difficult to conceive of forces acting to assemble the critical mass that would be strong enough to give a higher rate of assembly. See for example Reference 1.

$$\frac{dC_i}{dt} = \frac{k\beta_i}{\ell}\frac{dQ}{dt} - \lambda_i C_i \qquad (i = 1 \text{ to } 6) \ . \qquad (2)$$

Here C_i is a quantity proportional to the concentration of delayed neutron precursors of type i, but having the dimensions of power density.* Similarly, S is proportional to the extraneous neutron source strength. These equations are employed in Chapters IV and V but in Chapters III and VI the delayed neutrons are ignored, leaving only Equation (1) without the summation term. Q gives the time dependence of the energy production:

$$E(\underline{r}, t) = N(\underline{r})\, Q(t) \ . \qquad (3)$$

The separability in space and time is assured because the prompt neutron generation time is very small compared to the periods which are encountered.

The neutron multiplication constant as a function of time is given by

$$k(t) = k_0 + k_1(t) + k_2(t) \ , \qquad (4)$$

---

*If dQ/dt were neutron density rather than power density then Eq. (1) and (2) would be the standard equations for reactor kinetics[27]. In the usual notation, k is the multiplication constant, β the delayed neutron fraction, ℓ the prompt neutron generation time, C_i the concentration of delayed neutron precursors of type i, λ_i the decay constant for precursors of type i, and S the extraneous neutron source. The power density is of course directly proportional to the neutron density, and so the kinetics equations for power density are obtained from those for neutron density by multiplying each term in the equations by the proportionality constant. Call this constant A. Then, our dQ/dt is A times the neutron density, our C_i is A times the concentration of precursors, and our S is A times the extraneous source.

where k_0 is the initial multiplication constant and $k_1(t)$ is the reactivity insertion which is responsible for initiating the excursion: It is always taken to be either a linear function of time or a step function. The reactivity $k_2(t)$ is the feedback which comes from material displacement $\underline{u}(\underline{r}, t)$ due to the pressure buildup from the power excursion; thus, it is the effect which terminates the excursion:

$$k_2(t) = \int \underline{u}(\underline{r}, t) \cdot \underline{\text{grad}}\, D(\underline{r})\, d^3r \quad , \tag{5}$$

where $D(\underline{r})$ is the reactivity worth per unit volume* of material at location $\underline{r}$. The integral extends over all the volume for which $\underline{u}(\underline{r}, t)$ and $D(\underline{r})$ are non-vanishing. The quantity $D(\underline{r})$ is assumed known either from a perturbation theory calculation or a critical experiment measurement.

HYDRODYNAMICS

The displacement $\underline{u}(\underline{r}, t)$ is related to the pressure $P(\underline{r}, t)$ through the equations of hydrodynamics:[28]

$$\frac{d^2\underline{u}(\underline{r}, t)}{dt^2} = -\frac{1}{\rho}\underline{\text{grad}}\, P(\underline{r}, t) \quad , \tag{6}$$

---

*i.e., $-D(r)$ is the reactivity change which would occur if a unit volume of homogenized core material at position $\underline{r}$ were to be removed from the core; hence $\underline{u}(\underline{r}, t) \cdot \underline{\text{grad}}\, D(\underline{r})$ is the reactivity change which occurs when a unit volume of material is displaced from its initial location $\underline{r}$ to the position $\underline{r} + \underline{u}(\underline{r}, t)$.

$$\frac{\partial \rho(\underline{r}, t)}{\partial t} + \operatorname{div}\left[\rho(\underline{r}, t) \frac{d\underline{u}(\underline{r}, t)}{dt} \right] = 0 , \qquad (7)$$

$$P(\underline{r}, t) = P(E(\underline{r}, t), \rho) , \qquad (8)$$

where ρ is the material density and P is the pressure. At this point Assumption 2 above is utilized. It states that we neglect the small changes in density and pressure due to material movement. Therefore, we have no need for Eq. (7), and ρ in Eq. (6) and (8) is assumed constant, then $P(\underline{r}, t)$ is the pressure generated by the power excursion, and it is determined by the energy density $E(\underline{r}, t)$ at a position $\underline{r}$ and time t and the density ρ which exists at the beginning of the power excursion.*

Eq. (5) is differentiated twice with respect to time and combined with Eq. (6) to give

$$\frac{d^2 k_2}{dt^2} = -\frac{1}{\rho} \int [\operatorname{grad} P(\underline{r}, t)] \cdot [\operatorname{grad} D(\underline{r})] d^3 r . \qquad (9)$$

Eqs. (1), (2), (3), (4), (8), and (9) constitute a complete set of coupled differential equations, and they have a unique solution if the appropriate initial conditions are specified. The initial conditions used are:

$$Q(0) = Q_0 \text{ (initial energy content)} ,$$

$$dQ/dt(0) = P_0 \text{ (initial power level)}, \qquad (10)$$

---

*We refer to Eq. (8) relating the pressure to the energy and the density as the equation of state. It is discussed in Appendix A. In Chapters III and VI we approximate P by a linear function of the energy, and in Chapters IV, and V, on the other hand, we use a negative exponential whose exponent is inversely proportional to the energy.

$k(0) = k_0$ (initial multiplication constant). (10 cont.)

CONDITIONS AT THE CORE SURFACE

Our Assumption 2 above leads to grad $P(r, t) \to -\infty$ at the edge of the core because the energy density changes discontinuously across the core boundary. (We assume that there is no energy generated outside the core.) It is therefore necessary to specify whether the integral in Eq. (9) goes just up to the inner edge of the core surface or just beyond the core surface. In previous calculations,[14-16] using the Bethe-Tait method, the integral has been carried just beyond the core edge. Under certain conditions we find that is the better approximation, and under other conditions it is better to integrate just up to the edge and not include the contribution from the infinite gradient at the surface.

What really happens near the surface depends upon the nature of the restraint offered by the reflector. The supercritical assembly is supposed to have been produced by rearrangement of the reactor fuel subsequent to core meltdown. While there may have been a rather well-defined boundary between core and reflector before meltdown it is not likely to be so well defined after meltdown. If, in the rearranged core, a large fraction of the surface is separated from the reflector by void (gas) space, then the reflector will have little influence on the motion of the core material, and it would be appropriate to use a treatment that approximates a free surface. On the

other hand, if the molten core is in more or less intimate contact with a reflector, then, because of its inertia, the reflector will tend to inhibit the motion of the core surface. The extent to which it slows down the surface movement depends upon how dense and how compressible the reflector is relative to the core material. A very dense material of low compressibility will provide more resistance than a light or highly compressible material.

There are several possible simple models which might be visualized for the treatment of the reflector effects.

a. The core surface is free to move unimpeded by the reflector.

b. The core surface is completely restrained from moving.

c. The existence of the core surface is completely ignored, i.e., the pressure gradient is assumed to be continuous through the surface, and then the integral in Eq. (9) is simply carried up to the surface.

d. The surface is in contact with a reflector which has a given thickness and average composition, and it is treated as homogeneous.

e. The surface is in contact with a reflector composed of alternate layers of material and each layer is treated as homogeneous.

Models a. and d. or e. describe situations that could actually exist. Models b. and c. are two idealized models which might be

chosen to approximate situations better described by Model d. or e. All of our calculations employ either Model a. or Model c. In Appendix C we show that Model c. is a reasonable one for the purpose of calculating the energy release when the core is surrounded by a typical reflector. It is also concluded that the energy release is not very sensitive to the nature of the surface restraint. InChapter III it is shown directly that the calculated energy release is approximately the same for Models a. and c. Furthermore, it is shown in Appendix C that Model c. usually tends to cause a slight overestimate of the energy release for a typical situation, while Model a. tends to give a slight underestimate; therefore the two models can often be used to bracket the energy release, although that would usually be unnecessary since they both give very nearly the same result.

To use Model c. it is only necessary to carry the integral in Equation (8) up to the inner edge of the core and stop short of the infinite pressure gradient. But in Model a. the surface is free to move, and it is clear in a qualitative sense what would happen near the core surface under these conditions. As soon as the pressure began to build up, the surface would move to relieve the pressure and the pressure would always vanish on the surface. Slightly inside the core the pressure would be positive but smaller than that predicted by Assumption 2.* The pressure increases with distance into

---

* i. e. that the pressure is not influenced by expansion.

the surface and asymptotically approaches the value predicted by Assumption 2. Thus the free surface causes a rarefaction wave to move into medium. Our calculations in Appendix C show that in the times involved the rarefaction wave can only move one cm or so. Because of this it is possible to approximate accurately the movement near a free surface by a simple scheme.

In the real situation there is a rapid drop in pressure from the asymptotic value to zero through a thin surface layer. As long as the layer is sufficiently thin that the gradient of the reactivity distribution does not change much through it, the layer can be treated as a unit, and the rate of reactivity change due to the motion of this material is proportional to the total momentum of the material. This means further that the result is independent of the actual magnitude of the thickness of the layer (as long as it is thin), and it is permissible to go to the limit of an infinitesimally thin layer in which $\underline{\text{grad}}\ P(\underline{r}, t)$ in Eq. (7) becomes the sum of a smooth function plus a delta function at the surface. Thus

$$\underline{\text{grad}}\ P(\underline{r}, t) = \underline{\text{grad}}\ P_i(\underline{r}, t) - \underline{n}\, P_s(\underline{r}, t)\, \delta(\underline{r} - \underline{r}_s) \qquad (11)$$

where P_i is always evaluated inside the core and is a continuous function approaching the value $P_s(\underline{r}_s, t)$ at the surface, and $\underline{n}$ is a unit vector directed outward, normal to the surface. Thus, in the free surface approximation Eq. (9) becomes

$$\frac{d^2 k(t)}{dt^2} = -\frac{1}{\rho}\int_{\text{volume}} [\underline{\text{grad}}\, P_i(\underline{r}, t)]\cdot[\underline{\text{grad}}\, D(\underline{r})]\, d^3 r + \frac{1}{\rho}\int_{\text{surface}} P_s(\underline{r}_s, t)\,\underline{n}\cdot \underline{\text{grad}}\, D(\underline{r}_s)\, ds \quad , \tag{12}$$

where the integration over the coordinate normal to the surface has been done in a trivial manner because of the δ function. This free surface approximation was introduced by Bethe and Tait[14] in the special case of spherical symmetry, in which case the surface integral can also be done.

Eq. (12) is the mathematical statement of Model a. Model c. is derived from this by simply dropping the surface integral term. These two models are the ones applied in the actual energy release calculations of Chapters III - VI.

In the original Bethe-Tait[14] and Jankus[1] calculations there was a reason for preferring to include the surface integral contribution to Equation (12), even when the core was assumed to be surrounded by a dense reflector. The reason was that in one-energy-group perturbation theory, if the reflector has about the same transport cross section as the core, a unit displacement of the reflector material near the boundary produces the same reactivity effect as a unit displacement of the core material near the boundary.[1] Since the reflector can only inhibit the motion of the core to the extent that it is set in motion itself,* the same reactivity effect is produced whether one

---

*The reflector slows down the movement of core material by causing a pressure to exist at the interface. But this pressure sets the

considers the tamping effect or not. That is the result of one group perturbation theory. However, when the reactivity changes are calculated more accurately, using multigroup perturbation, then it is found that the displacement of reflector material has a much smaller reactivity effect than displacement of core material near the boundary. For this reason the tamping does decrease the contribution of surface movement to the reactivity reduction,and we prefer to omit the surface integral in situations where the tamping effect does exist. Fortunately, as pointed out already and illustrated in Fig. 1, the difference in calculated energy release for Models a. and c. is quite small.

---

reflector material in motion and the total momentum of core material plus reflector material is the same as if the reflector were not present.

CHAPTER III

THE MODIFIED BETHE-TAIT METHOD

Much of the analysis of the power excursions from hypothetical fast reactor meltdown accidents has previously been based on a simple model which reduces the necessary numerical work to the solution of a pair of differential equations which can be solved numerically with great ease. This method can be developed from the basic method of Chapter II with the treatment of surface movement which leads to Eq. (12). Some further approximations are used which were introduced by Bethe and Tait.[14] The method presented here, however, follows more closely the treatment of Jankus,[1] who improved it by eliminating an approximation that was found to introduce appreciable error. We refer to our modified method as the modified Bethe-Tait, or M-B-T method.

The simple Bethe-Tait and Jankus method is reproduced here in some detail. The method is generalized by writing the reactivity changes in terms of the function $D(\underline{r})^*$, which could be an experimentally known function or calculated from transport theory or multigroup diffusion theory. Jankus expressed his equations in terms of reactivity changes calculated from one-energy-group perturbation

---

*See the footnote on page 19.

theory. While the one-group calculation is sufficient for most purposes, it is not difficult to obtain better approximations. The use of $D(r)$ also simplifies the development of the equations and makes it easier to compare the results of this method with those of the method in Chapter IV, where the reactivity changes are again expressed by a function $D(r)$. In addition, we show how to utilize higher order polynomial approximations to the power distribution, whereas Jankus restricted his analysis to parabolic power distributions.

ADDITIONAL APPROXIMATIONS

The major simplifications of the Bethe-Tait method beyond those already introduced in Chapter II are restriction of the analysis to spherical geometry, neglect of delayed neutrons, and division of the power excursion into two phases. Also the pressure is assumed to be a linear function of the energy. The first phase corresponds to the time during which the reactivity is being added (at an assumed constant rate) and the power is rising, but before the total energy generated from time zero has become sufficiently large to produce pressures which introduce significant material movement. During Phase I, therefore, the reactivity is taken to be a linear function of the time and reactivity feedback is neglected. This method of analysis is thus restricted to situations in which either the initial power is relatively low or else the rate of reactivity input is quite high, for otherwise there would be no time during which reactivity feedback could

be neglected. Phase II begins just as the reactivity feedback begins to be important. It is found that the ratio of the time interval between the beginning of Phase II and the termination of the power excursion to the time interval covered in Phase I is so small that the reactivity added during Phase II can be neglected as small compared to that added during Phase I. Therefore, during Phase II, the only reactivity effect accounted for is that coming from disassembly, i.e., from Eq. (12). It has been found directly in the calculations that the neglect of reactivity added during Phase II from the constant rate used in Phase I is completely justified for a wide range of conditions.

PHASE I

The energy generation as a function of time during Phase I is thus assumed governed by the neutron kinetics Eq. (1) with no delayed neutrons:

$$\frac{d^2Q(t)}{dt^2} = \frac{(k-1-\beta)}{\ell}\frac{dQ}{dt} + S \ . \qquad (13)$$

The initial conditions can be the values of Q and dQ/dt at any particular convenient reference. They are taken at prompt critical ($k = 1 + \beta$). The rate of reactivity increase is α, a constant, and so if the zero of time is when $k = 1 + \beta$, then Eq. (13) becomes

$$\frac{d^2Q}{dt^2} = \frac{\alpha t}{\ell}\frac{dQ}{dt} \ , \qquad (14)$$

where the source S has been dropped, since it is negligible above prompt critical. This equation can be immediately integrated once

to give

$$\frac{dQ}{dt} = \frac{dQ(0)}{dt} e^{\frac{\alpha t^2}{2\ell}} , \qquad (15)$$

and once again to give

$$Q(t) = \frac{dQ(0)}{dt} \int_0^t \exp[\alpha t'^2/2\ell]\, dt' + Q(0) \qquad (16)$$

Equation (16) gives the time dependence of the energy generation during Phase I in terms of the values $\frac{dQ(0)}{dt}$ and $Q(0)$ at prompt critical. To apply the equation, it is necessary to know these quantities, whereas one would normally know instead the corresponding quantities at delayed critical or even at some subcritical point. However, if the equations are applied only for high rates of reactivity increase, there is not time for large changes in power level until prompt critical is reached and the period becomes very short. It is therefore sometimes satisfactory to just use the subcritical power level for $\frac{dQ(0)}{dt}$, i.e., assume the power has not increased at all between delayed critical and prompt critical. Alternatively, one can make an estimate of the increase in power.[29] It is shown in the calculations of Chapter IV that this is necessary for low rates of reactivity increase. In the calculations it has been found that the results are not sensitive to the precise value of $\frac{dQ(0)}{dt}$. $Q(0)$ is the total energy content at time zero and we are free to set it equal to zero, thus establishing the reference point of the energy scale.

The end of Phase I was said to come at a time t_1 such that $Q(t_1)$ was sufficiently large to begin to produce pressure, and hence

material displacement. This is a very loose definition for the time t_1 , but here again it is found in the calculations that the final result is rather insensitive to the value chosen for $Q(t_1)$. Whether it is the value that produces a pressure of 1 atm at the core center or 100 atm makes little difference to the total energy release calculated. In actual calculations using this method the equation of state (8) is approximated by a linear function:*

$$\begin{aligned} P(r, t) &= (\gamma-1)\rho(E(r, t) - Q^*) && E(r, t) > Q^* \ ; \\ &= 0 && E(r, t) < Q^* \ . \end{aligned} \tag{17}$$

PHASE II

With this type of equation of state the obvious choice for $Q(t_1)$ is Q^* . Thus Q^* defines the end of Phase I and is an initial condition for Phase II. The other initial conditions for Phase II are $k(t_1)$ and $\frac{dQ(t_1)}{dt}$, the multiplication constant and power level at time t_1:

$$k(t_1) = 1 + \beta + \alpha t_1 \ . \tag{18}$$

To obtain t_1 it is necessary to invert Eq. (16) and solve for t as a function of Q . Since the integral in Eq. (16) is a tabulated function[30] there is no need to obtain an analytic expression. Jankus did obtain an asymptotic formula,[1] which is instructive in that it shows why the results are often insensitive to $Q(t_1)$ and $\frac{dQ(0)}{dt}$. He found

---

*The equation of state is discussed in Appendix A. In Eq. (17), ρ is the uranium density, and $(\gamma-1)$ and Q^* are parameters determining the slope and intercept of the linear function. For typical values see Table A. II.

$$t_1 \sim \sqrt{\frac{\ell}{\alpha}}\,\sqrt{\ell n\, y + \ell n(\ell n\, y)} \qquad y \gg 1 \quad ; \tag{19}$$

$$y \equiv \frac{\alpha Q^2(t_1)}{\ell}\left[\frac{dQ(0)}{dt}\right]^{-2} \quad . \tag{20}$$

Since y is a very large number the $\ell n(\ell ny)$ term is a fairly small correction, and it can be seen that the dependence of t_1 on $Q(t_1)$ and $\frac{dQ(0)}{dt}$ is as the square root of a logarithm. A typical value of $\ell n\, y$ is ~ 50, and Jankus[1] shows that a factor of e in $Q(t_1)$ or $\frac{dQ(0)}{dt}$ makes a difference of only 2% in t_1.

An initial condition for $\frac{dQ}{dt}$ for Phase II is also needed. This could be obtained from Eq. (15) and the calculated value of t_1. Instead it is perhaps more convenient again to employ the asymptotic formula for $Q(t_1)$ in order to express this initial condition in terms of $Q(t_1)$ and hence Q^* instead of $\frac{dQ(0)}{dt}$. The asymptotic relation is

$$Q(t_1) \sim \frac{dQ(0)}{dt}\,\frac{\ell}{\alpha t_1}\exp\left(\frac{\alpha t_1^2}{2\ell}\right) \qquad \frac{\alpha t_1^2}{2\ell} \gg 1 \quad . \tag{21}$$

This combined with Eq. (15) gives

$$\frac{dQ(t_1)}{dt} = \frac{\alpha t_1}{\ell}\,Q(t_1) = \frac{k(t_1) - 1 - \beta}{\ell}\,Q^* \quad . \tag{22}$$

The initial conditions (18), (22) and $Q(t_1) = Q^*$, combined with Eqs. (13) (with $S = 0$), (3), (12), and (17) constitute the mathematical statement of the problem during Phase II. The first step towards a solution is integration of the volume term in Eq. (12) once by parts. The boundary term obtained in this way just cancels the surface integral

in Eq. (12) to give

$$\frac{d^2 k(t)}{dt^2} = \frac{4\pi}{\rho} \int P_1(r,t) \frac{d}{dr}\left[r^2 \frac{dD(r)}{dr}\right] dr \quad , \tag{23}$$

when in addition the problem is restricted to spherical symmetry.

POWER AND REACTIVITY DISTRIBUTIONS

In order to arrive at formulae that have the same form as Jankus' results,[1] starting with our more general treatment of reactivity changes, we assume a parabolic distribution for the power:

$$N(r) = 1 - q \frac{r^2}{a^2} \quad , \tag{24}$$

just as he did. The constant a is the core radius and q is the shape parameter. But now $D(r)$ must still be specified, whereas in the one group perturbation theory used in the unmodified Bethe-Tait method the spatial shape of $D(r)$ is actually forced by Eq. (24) also to be parabolic, i.e., in the one group theory the flux distribution and reactivity worth are very closely tied.* So to obtain the Jankus formulae we assume

$$D(r) = D(0) - \frac{d}{2} \frac{r^2}{a^2} \quad , \tag{25}$$

---

*In the one group perturbation theory the equation corresponding to our Eq. (23) is

$$\frac{d^2 k}{dt^2} = A \int P_1(r,t) \frac{d}{dr}\left[r\left(\frac{d\phi}{dr}\right)^2\right] dr$$

where ϕ is the neutron flux and A is a constant involving neutron cross sections and uranium density. If a parabolic shape is chosen for ϕ the integrand is proportional to $r^2 P_1(r,t)$. To obtain an integrand of the same form in our Eq. (23) $D(r)$ must be chosen to be parabolic as in Eq. (25).

where d is a shape parameter for the reactivity worth function. While a parabolic shape is usually a reasonable approximation for the power distribution in a fast reactor, it is usually not very good for the reactivity worth. Table D.I shows power and reactivity worth distributions for a particular fast reactor core calculated by multigroup diffusion theory, and a comparison is made to the parabolic distributions used in our calculations of Chapter IV. The parabola, of course, has its maximum slope at $r = a$. The slope of $D(r)$ is actually about a factor of 2 less at $r = a$ than that predicted by our parabolic approximation. It is shown in Appendix B that a large fraction of the reactivity reduction in a strong excursion comes from material movement within several centimeters of the core edge, whereas in a weak excursion most of the reactivity reduction comes from material movement closer to the core center. Therefore, if the one-group parameters give the correct reactivity reduction for a weak excursion they will tend to cause an overestimate for strong ones, or if they are satisfactory for strong ones they will tend to underestimate the reactivity reduction in the weak ones. In Chapter IV we compare the energy release obtained for various shapes of the function $D(r)$, which shows the extent to which the shape can be important.

SOLUTION OF THE EQUATIONS

When Eq. (25) is inserted in (23) the latter becomes

$$\frac{d^2k(t)}{dt^2} = -\frac{12\pi d}{\rho a^2}\int P_1(r,t)\,r^2\,dr \quad . \tag{26}$$

Because of the form of the pressure, Eqs. (17), (24), and (3), Jankus found it convenient to change the integral over volume to an integral over the quantity N. A straightforward change of variable gives

$$\frac{d^2k}{dt^2} = -\frac{6\pi a d q^{-3/2}}{\rho}\int_{1-q}^{1} P(NQ(t))(1-N)^{1/2}dN \quad . \tag{27}$$

With the pressure function (17) this integral can be performed explicitly and gives

$$\frac{d^2k}{dt^2} = -\frac{8\pi}{5}a d\, q^{-3/2}(\gamma-1)Q^*\frac{Q}{Q^*}\left(1-\frac{Q^*}{Q}\right)^{5/2} \qquad Q^* < Q < \frac{Q^*}{1-q}\ ; \tag{28}$$

$$\frac{d^2k}{dt^2} = -4\pi a d(\gamma-1)Q^*\left[\left(1-\frac{3}{5}q\right)\frac{Q}{Q^*}-1\right] \qquad Q > Q^*(1-q)^{-1}\ . \tag{29}$$

These equations correspond to Eqs. (28b) and (28c) of Reference 1.*

Eqs. (28) and (29) are to be solved simultaneously with Eq. (13) (with $S = 0$) and the initial conditions Eqs. (22) and (18), with t_1 calculated from Phase I and $Q(t_1) = Q^*$. Jankus observed that the solution of these equations, which contain many parameters, is really dependent only upon a group of parameters x and the paramater

---

*There was a minor error[31] in this reference. The error is in the denominator of Eqs. (28b) and (28c), where the quantity (1-0.6q) should be replaced by $\left(1-\frac{6}{5}q+\frac{3}{7}q^2\right)$. The error is also carried through to subsequent equations. The factor (1-0.6q) which occurs in the numerator of Jankus' Eq. (28c) and a number of succeeding equations is correct and also appears in Eq. (29) of this work.

q . This can be shown as follows. The quantity x is defined here by

$$x = \frac{5(k_1 - 1 - \beta)^3 q^{3/2}}{8\pi a d(\gamma - 1) Q^* \ell^2} \tag{30}$$

Then the following changes of variable are made:

$$y = \frac{Q - Q^*}{Q^*} \; ; \quad \kappa(t) = \frac{k(t) - 1 - \beta}{k_1 - 1 - \beta} \; ; \quad \tau = t \cdot \frac{k_1 - 1 - \beta}{\ell} . \tag{31}$$

With these changes the problem becomes

$$\frac{d^2\kappa}{d\tau^2} = -\frac{(y+1)}{x}\left(\frac{y}{y+1}\right)^{5/2} \qquad 0 < y < \frac{q}{1-q} \; ; \tag{32}$$

$$\frac{d^2\kappa}{d\tau^2} = \frac{5q^{3/2}}{2x}\left[\left(1 - \frac{3}{5}q\right)y - \frac{3}{5}q\right] \qquad y > \frac{q}{1-q} \; ; \tag{33}$$

$$\frac{d^2y}{d\tau^2} - \kappa \frac{dy}{d\tau} = 0 \; ; \tag{34}$$

with initial conditions

$$\begin{aligned} y(0) &= 0 \; ; \; \frac{dy(0)}{d\tau} = 1 \; ; \\ \kappa(0) &= 1 \; ; \; \frac{d\kappa(0)}{d\tau} = 0 \; ; \end{aligned} \tag{35}$$

and it is seen that the only parameters entering are x and q .

Equations (32) - (34) have been solved numerically. In Figure 1 $y(\infty)$, i.e., the total energy release, is plotted as a function of x for $q = 0.6$. These results are found to be consistent with those presented in Reference 1. They were calculated and presented here because one cannot read the values from the curves of Reference 1 with sufficient accuracy to make comparisons between methods.

The set of Eqs. (32) - (34) which have been solved simultaneously are seen to be non-linear, Eq. (32) having a complicated dependence upon y . The functions, however, are smooth monotonic functions of τ, and the non-linear nature causes no difficulty whatever in the numerical solution. In fact, the solution is found very easily by iteration. The first guess for y is taken to be the solution of Equation (34) with $\kappa(\tau) = 1$, a constant. This solution is

$$y(\tau) = e^{\tau} - 1 \qquad \text{(first guess)} \qquad (36)$$

This is an overestimate for $y(\tau)$ since $\kappa(\tau)$ is a monotonically decreasing function of τ . Equation (36) is substituted into Eqs. (32) and (33) which are then integrated twice numerically to obtain a first estimate of $\kappa(\tau)$; which will be an underestimate and hence give an underestimate for $y(\tau)$ on the first iteration. The solution thus oscillates around the final answer with successive iterations. The convergence is extremely rapid due to the four-fold integration involved in going from one estimate of $y(\tau)$ to the next. For most purposes the first approximation is sufficient, giving an error of the order of 1% in the asymptotic value of y .

ADDITIONAL MODIFICATIONS

We have extended the treatment of this method to allow for better polynomial approximations for the power distribution and reactivity distributions. To do this, we found it more convenient to start with the spherically symmetric form of Eq. (12) rather than Eq. (23):

$$\frac{d^2k}{dt^2} = -\frac{4\pi}{\rho}\int_0^a r^2 \frac{dP(r,t)}{dr}\frac{dD(r)}{dr}\,dr \qquad (37)$$

$$+\frac{4\pi a^2}{\rho} P(a,t)\frac{dD(a)}{dr} .$$

When Eqs. (17) and (3) are used for the pressure, Eq. (37) becomes

$$\frac{d^2k}{dt^2} = -4\pi(\gamma-1)Q(t)\int_0^{r_t} r^2 \frac{dN(r)}{dr}\frac{dD(r)}{dr}\,dr \qquad r_t \le a ; \qquad (38)$$

$$\frac{d^2k}{dt^2} = -4\pi(\gamma-1)Q(t)\int_0^a r^2 \frac{dN(r)}{dr}\frac{dD(r)}{dr}\,dr$$

$$+ 4\pi a^2(\gamma-1)\frac{dD(a)}{dr}[N(a)Q(t) - Q^*] \qquad r_t > a , \qquad (39)$$

where r_t is the smallest positive solution of the equation

$$N(r_t) = \frac{Q^*}{Q(t)} . \qquad (40)$$

This, of course, assumes that the density ρ is a constant and that the power distribution $N(r)$ is a monotonically decreasing function of r for all $r \le a$.

Now it is simple to do the integrations in Eqs. (38) and (39) if $N(r)$ and $D(r)$ are approximated by polynomials. Then we can write

$$\frac{dN(r)}{dr}\frac{dD(r)}{dr} = a_0 + a_1\frac{r}{a} + a_2\frac{r^2}{a^2} + \cdots a_n\frac{r^n}{a^n} , \qquad (41)$$

and the expression for $\frac{d^2k}{dt^2}$ becomes

$$\frac{d^2k}{dt^2} = -4\pi a^2(\gamma-1)Q(t)\left[\frac{a_0}{3}\frac{r_t^3}{a^3} + \frac{a_1 r_t^4}{4a^4} + \cdots \frac{a_n r_t^{n+3}}{(n+3)a^{n+3}}\right] \quad r_t < a \quad ; \tag{42}$$

$$\frac{d^2k}{dt^2} = -4\pi a^2(\gamma-1)Q(t)\left[\frac{a_0}{3} + \frac{a_1}{4} + \cdots \frac{a_n}{n+3}\right]$$

$$+ 4\pi a^2(\gamma-1)Q(t)\frac{dD(a)}{dr}\left[N(a) - \frac{Q^*}{Q(t)}\right] \qquad r_t > a \; . \tag{43}$$

The coefficients a_0, a_1, ... a_n are easily obtained from the coefficients in the given distributions $N(r)$ and $D(r)$.

We do not present any actual calculations by this method using polynomial distributions (other than parabolic), but it is evident that they could be treated with only slightly more numerical effort than is required to solve the problem with Eqs. (28) and (29). Instead, we have compared polynomial approximations using the method of Chapter IV, which also incorporates some other improvements and has been programmed for solution on a digital computer.

In the method of Chapter IV we have chosen not to use the free surface assumption that has always been used up to now in the Bethe-Tait method. Instead, we use the more conservative approximation for surface movement referred to in Chapter II as Model c. In Appendix C it is shown that this model usually tends to overestimate the energy release. The free surface Model a tends to underestimate the energy release. In order to compare the two models and to make valid

comparisons between the Bethe-Tait method and our method of Chapter IV, we have altered the Bethe-Tait equations to incorporate the Model c treatment of surface movement. As explained in Chapter II, in this method we just drop the surface integral that provided the second term on the right hand side of Eq. (43). If this assumption is used with the parabolic power and reactivity worth distributions leading to Eqs. (28) and (29), we get no change in Eq. (28), but Eq. (29) is replaced by

$$\frac{d^2k}{dt^2} = -\frac{8\pi}{5} aqd(\gamma-1)Q(t) \qquad Q(t) > Q^*(1-q)^{-1} \qquad (44)$$

In Figure 1 the solution of Eqs. (28) and (44), coupled to Eq. (13) (with S = 0), is plotted in terms of the dimensionless quantities x and y of Eqs. (30) and (31) for q = 0.6. The solution of these equations was carried out in the same way as described above for solving Eqs. (28) and (29).

Figure 1 displays the difference in the results according to whether one uses Model a or c for the surface condition. The two methods of course give the same result for $Q(\infty)$ as long as $Q(\infty) < Q^*(1-q)^{-1}$, since then Eqs. (30) and (44) are never involved, i.e., the energy density at the core surface has not reached the threshold Q^*. For the case presented, q = 0.6, this point is reached at y = 1.5. Beyond that point the two models begin to differ. The difference, however, is not noticeable until y becomes greater

than about three. At $y = 10$, the difference is still only 15 per cent. In Chapter V, where we make comparisons between the M-B-T model and a more accurate one, we see that rates of reactivity increase greater than $6.4\ \text{sec}^{-1}$ are required before the energy release is great enough to give $y > 10$.

The significance of the numbers plotted in Figure 1 is not too clear until they are applied to give an energy release for a particular reactor subjected to a given rate of reactivity increase and given initial conditions. In the more accurate treatment of Chapter IV, it is not possible to reduce the dependence of the energy release to two dimensionless parameters, and so there we have been forced to choose a particular reactor model. For purposes of comparison, in Table II of Chapter IV we have compared the results of the modified Bethe-Tait calculation, using Model c for the surface movement, with the results of the more accurate method. The main difference in the results is due to the use of the vapor pressure Eq. (47) in place of the threshold expression (17).

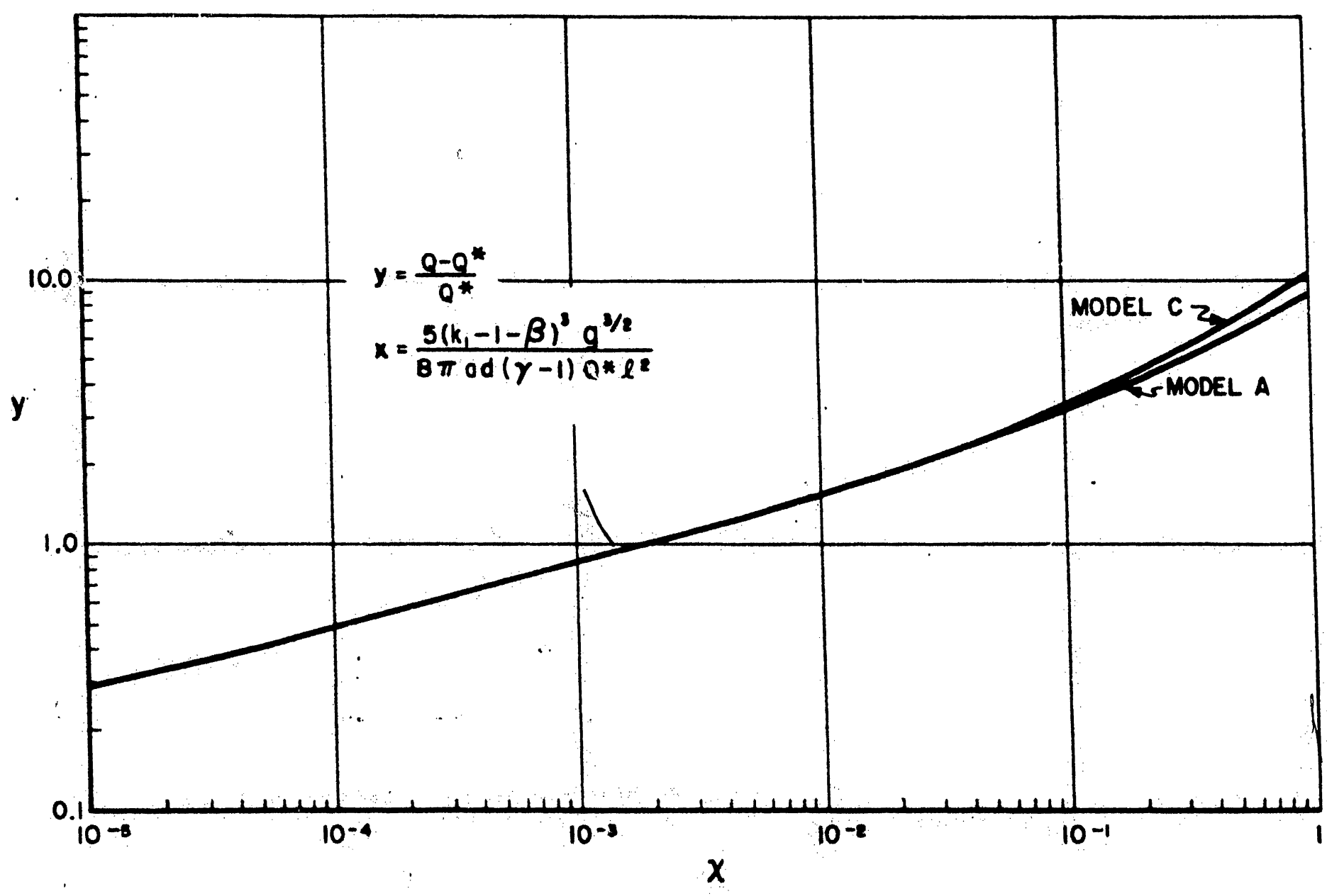

FIG. 1 y AS A FUNCTION OF χ IN THE M-B-T CALCULATION

CHAPTER IV

IMPROVEMENTS ON THE MODIFIED BETHE-TAIT METHOD

In Chapter III, a number of additional approximations were made beyond the general approximations described in Chapter II* in order that the problem could be carried further analytically, leaving only a simple numerical integration to obtain the energy release. That is, delayed neutrons were omitted; and the excursion was broken into two phases with reactivity feedback neglected in the first phase and reactivity insertion neglected during the second phase. However, more important was the restriction to a particularly simple equation of state, Equation (17), which assumed the pressure to be zero until the energy density exceeded a given threshold Q^*, and that a linear relation between the pressure and energy existed for $E > Q^*$. Largely in order to determine the influence of pressures which actually exist before the energy exceeds Q^*, a digital computer program was developed to solve the problem with a more realistic equation of state. At the same time the other approximations introduced in Chapter III were also dropped. Thus, the delayed neutrons are included in the computer calculation, and we show to what extent they influence the

---

*i.e., Assumptions 1 and 2, the use of perturbation theory to calculate reactivity changes and the neglect of density changes in the hydrodynamic equations.

results. There is no division into two phases. The reactivity is inserted throughout the calculation, and reactivity feedback is included throughout the calculation.*

AN IMPROVED METHOD

We use as a starting point for this method the basic method of Chapter II with the core surface movement treated by Model c, i.e. Eq. (12) with the surface integral dropped. The calculation is specialized to spherical symmetry. Then Eq. (12) becomes

$$\frac{d^2 k_2(t)}{dt^2} = -\frac{4\pi}{\rho} \int \frac{dP(r,t)}{dr} \frac{dD(r)}{dr} r^2 dr \ . \qquad (45)$$

The time dependence of the energy generation is given by Eqs. (1) and (2). However, in the digital program, in order to minimize computation time, it is found convenient to approximate Eq. (1) by setting $\frac{d^2Q}{dt^2} = 0$,

$$0 = \frac{(k-1-\beta)}{l} \frac{dQ}{dt} + \sum_{i=1}^{6} \lambda_i c_i + S \ , \qquad (46)$$

until the reactivity approaches prompt critical and switch to Eq. (1) for the remainder of the calculation. Because of the short neutron generation time this is a highly accurate procedure for a fast reactor as long as the rate of change of reactivity is not too great and the changeover is made when the reactivity is at least a few cents or

---

*although it has been found that the neglect of reactivity added during Phase II of the M-B-T method is a reasonable one.

more below prompt critical. Although Eq. (46) still appears to contain the lifetime, dropping $\frac{d^2Q}{dt^2}$ actually corresponds to going to the limit of an infinitely short prompt neutron generation time, and this is clearly a good approximation in a fast reactor below prompt critical where the time behavior is essentially completely determined by the delayed neutrons.* That it is a good approximation has also been demonstrated directly by showing that the results are independent of the point at which the changeover from approximate to more nearly exact equations is made.

Equations (45) and (46) or (1) are connected by the equation of state (9), relating the pressure and energy. In this method the equation of state is approximated by an exponential function:

$$P(r,t) = B \exp\left(\frac{-A}{E(r,t) + E_0}\right) . \qquad (47)$$

The basis for such a form for this function is explained in Appendix A. It is believed to be a considerably better approximation than the linear expression used in Chapter IV if the uranium density is not much greater than 7.5 gm/cc. $E(r,t)$ is again assumed separable in space and time:

$$E(r,t) = N(r)Q(t) .$$

---

*The quantity C_1 is inversely proportional to ℓ as can be seen from Eq. (2). Therefore, when $\ell \to 0$, the first two terms on the right hand side of Eq. (1) dominate the equation and d^2Q/dt^2 can be dropped. The extraneous source S is a constant, and once the power level dQ/dt becomes large S is also negligible. Then C_1 can be replaced by some other quantity B_1/ℓ, and ℓ cancels out of the equations.

The distributions $N(r)$ and $D(r)$ are assumed to be known from either a multigroup diffusion theory calculation or a critical experiment measurement, and are here fitted by polynomials of the fourth and fifth degree, respectively*

$$N(r) = N_0 + N_1 r + N_2 r^2 + N_3 r^3 + N_4 r^4 \quad ; \tag{48}$$

$$D(r) = D_0 + D_1 r + D_2 r^2 + D_3 r^3 + D_4 r^4 + D_5 r^5 \quad . \tag{49}$$

The reactivity insertion that initiates a power excursion is assumed to be linear with time. Thus the net reactivity as a function of time is

$$k(t) = k_0 + \alpha t + k_2(t) \quad , \tag{50}$$

where k_0 is the initial reactivity, αt the inserted reactivity, and $k_2(t)$ the feedback calculated by a two-fold time integration of Eq. (45).

Equations (1) - (3) and (46) - (50) constitute the formulation of the problem with the following initial conditions. The power $\frac{dQ}{dt}$ and delayed neutron precursors are assumed to be in a steady-state prior to time zero so that from Eqs. (1) and (2):

$$\left.\begin{aligned} \frac{dQ(0)}{dt} &= \frac{S\ell}{1 - k(0)} \\ C_i(0) &= \frac{\beta_i S}{\lambda_i (1 - k(0))} \end{aligned}\right\} \text{subcritical initial conditions.} \tag{51}$$

Alternatively $k(0)$ can be specified to be unity, in which case

*We believe that polynomials of this degree are sufficient to fit the calculated distributions to an accuracy which is more than sufficient. We provided for a fifth degree polynomial for $D(r)$, because it is the gradient of $D(r)$ which enters the calculations, and it is then a fourth degree polynomial.

the source term in Eq. (46) is dropped and Eq. (51) replaced by

$$\left.\begin{aligned} \frac{dQ(0)}{dt} &= P_0 \\ C_i(0) &= \frac{\beta_i \ell P_0}{\lambda_i} \end{aligned}\right\} \text{ critical initial conditions.} \qquad (52)$$

Thus we cover both the case of a shutdown reactor and one that is operating at some power when the excursion is initiated.

In practice, it is found that the results are very nearly the same for the subcritical and critical initial conditions. This is because the calculation proceeds through several decades in power before any significant feedback reactivity begins, and at that time there is very little "memory" left of the initial conditions. (This is one of the reasons the two phase procedure of the Bethe-Tait model of Chapter III works as well as it does.)

Since the calculation begins with the approximate equation, (46), no further initial condition is needed. The initial conditions on k are

$$k(0) = k_0 \; ; \quad k_2(0) = 0 \; ; \quad \frac{dk_2(0)}{dt} = 0 \qquad (53)$$

When the change is made over to the "exact" equations, the computer sets up new initial conditions which are essentially the terminal conditions from the solution of the approximate equations. Then $\frac{d^2Q}{dt^2}$ is needed, and it is derived from the calculated dQ/dt by differentiation.

The computer program which solves the equations with the stated initial conditions was developed for the author by J. W. Stephenson.*

*M. Friedman, A. Klickman, Y.J. Shin, and R. Mueller of Atomic

It is described in greater detail in Reference 32.

The method of calculation of this Chapter is very nearly an exact solution of the basic method of analysis described in Chapter II, except that it has been specialized to a spherical reactor of uniform homogeneous composition. The attempt at greater accuracy causes the results to depend upon each of many parameters of the theory individually in contrast to the M-B-T method of Chapter III, where it was possible to express the results as a function only of the parameter q and the group of parameters x, Eq. (30). For this reason the calculations by the method of this chapter must be defined by a particular hypothetical situation.

COMPARISON WITH THE MODIFIED BETHE-TAIT METHOD

For the purpose of demonstrating the influence of various parameters, and to compare with the M-B-T calculation and show the errors introduced by the additional approximations of the M-B-T model, we have thus defined a hypothetical reactor. It is a spherical reactor with a core radius of 40 cm. The core is composed of pure uranium at a density of 7.5 gm/cc, while the power distribution and reactivity worth distribution are specified polynomial functions of the form of Eqs. (48) and (49). This model is discussed in further detail in Appendix D.

Power Development Associates, Inc. also contributed to the development of the program.

As a first application of our more accurate method of calculation, we compare the energy release calculated by this method to that obtained by the M-B-T method for various rates of reactivity increase. In this comparison the power and reactivity worth distributions are assumed to be parabolic. The reactor is assumed to be initially critical at a given power level, and the initial energy content is that corresponding to molten uranium at the melting point. Power levels of 10 watts and 10^8 watts are treated, corresponding roughly to the normal shutdown power level and full power level for a power reactor of this size. The equation of state for the M-B-T calculation is the threshold equation, (17), with the parameters from Table A. II for a density of 7.5 gm/cc. The equation of state for the improved method is taken to be Eq. (4). Figure A. 1 compares the two, showing that they differ only at energies near and below Q^*. The prompt neutron generation time ℓ is taken to be 10^{-7} sec. The parameters of the calculation are summarized in Table I.

In the M-B-T calculation, the required initial condition is the power at prompt critical. We have determined it from our computer calculation so the two calculations agree at that point. The first step in the M-B-T method is a calculation of k_1, the maximum reactivity attained, from Eq. (18). Given k_1 and the parameters from Table I, the energy density at the core center Q is read from the upper curve in Figure 1. Then the total energy E_T generated is Q times the material density,

multiplied by the integral of the power distribution:

$$E_T = \rho Q \left[4\pi \int_0^a \left(1 - q \frac{r^2}{a^2}\right) r^2 \, dr \right]$$

$$= \frac{4}{3}\pi a^3 \rho Q \left(1 - \frac{3}{5}q\right) \quad . \qquad (54)$$

In the improved method the total energy is calculated directly by the computer. Table II summarizes the maximum reactivity attained and the total energy release as calculated by the two methods for various rates of reactivity increase. It can be seen that the M-B-T method of estimating the maximum reactivity attained is reasonably accurate for all rates of reactivity increase studied. However, the improved method of calculation gives substantially lower energy release except at very high rates of reactivity increase. This lower energy is almost completely a reflection of the different equation of state.

Even if the same maximum reactivity were to be attained in the two methods, the improved method would predict a lower energy release. This might at first seem surprising since in the M-B-T calculation the energy density at the core center attains values sufficiently large that the two equations of state, (17) and (47), become almost identical towards the end of the calculation.* However, we can easily see why the difference occurs. The discussion of Appendix B shows that most of the reactivity feedback comes from positions well out from the core

*See the comparison in Fig. A. 2 of Appendix A.

TABLE I

PARAMETERS FOR THE ENERGY RELEASE CALCULATION

		M-B-T	Our Method
ℓ	(prompt neutron generation time)	10^{-7} sec	10^{-7} sec
a	(core radius)	40 cm	40 cm
ρ	(uranium density)	7.5 gm/cc	7.5 gm/cc
q	(Eq. (24))	0.6	0.6
d	(Eq. (25))	6.4×10^{-6} cm^{-3}	6.4×10^{-6} cm^{-3}
Q*	(Eq. (17))	1.16×10^{3} joules/gm	--
$\gamma - 1$	(Eq. (17))	.82	--
A	(Eq. (47))	--	4.41×10^{4} joules/cm^{3}
B	(Eq. (47))	--	7.6×10^{11} dynes/cm^{2}
E_0	(Eq. (47))	--	1.12×10^{3} joules/cm^{3}

For delayed neutron parameters see Table D. II.

TABLE II

COMPARISON OF ENERGY RELEASE FOR TWO METHODS

$\alpha(\text{sec}^{-1})$	$(k_1-1-\beta)$ M-B-T Method	$(k_1-1-\beta)$ Our Method	Energy (joules $\times 10^{-9}$) M-B-T Method	Energy (joules $\times 10^{-9}$) Our Method
Power at k = 1 is 10 watts				
0.0013	--	0.000058	---	0.63
0.0040	0.00012	0.00010	1.9	0.98
0.012	0.00022	0.00020	2.1	1.14
0.056	0.00050	0.00048	2.6	1.7
0.18	0.00092	0.00089	3.2	2.4
0.62	0.0018	0.0017	4.3	3.8
1.9	0.0032	0.0031	6.8	6.4
6.4	0.0059	0.0058	15.0	14.5
Power at k = 1 is 10^8 watts				
0.0063	--	-0.0012	---	0.28
0.056	0.00025	0.00019	2.15	1.04
0.62	0.0010	0.00093	3.4	2.4
6.4	0.0037	0.0035	8.0	7.3

center where the power density is lower. Furthermore, since the material movement is given by a two-fold time integration of the pressure gradient, it is the pressures which occur when the energy generation is only ~1/2 to 3/4 complete which are mainly responsible for terminating the power excursion. If these pressures are compared for the two equations of state, we see that the vapor pressure equation predicts substantially higher pressures than the threshold equation used in the M-B-T method. In fact, for low rates of reactivity increase, the pressure is already terminating the excursion at a time when the threshold model predicts no pressure at all. The two calculations nearly agree for the highest rate of reactivity insertion considered here, i.e., 6.4 sec^{-1}. In that case the energy release is so high that the pressures effecting the shutdown are very nearly equal for the two calculations.

The lower energy release predicted by our calculation is mainly due to the effect noted above but also partly to the lower maximum reactivity attained. But the lower reactivity is again due to the different equation of state. The material movement in the improved method begins before the energy density reaches Q^*. In the M-B-T calculation no reactivity feedback is considered until the energy exceeds Q^*. If the excursion is initiated from lower power, the maximum reactivity attained differs in the two methods only for very low rates of reactivity increase. However, if the accident is initiated from near the normal

full reactor power, then the effect is important for rates of reactivity increase up to about 0.64 sec^{-1}. We see from Table II that if the excursion is initated from a power of 10^8 watts the difference in maximum reactivity for an $\alpha = .064$ sec^{-1} accident is about 30 percent, and for an $\alpha = 0.0064$ sec^{-1} accident the reactor does not even reach prompt critical. The M-B-T method is of course completely inapplicable in excursions that do not reach prompt critical.

The behavior of the energy release as a function of the rate of reactivity increase in Table II is quite interesting. We have covered a range of reactivity rates from 0.0013 sec^{-1} to 6.4 sec^{-1}, a ratio of about 5,000, and obtain a range of energy release from 0.63×10^9 joules to 14.5×10^9 joules, a ratio of only 22. Except for the extreme high rates and extreme low rates a factor of ten in rate produces about a factor of two in energy. This is because even our equation of state has somewhat of a threshold character. Very little pressure is produced until the energy density becomes quite large, and then the pressure increases rapidly and approaches the straight line expression of the M-B-T method. However, at the higher rates the presence of the threshold is no longer so important, and the energy release becomes more or less proportional to the rate of reactivity insertion. At the lower rates the energy release again becomes quite sensitive to rate of reactivity increase if the maximum reactivity attained is just about prompt critical, due to the very strong variation with reactivity of the reactor period in the neighborhood of prompt critical. The Bethe-Tait model

cannot show this effect since the delayed neutrons are omitted from the calculation.

INFLUENCE OF THE DELAYED NEUTRONS

The calculations reported in Table II gave some indication that the delayed neutrons are important if the excursion is initiated by a low rate of reactivity increase or if the excursion is initiated from high power. However, it was pointed out above that most of the difference in the two methods of calculation was probably due to the different pressure relations. In order to see more directly what role the delayed neutrons play, we have done a few special calculations with the computer code. Two pairs of calculations were done, and in each pair all parameters were identical except that in one member of the pair the delayed neutron fraction was reduced by a factor of 10^3. The parameters for these calculations are those given in Table I. The initial power level was 10 watts. For a rate of reactivity increase $\alpha = 0.00132\ \text{sec}^{-1}$ the energy release was 6.3×10^8 joules with delayed neutrons and 7.6×10^8 joules without delayed neutrons. For a rate of reactivity insertion $\alpha = 0.0040\ \text{sec}^{-1}$, the corresponding results were respectively 8.7×10^8 joules and 9.6×10^8 joules. At higher rates of reactivity increase, the effect rapidly becomes negligible. There are two effects involved which contribute to the differences observed. One is the effect of delayed neutrons between critical and prompt critical and the other is their effect beyond prompt critical; it turns out that the former

effect is much more important as might be expected. The calculations started from a critical condition $k = 1$. In the calculation with delayed neutrons the power rises through a few decades while the reactivity increases from critical to prompt critical. In the calculation without delayed neutrons the system starts at prompt critical. Suppose we neglect the delayed neutrons only after prompt critical. Then one can make an estimate of the increase in power up to prompt critical including delayed neutrons,[29] and begin the explosion calculation at that point. We have done this for the two cases discussed above. When the calculations with and without delayed neutrons were in this way forced to agree at prompt critical, the energy release was found to agree within two or three percent.

When the rate of reactivity increase was $0.0013\ \text{sec}^{-1}$, the maximum reactivity exceeded prompt critical by only 3.8×10^{-5}. Still, it should not be too surprising that the delayed neutrons could be neglected. The prompt neutron generation time of a typical fast reactor is $\sim 10^{-7}$ sec; for $\Delta k = 3.8 \times 10^{-5}$ the period turns out to be about 3 milliseconds, which is still much shorter than the lifetime of the delayed neutron precursors.

Thus, so long as one observes a few simple precautions, it is safe to neglect the delayed neutrons in fast reactor explosion studies. First of all, it is necessary to be certain that the combination of initial power level and rate of reactivity increase are such that the reactivity does

reach a value that is above prompt critical. For initial power levels near normal full power, our work indicates that this criterion is well satisfied for rates of reactivity increase of 0.05 sec^{-1} or greater. A rate of 0.004 sec^{-1} was found too low to produce a reactivity above prompt critical. Thus the break point lies somewhere between these two values—to be sure use the larger of the two. For an initial power level of 10 watts, all rates of reactivity increase treated down tc 0.0013 sec^{-1} were found to produce a reactivity above prompt critical.

Secondly, one should check to be sure that the total energy generation up to the time of prompt critical is a small fraction of the energy generated after the time of prompt critical. This will automatically be true if the shortest period achieved is small compared to the period at prompt critical. Finally, it is sometimes important to make a good estimate of the power level at prompt critical as the initial condition for the calculation. This is necessary when the rate of reactivity increase is small,so that there are several decades increase in power up to prompt critical, or when the initial power is high, so that there are only a few decades between initial power and the peak power in the excursion. If the initial power is low and the rate of reactivity increase is high, then one can forget about the delayed neutrons altogether.

INFLUENCE OF INITIAL POWER LEVEL

Using the computer code, we have investigated the influence of

various parameters upon the calculated energy release. Table II shows the variation of energy release with rate of reactivity increase, which has already been discussed. We have also discussed the fact that the energy release is dependent upon the initial power. Table II shows the difference between the results for initial powers of 10 watts and 10^8 watts. In addition, the energy release has been calculated as a function of initial power level for a rate of reactivity increase $\alpha = 0.06\ \text{sec}^{-1}$. The other parameters of the calculation are those given in Table I. The results are given in Table III.

TABLE III

ENERGY RELEASE AS A FUNCTION OF INITIAL POWER-$\alpha = 0.06\ \text{sec}^{-1}$

Initial Power Level (watts)	Energy Release (joules)
10	1.7×10^9
10^5	1.4×10^9
10^8	1.0×10^9
10^9	$.46 \times 10^9$

Table III shows a rather weak dependence of energy release upon initial power except that there is a rather sharp drop between the initial powers 10^8 and 10^9. That effect is due to the delayed neutrons. The case starting from 10^9 watts did not quite reach prompt critical, the maximum reactivity attained in that problem being 0.00612 compared

tc prompt critical reactivity 0.0064. The dependence of energy release upon initial power is weaker for the higher rates of reactivity increase as can be seen in Table II.

INFLUENCE OF PROMPT NEUTRON GENERATION TIME

We have investigated the influence of the prompt neutron generation time ℓ on the energy release. Again using the other parameters of Table I, a rate of reactivity increase $\alpha = 0.6\ \text{sec}^{-1}$ and $0.05\ \text{sec}^{-1}$, and an initial power level of 10 watts, we have varied ℓ from 10^{-5} to 10^{-7}. In Table IV we give the maximum reactivity attained above prompt critical and the energy generation.

TABLE IV

THE INFLUENCE OF PROMPT NEUTRON GENERATION TIME

	$\alpha = 0.6\ \text{sec}^{-1}$		$\alpha = 0.05\ \text{sec}^{-1}$	
ℓ (sec)	$k_1 - 1 - \beta$	Energy (joules)	$k_1 - 1 - \beta$	Energy (joules)
10^{-5}	0.017	2.2×10^9	-	-
10^{-6}	0.0054	2.9×10^9	0.0016	1.4×10^9
10^{-7}	0.0017	3.8×10^9	0.00048	1.7×10^9

Table IV shows that the energy generated is not a strong function of neutron lifetime. There is thus no very strong incentive to try to make fast reactors safer by various tricks which have been considered, such as coupling the fast reactor to a thermal reactor, in order to increase

the prompt neutron generation time. The reason for the rather weak dependence is evident when one examines the maximum reactivity attained above prompt critical. From Table IV we note that the maximum reactivity above prompt critical is roughly proportional to the square root of ℓ. Thus the minimum period of rise of the power is only inversely proportional to the square root of ℓ rather than to the first power of ℓ. The higher values of k are attained for the longer lifetime because of the longer periods. It takes longer for the power to rise high enough to begin disassembly and so there is more time for reactivity insertion.

INFLUENCE OF THE SHAPE OF D(r)

In Chapter III we mentioned that the parabolic distributions for power and reactivity worth which have generally been used in the Bethe-Tait method of calculation (and which we have also used in all the calculations of this section up to this point) tend to cause an underestimate of the energy release for the more severe accidents. This happens because in a severe accident if the power distribution is assumed parabolic, the pressure gradients are a maximum near the edge of the core.* In addition, the gradient of a parabolic reactivity distribution is a maximum there. In reality, the reactivity distribution in a typical fast reactor (see Appendix D) is apt to flatten appreciably

*See for example the discussion near the end of Appendix B.

near the core edge, and the slope of the distribution at that point may be only about half that predicted by a parabolic distribution. We have therefore made an investigation of the importance of the shape of the reactivity distribution. In this study we have held constant the difference in reactivity worth between center and edge of the core, and varied the shape of reactivity as a function of position. We have treated three shapes, a straight line, a parabola, and a fourth order curve which is forced to have a slope at the core edge equal to half the average slope between center and edge. It is of course only the gradient of the distributions which enters our calculations. The three curves are:

$$\text{Case A:} \quad \frac{dD}{dr} = -0.8 \times 10^{-7}$$

$$\text{Case B:} \quad \frac{dD}{dr} = -0.4 \times 10^{-8} r$$

$$\text{Case C:} \quad \frac{dD}{dr} = -0.7 \times 10^{-8} r + 0.375 \times 10^{-11} r^3$$

In Appendix D these are compared to the shape of a reactivity distribution actually calculated for a fast reactor, and it is seen that Case c is the most realistic of the three. The energy release was calculated for these three distributions for rates of reactivity insertion $\alpha = 6.4 \text{ sec}^{-1}$ and 0.05 sec^{-1} and an initial power of 10 watts. The other parameters are those of Table I. The results are given in Table V.

TABLE V

EFFECT OF THE SHAPE OF THE REACTIVITY DISTRIBUTION

Case	$\alpha = 6.4\ \text{sec}^{-1}$ Energy (joules)	$\alpha = 0.05\ \text{sec}^{-1}$ Energy (joules)
A	1.86×10^{10}	1.75×10^{9}
B	1.45×10^{10}	1.69×10^{9}
C	1.74×10^{10}	1.68×10^{9}

We see that Case B, the parabolic distribution, does tend to give a lower energy release, but the effect is not very great. We would expect the true distribution for most fast reactors would actually have a shape lying somewhere between Cases B and C. If our calculations had been done with the assumption that the core surface was free, then a larger fraction of the reactivity reduction would have come from material movement near the core surface, and the differences would have been somewhat greater. However, we have shown in Chapter III and Appendix C that the treatment of surface movement does not have a major effect on the results, and it can be concluded that the precise shape of the reactivity distribution is not of extreme importance. There is a sufficiently large effect however to warrant the use of a carefully calculated curve if the use of such a curve does not greatly complicate the energy release calculation. In our method it is certainly easy to use such a curve, and we have shown in Chapter III that this can also be done with no great inconvenience in the M-B-T method.

PRESSURE AND THE TIME WIDTH OF THE EXCURSIONS

The results presented in this Chapter have been mostly concerned with the total energy released in the power excursion. Other quantities of some interest are the pressures produced and the time for release of the energy. We have plotted in Figure 2 the pressure at the core center as a function of total energy release. By referring to this figure, one can see how high the pressure rises in any of the cases presented in this chapter. Figures 3 and 4 are plots of the power excursion for two extreme cases, $\alpha = 6.4$ sec^{-1} and $\alpha = 0.0013$ sec^{-1}. At the high rate of reactivity increase, the pressure attains a value of 4.5×10^5 atmospheres, and the time width of the power excursion at half maximum was 30 microseconds. This is a pressure slightly more severe than that encountered in a TNT explosion. At the lower rate of reactivity increase the maximum pressure was calculated to be 70 atmospheres and the time width was 2.5 milliseconds. This is still quite a rapid and severe pressure excursion that would disrupt most reactor core structures, but it is not so severe as a typical chemical explosion. Most of the other cases treated fall between these limits, an exception being those few cases in which the reactivity does not quite reach prompt critical. In such cases the pressure remains near atmospheric pressure.

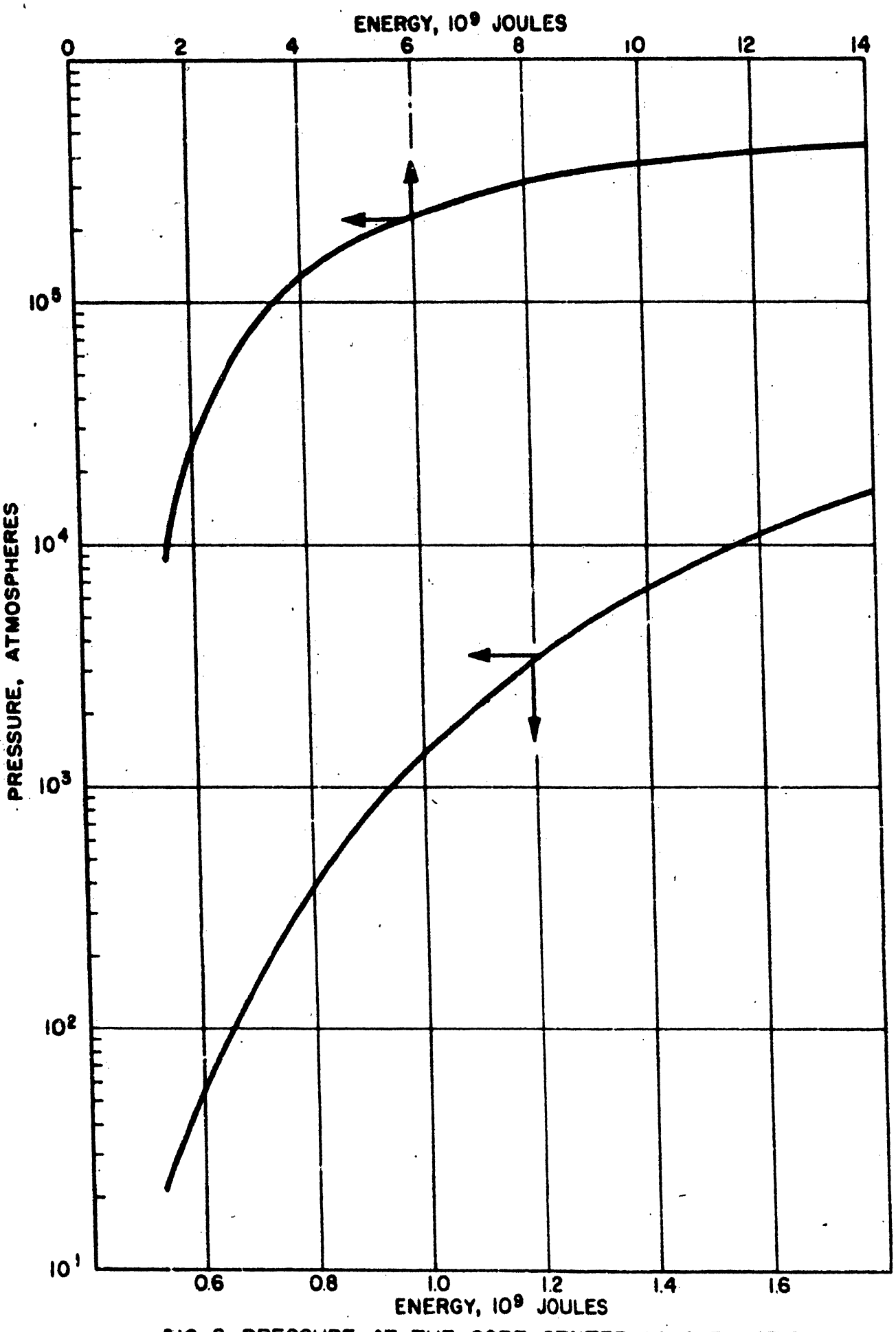

FIG. 2 PRESSURE AT THE CORE CENTER AS A FUNCTION OF TOTAL ENERGY RELEASE

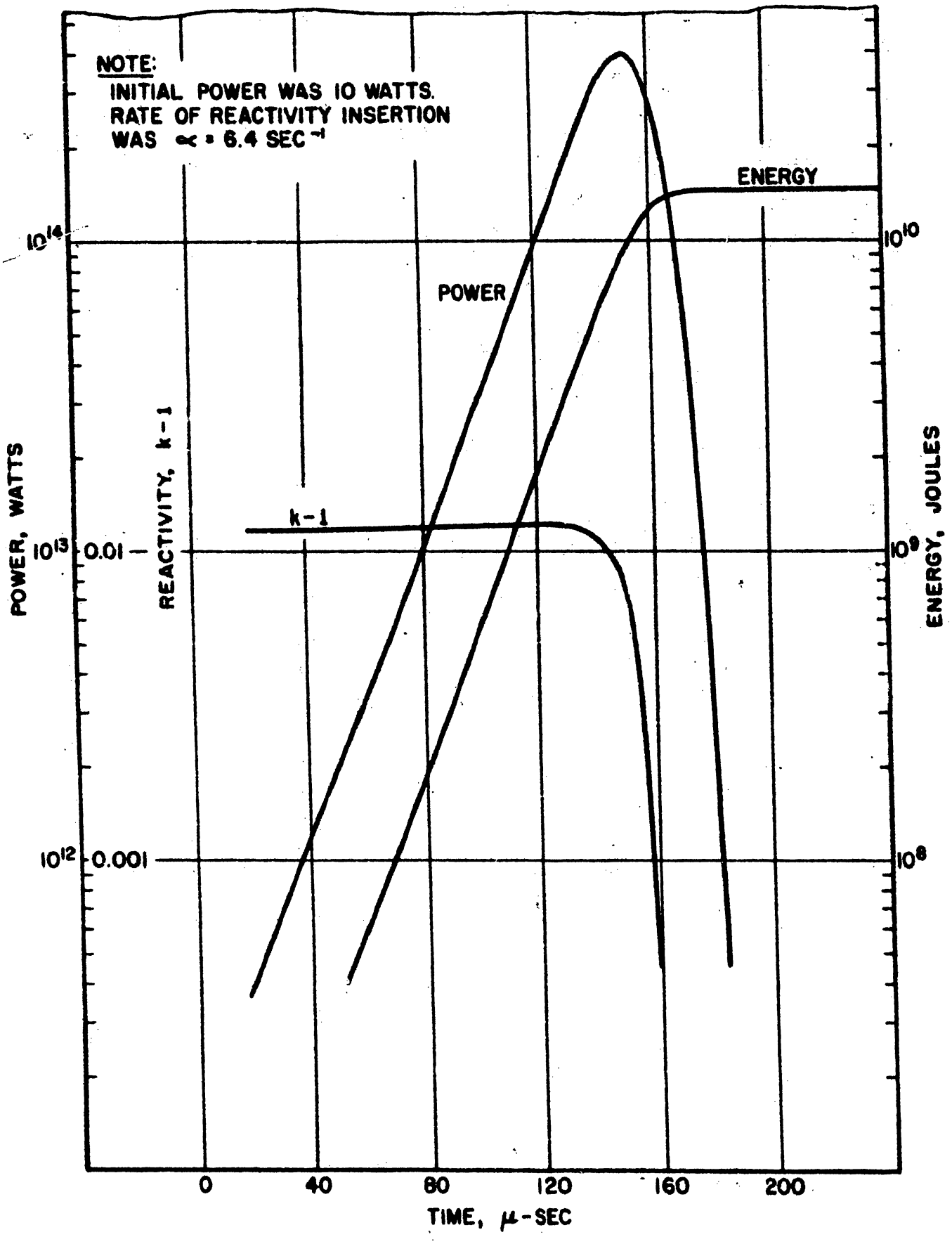

FIG. 3 A TYPICAL STRONG POWER EXCURSION

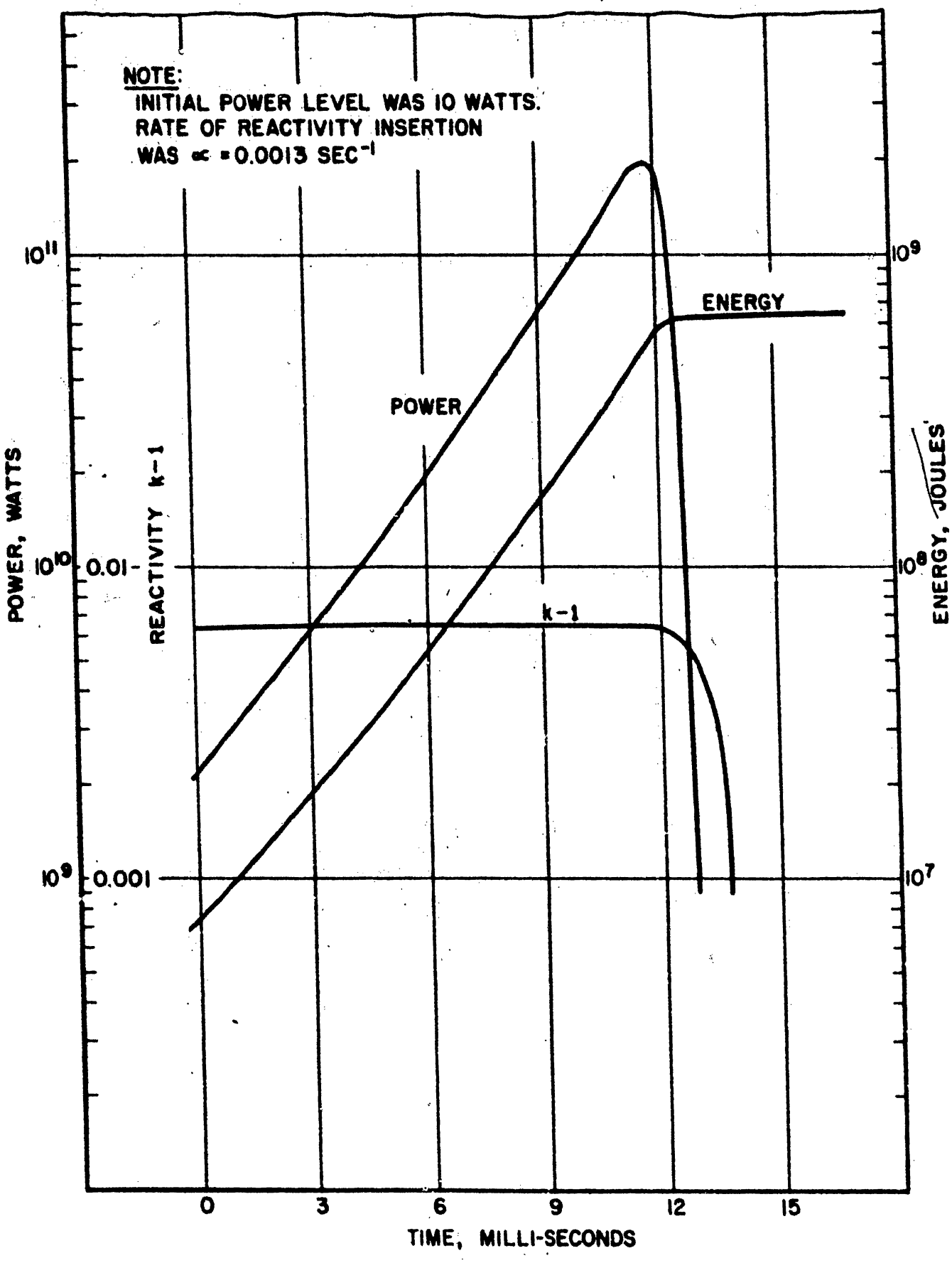

FIG. 4 A TYPICAL WEAK POWER EXCURSION

CHAPTER V

THE INFLUENCE OF DOPPLER EFFECT

In all of the work of the preceding chapters, we ignored the existence of the Doppler effect, which can be of great importance in the analysis of severe power excursions. The Doppler effect, as we use the term here, refers to the change in reactivity of a reactor with temperature, independent of the expansion effects that result from temperature changes.* This effect is caused by the change in the effective neutron resonance cross sections of the reactor materials as the temperature changes[24, 34]. The Doppler effect has been extensively investigated in studies of thermal neutron reactors,[35] and it has also been studied for fast reactors.[24, 25, 36] In thermal reactors of low uranium enrichment, the Doppler effect generally provides a large negative temperature coefficient of reactivity which is often larger than any other of the temperature coefficients of reactivity.

In the fast power reactors that have been built or are now under construction, e.g., EBR-I, EBR-II, Enrico Fermi, and the British Dounreay Fast Reactor, the Doppler effect has been predicted[24, 36, 37]

---

*In fast reactors, these are essentially the only contributions to the temperature coefficient of reactivity. In thermal reactors, of course, there are also effects due to changes in the thermal spectrum.

to be considerably smaller than the other temperature effects on reactivity which occur during slow temperature transients. However, in the extremely rapid transients which occur in our studies, material movement is held back by inertia, whereas the Doppler effect is an instantaneous function of the temperature. We find that even quite small Doppler temperature coefficients, which can safely be ignored in the usual reactor transient studies, can exert an important influence on the energy release in severe excursions.

Some of the fast breeder reactors that are now being studied for possible future construction[25, 38] have a larger fraction of their neutron energy spectrum in the lower energy range where the resonance effects are stronger than is the case for the reactors mentioned above; hence, the predicted Doppler temperature coefficients of reactivity for these reactors are higher. The coefficient calculated[24, 25] for a large uranium-oxide fueled fast reactor is of the order of magnitude $-1 \times 10^{-5}/C$ at the normal reactor operating temperature. This compares to the value $-1.7 \times 10^{-6}/C$ predicted[24, 36] for the Enrico Fermi fast reactor. The coefficients for EBR-I, EBR-II, and the Dounreay reactor are expected to be smaller yet. Since U^{238} contributes a negative Doppler coefficient and U^{235} a positive coefficient, a fast reactor fueled with fully enriched uranium has a positive Doppler coefficient. It has been estimated[36] that in a reactor having equal amounts of U^{235} and U^{238} the positive and negative effects approxi-

mately cancel one another. This is not true in general[24] and requires investigation for each particular case. The studies[24] show that it is unlikely for the coefficient to be very large and positive in a fully enriched U^{235} reactor, whereas it can be quite large and negative in a reactor of low enrichment. Hence, in our studies of the influence of Doppler effect on energy release, we have varied the Doppler coefficient as a parameter from small positive values to large negative values.

The reactivity changes from Doppler effect are easily incorporated in our calculations of the energy release by the method of Chapter IV. It is only necessary to add a term to Eq. (50) which is a specified function of the energy content. Thus Eq. (50) is replaced by

$$k(t) = k_0 + \alpha t + k_2(t) + k_D(t) \quad , \tag{55}$$

where $k_D(t)$ is the reactivity change due to Doppler effect. It is determined by the temperature (energy content) as a function of time. We assume that it is only a function of the average energy content and do not account for the non-uniform distribution of temperature through the core. The calculations of Doppler effect in fast reactors are not yet sufficiently refined to account for such details. However, we do know that the quantity dk_D/dT is temperature dependent, so that $k_D(t)$ is not simply proportional to energy content. It has been shown[24, 36] that for fast reactors like EBR-II and the Enrico Fermi reactor dk_D/dT is inversely proportional to the three halves power of the temperature. In Appendix E we sketch a derivation of this

temperature dependence and discuss also the temperature dependence for the large uranium-oxide reactors. We have assumed the $T^{-3/2}$ dependence for all the calculations of this section. We have further assumed the heat capacity to be temperature independent so that there is a direct proportionality between temperature and energy content. The heat capacity used was 6 calories per gram mole per degree Kelvin.* Then integration of the coefficient dk_D/dE with respect to energy gives

$$k_D(t) = K_D\left(1 - \frac{\sqrt{E_0}}{\sqrt{E_0 + \overline{E(t)}}}\right) , \qquad (56)$$

where K_D is the total amount of Doppler reactivity change which would result if the temperature were raised from the initial temperature, corresponding to energy E_0, to infinite temperature, and $\overline{E(t)}$ is the energy content added to the reactor by the power excursion, averaged over the volume. In our calculations we vary K_D from +.00064 to -.0128. The relationship between K_D and dk_D/dT is

$$K_D = \int_{T_0}^{\infty} (dk_D/dT)\, dT = \frac{dk_D(0)}{dT} T_0^{3/2} \int_{T_0}^{\infty} \frac{dT}{T^{3/2}} \qquad (57)$$

$$= 2\, T_0 \frac{dk_D(0)}{dT} ,$$

where $\frac{dk_D(0)}{dT}$ is the value at $T = T_0$.

---

*See the discussion on page 114 of Appendix A.

Since our excursions start with the uranium at the melting temperature $T_0 \approx 1400$ K, the range of temperature coefficients treated is roughly

$$\frac{dk_D(0)}{dT} = \frac{.00064}{2800} \approx 2 \times 10^{-7}/°K \quad \text{to}$$

$$\frac{dk_D(0)}{dT} = -\frac{.0128}{2800} \approx -5 \times 10^{-6}/°K .$$

(Because of the assumed temperature dependence, the Doppler temperature coefficients at a normal reactor operating temperature of about 700 K are roughly three times larger.)

Using Eq. (56) to represent the Doppler reactivity effect, and applying the method of Chapter IV, we have calculated the energy release as a function of the Doppler effect parameter K_D. The other parameters of the calculation were those used in the calculations of Chapter IV and are shown in Table I. The results for several rates of reactivity increase are given in Table VI. The initial power level was 10 watts except for the case in the right hand column for which the initial power level was 10 watts.

From Table VI it can be seen that the Doppler effect can have a very important influence on the energy release. At the low rates of reactivity increase even the very small Doppler effect $K_D = -.00064$ reduces the energy release by about a factor of two. At the higher rates it has about 20 percent effect. We see that a small positive coefficient increases the energy by about the same amount that a negative coefficient decreases it.

TABLE VI

THE INFLUENCE OF DOPPLER EFFECT ON CALCULATED ENERGY RELEASE (10^9 joules)

K_D	α (sec^{-1})						
	0.012	0.056	0.18	0.62	1.9	6.4	0.62*
+0.00064	--	--	--	4.5	--	--	3.0
0	1.1	1.7	2.4	3.8	6.4	14.5	2.4
-0.00064	0.5	1.2	1.8	3.1	5.4	--	1.9
-0.00192	--	0.4	--	2.0	--	9.2	1.0
-0.0032	--	--	--	--	--	7.1	--
-0.0064	--	--	--	0.75	--	3.6	--
-0.0128	--	--	--	--	--	1.0	--

*In this case the initial power level was 10^8 watts. In all other cases the initial power level was 10 watts.

It is particularly interesting that a large negative Doppler effect, e.g., $K_D = -.0128$, can hold the energy release to a very low level even for extremely high rates of reactivity increase. If it can be shown conclusively that the large oxide fast breeder reactors under study at this time do have negative Doppler effects of this magnitude, then the core meltdown accident will be only a very minor consideration in the evaluation of the safety of such reactors.

An interesting behavior is seen to obtain if the parameter K_D and the rate of reactivity increase α have certain values. Figure 5 is a

plot of the power, Doppler reactivity, and net reactivity as a function of time for a case in which the initial power is 10 watts, $\alpha = 0.6\ \text{sec}^{-1}$, and $K_D = .0064$. In this case a first power peak develops and is terminated by the reactivity from Doppler effect before the total energy generated is great enough to produce the high pressures required for rapid disassembly of the core. Since the insertion of reactivity is assumed to continue at a constant rate, the reactivity builds up again above prompt critical, and a second excursion develops. The second excursion raises the pressure to a sufficiently high value that disassembly begins, and then the reactivity decreases monotonically from that point on.

For this double peak to develop, it is necessary that the Doppler effect be strongly negative so that the energy generated in the first peak is not large enough to disassemble the core. Of the cases presented in Table VI, only this one involved a double peak. If a much stronger Doppler effect were used, it is likely that multiple peaks would occur, each one raising the temperature by a certain amount until the pressure became great enough for disassembly to occur. If the Doppler constant for the $\alpha = 0.62\ \text{sec}^{-1}$ case were increased from $K_D = 0.0064$ to ~ 0.01, it is probable that a third peak would begin to develop. The multiple peaks have been observed in some calculations by D.C. Menzies[39] of the U.K.A.E.A., who has also recently studied the influence of Doppler effect on severe power excursions using Eq. (17) for the pressure.

With this threshold equation it is easy to see that multiple peaks will occur, since no pressure at all exists until the threshold energy Q^* is exceeded.

With our Eq. (47), there is no threshold, and the usual behavior is that shown in Figure 6, which is a plot of power, Doppler reactivity, and net reactivity as a function of time, for a case in which the initial power is 10 watts, $\alpha = 0.62$ sec^{-1} and $K_D = -0.00192$. In that case the excursion is mainly terminated by the negative reactivity from the Doppler effect, with only a little help from material movement. But at that point the material velocities are great enough to overcome the assumed rate of reactivity insertion, and the net reactivity continues monotonically downward at an accelerated rate. The difference in behavior between Figures 5 and 6 was due to the smaller negative Doppler parameter K_D used in the calculations for Figure 6.

Figure 6 also displays the power excursion for the case in which $K_D = 0$. By comparison of the two power curves, we see that the Doppler effect broadens and lowers the power peak. The broadening is due to the fact that the Doppler effect has decreased the energy release, and so the pressures are lower and the disassembly is less rapid. From Table VI we see that the total energy release for the cases shown in Figure 6 was 3.8×10^9 joules with no Doppler effect, compared to 2×10^9 joules when $K_D = -0.00192$.

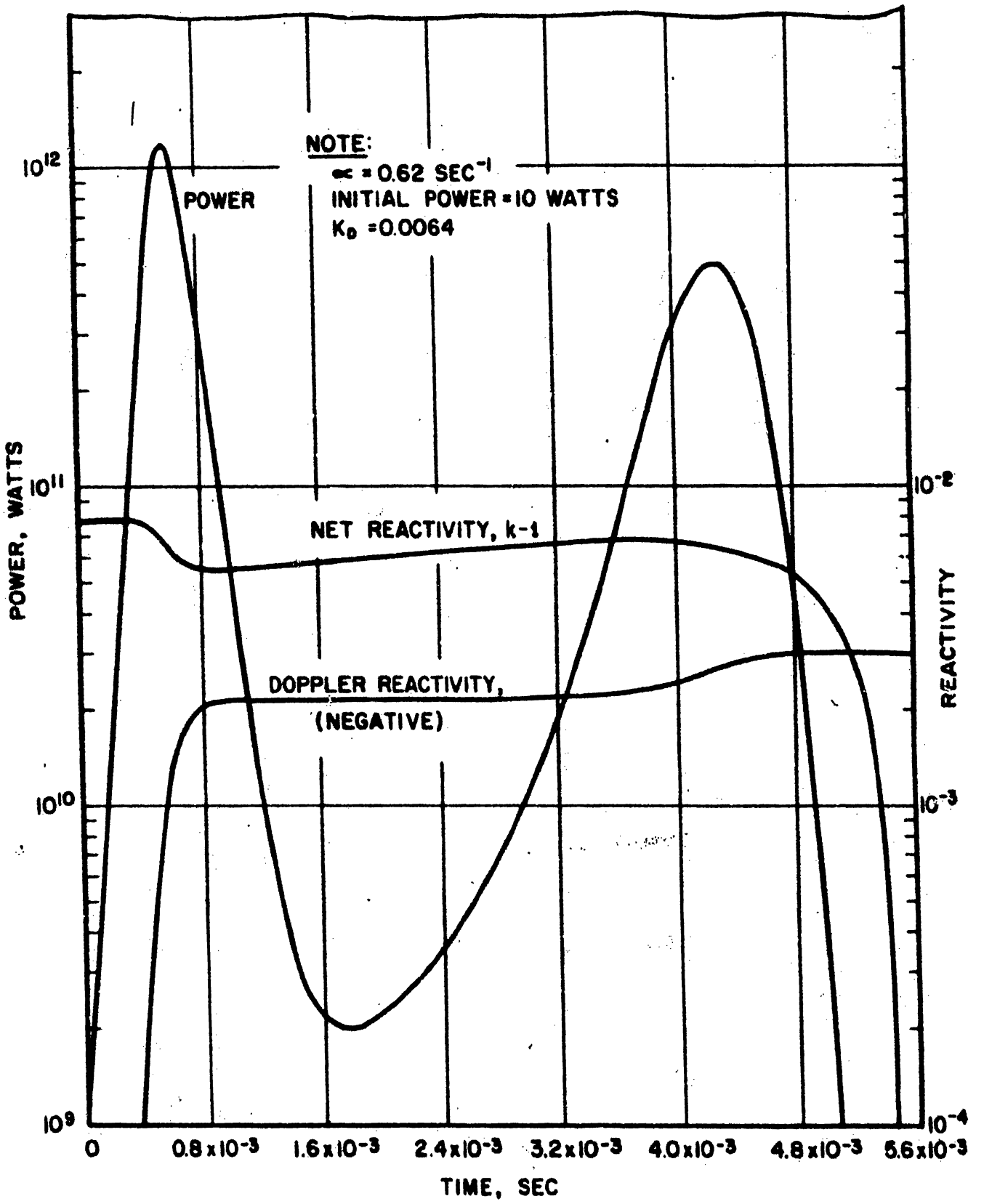

FIG. 5 POWER EXCURSION WITH LARGE DOPPLER EFFECT

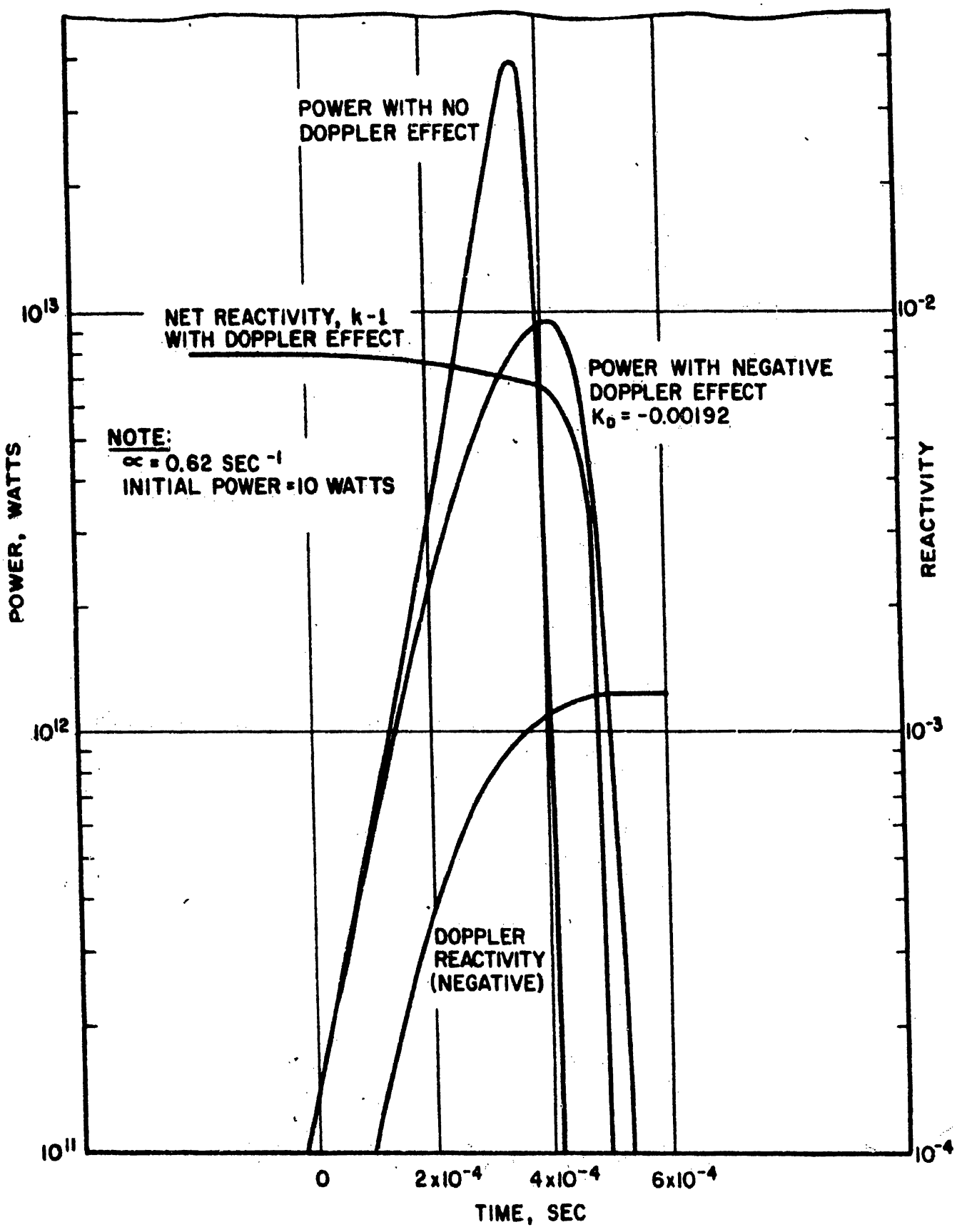

FIG. 6 POWER EXCURSION WITH NEGATIVE DOPPLER EFFECT

CHAPTER VI

TWO-DIMENSIONAL AND NON-UNIFORM EFFECTS

The methods of Chapters III, IV and V were restricted to situations which can be described by, or at least approximated by, a spherical uniform homogeneous core. It is believed that such a model is adequate for many interesting cases. However, the hypothetical excursions are generally supposed to result from meltdown of the reactor core, and it is not difficult to visualize fuel configurations from meltdown which cannot be well represented by a uniform homogeneous sphere. To study the non-spherical configurations we here develop a procedure for solving the equations (using the basic method of analysis of Chapter II) in two-dimensional cylindrical geometry.

There are two principle new effects which arise in non-spherical non-uniform situations. The equation of state (17) predicts that for a given energy input per unit mass the pressure in a high density region may be much higher than in a low density region. This means that the reactivity effects produced by expansion of high density material can, in some cases, shut the reaction down before there is any significant pressure produced in the low density region.

The second new effect when non-spherical geometries are considered is that it is possible that the maximum of the reactivity distribution and the maximum of the pressure distributions may not occur at the

same (spatial) point. Then the slope of reactivity and pressure distributions could be of opposite sign in some part of the core, so that the movement of material in that part would tend to produce an increase in reactivity rather than a decrease. In actual cases investigated, no significant separation of the peaks of reactivity and power distributions was found. However it is well to remember that such possibilities do exist.

THE TWO DIMENSIONAL METHOD

To solve the equations in two-dimensional geometry, a digital computer program[40] was developed for the author by J. W. Stephenson. The problem of programming the calculation for a digital computer was considerably simplified by restricting the geometry somewhat rather than allowing arbitrary two-dimensional cylindrical symmetry. The program was written for a core which can be approximated by one or two regions each having cylindrical symmetry and uniform homogeneous composition. The regions are further restricted in the axial direction to be bounded by plane surfaces. Thus the possible shapes are right circular cylinders or annular cylinders. This restriction is not believed to be a severe one, in that the two new effects discussed above can be investigated quite freely with this geometry, and it is believed that the results for more complicated shapes would not differ qualitatively. (But it would not be terribly difficult to develop a program that would

treat more complicated shapes if one wished to study some particular case.)

The method of analysis of this Chapter follows closely that of Chapter III except that it is generalized to two dimensions. Thus the power excursion is again divided into two phases (see page 28). Phase I is independent of geometry and so the discussion in Chapter III between Eqs. (13) and (22) also applies here. The Phase I calculation is used to determine the initial conditions for Phase II which begins when the energy generated at the hottest point in the reactor reaches Q^*. But now since there are two regions having different compcsitions, and hence different Q^*, Phase II starts whenever the maximum of $E(r, t)$ in either region equals Q^* in that region.

The equations solved numerically by the computer are (1) (with delayed neutrons and S omitted), (3), (4), (11), and (43). The initial conditions are the reactivity, energy, and power at the end of Phase I as calculated in Chapter III and the condition $\frac{dk(0)}{dt} = 0$. The program allows the choice as to whether or not the surface term in Equation (11) is to be included, according to whether Model a or Model c of Chapter II appears to be better. In fact, it is possible to include some segments of the surface and omit others as desired.

The reactivity $D(\underline{r})$ and power $N(\underline{r})$ distributions in this method are entered as a table of values at lattice points specified by their radial and axial position. The computer then makes a two-

dimensional polynomial fit to the input values and uses these smoothed distributions in the calculations.

It appears at first glance that at each increment of time in the numerical solution of the problem, the two-dimensional integrals over space in Eq. (11) must be done to provide the reactivity for the next time increment. However, since we have used the threshold Eq. (17) to represent the pressure, Eq. (9) can be written

$$\frac{d^2k}{dt^2} = -(\gamma-1)Q(t)\int[\underline{\text{grad}}\, N(\underline{r})]\cdot[\underline{\text{grad}}\, D(\underline{r})]d^3r \ , \qquad (55)$$

where now the integral extends over that part of the volume for which $N(\underline{r}) > Q^*/Q(t)$, i.e., the integral extends over a region of volume which is dependent upon how much energy has been generated, but the integral contains no other time dependence. Thus

$$\frac{d^2k}{dt^2} = -(\gamma-1)Q(t)\cdot F(Q) \ , \qquad (56)$$

where

$$F(Q) = \int_{N>Q^*/Q} [\underline{\text{grad}}\, N(\underline{r})]\cdot[\underline{\text{grad}}\, D(\underline{r})]d^3r \ ; \qquad (57)$$

and $F(Q)$ is a smooth function of Q that becomes a constant after the time when Q is sufficiently large that the entire core volume is included in the integration. The computer program therefore calculates the function $F(Q)$ at discrete values of Q before doing the time integration and then interpolates from this table of values. A similar treatment is used for the surface integral, Equation (12). The numerical solution of the equations is described in more detail in Reference 40.

TREATMENT OF CORE SURFACE MOVEMENT

In Appendix C, the various approximate treatments* of the motion of material near the core surfaces are discussed and shown to be reasonable. We show that the approximations introduce appreciable error in the motion of material right at the core surface but that the error is confined to a surface layer of ~ one cm thickness. In the case of a free surface, the motion of the material near the surface, integrated over volume, is reasonably accurate and leads to a good estimate of the reactivity effect. We also show that the results for the calculated energy release are not very sensitive to the treatment of surface movement for cases involving spherical cores. However, in more complicated geometries, it is sometimes necessary to pay more careful attention to the conditions at the surfaces. Two new situations can arise. It is possible to conceive situations in which the input pressure is nearly flat near a core surface or even decreases with distance from the surface into the core material. This could happen, for example, if there were two annular core regions separated by a void space or some material containing no uranium. The other new possibility which would be more commonly encountered is a surface separating two core regions each of which is generating pressure. It is difficult if not impossible to show in general that the Models a or c of Chapter III are adequate to treat these more compli-

---

*i.e., approximations for surfaces that are in contact with a reflector and surfaces that are completely free. See also pages 21-26.

cated situations. However, it is probable that one or the other of these approximate models for treatment of surface movement can be justified for most situations that might be encountered. After describing the two particular cases that we have analyzed, we show that the surface approximations are satisfactory for those cases.

TWO MELTDOWN CONFIGURATIONS

The two situations that we chose to analyze, and for which critical experiments were done at Argonne National Laboratory, * are idealizations of two fuel rearrangements of the Enrico Fermi Reactor which it was imagined might result from core meltdown accidents. We have designated the two cases Configuration A and Configuration B. Configuration A is supposed to arise when the fuel in a group of central fuel elements

---

*Over a period of several years the Argonne National Laboratory, using the ZPR-III facility,[41] has made many critical experiment measurements of power distribution and reactivity distribution in relatively simple geometries such as spheres and right circular cylinders surrounded by reflector. Calculational techniques have been developed that would predict the measurements to an accuracy that is sufficiently accurate for most purposes, and certainly good enough for our calculations. However, prior to the initiation of our work on two-dimensional power excursion studies, no complicated geometries had been done in ZPR-III. There was some doubt about the reliability of the available calculation techniques for reactivity and power distribution in cases, for example, where the core is an annular cylinder with a cylindrical void in its center. Since it is configurations such as this which are interesting in the study of two-dimensional problems, it was decided that some experiments should be done. We proposed a series of experiments on two particular configurations and these experiments were then carried out in the Argonne National Laboratory's ZPR-III facility. The experimental work was described in a paper presented to the American Nuclear Society. The author is grateful to the Argonne National Laboratory for making available some of the additional experimental data[43] which has not yet been published.

The experimental configurations were analyzed by Okrent, et al[44]

melts and settles towards the bottom of the core. We show this configuration schematically in Figure 7. The compositions of the four regions are given in Table VII.

TABLE VII

COMPOSITIONS FOR CONFIGURATION A

	% Volume Composition					
	U-235	U-238	Stainless Steel	Al	Mo	Zr
Region I	6.00	17.16	16.90	27.81	5.18	4.41
Region II	14.80	42.56	14.50	0	15.50	4.98
Region III	0	0	9.32	4.2	0	0
Region IV	0.11	48.7	21.0	0	0	13.47

The Argonne National Laboratory determined the power distribution in Configuration A by fission chamber measurements,[42] and they measured the reactivity worth as a function of position for a small sample having a composition approximating the average composition of the core material. From the experimental data furnished by the Argonne,[43] we have fabricated the power distributions and distributions of reactivity worth per unit volume shown in Table VIII and Table IX. We have shown the reactivity worth only for Region II because the reactivity worth in Region did not actually enter into the calculation. (The energy density in that region did not exceed the threshold, and therefore there was no material movement calculated in Region I.)

---

using two-dimensional, two-group diffusion theory. Their calculations of power distribution and reactivity worth agreed reasonably well with the experiments.

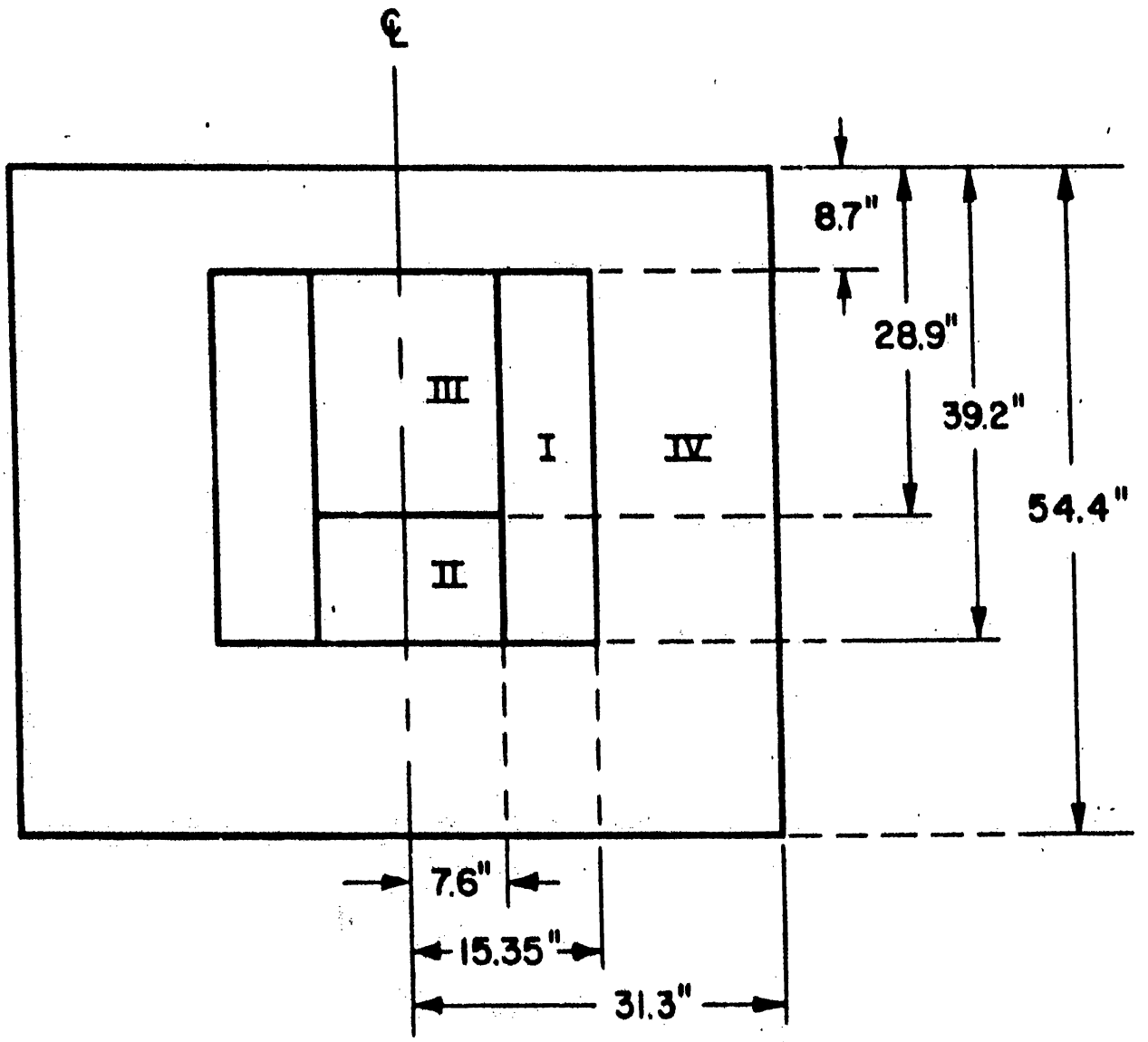

FIG. 7 DIMENSIONS OF CONFIGURATION A

TABLE VIII

POWER DISTRIBUTION* FOR CONFIGURATION A

Region I

Axial Position Measured from Bottom (cm)	Radial Position Measured From the Axis (cm)				
	19.2	24.3	29.4	34.4	41.4
74.3	4.8	4.5	4.0	3.3	2.0
50.8	7.6	7.0	6.1	5.2	3.5
30.5	10.3	9.3	8.1	6.7	4.6
20.3	12.8	10.6	9.1	7.0	4.8
15.2	13.4	10.8	9.0	7.0	4.8
10.2	12.9	10.3	8.4	6.6	4.5
5.1	10.7	8.9	7.2	5.6	3.7
0	8.0	6.6	5.0	4.0	2.7

*The normalization is arbitrary—no particular system of units.

Region II

Axial Position Measured from Bottom (cm)	Radial Position Measured From the Axis (cm)				
	0	5.1	10.2	15.2	19.2
26.3	12.8	12.3	10.9	9.0	7.8
20.3	18.3	17.7	15.8	13.4	11.4
15.2	20.4	19.7	18.2	15.4	13.1
10.2	20.3	19.6	18.1	15.6	13.5
5.1	17.5	16.9	15.6	14.1	12.4
0	12.5	12.2	11.8	11.3	10.8

TABLE IX

REACTIVITY* PER UNIT VOLUME FOR CONFIGURATION A

Region II

Axial Position Measured from Bottom (cm)	Radial Position Measured From the Axis (cm)				
	0	5.1	10.2	15.2	19.2
26.3	1.13	1.08	0.93	0.78	0.65
20.3	1.55	1.50	1.27	1.00	0.80
15.2	1.69	1.64	1.45	1.12	0.87
10.2	1.67	1.64	1.43	1.13	0.87
5.1	1.52	1.45	1.20	0.93	0.78
0	1.12	1.07	0.82	0.63	0.53

*Reactivity is expressed in units 10^{-5} $\Delta k/cm^3$. See the footnote on page 19.

Configuration B is shown in Figure 8. It supposedly arises from an accident in which the fuel in a group of the central fuel elements melts and either drains out of the core or is carried out by the pressure of the coolant stream. Then the outer fuel elements are assumed to collapse into the configuration shown. It is rather difficult to imagine that this could actually happen and so Configuration B might better be regarded as arbitrarily chosen for the purpose of studying the behavior of non-spherical configurations.

The compositions of the three regions are given in Table X.

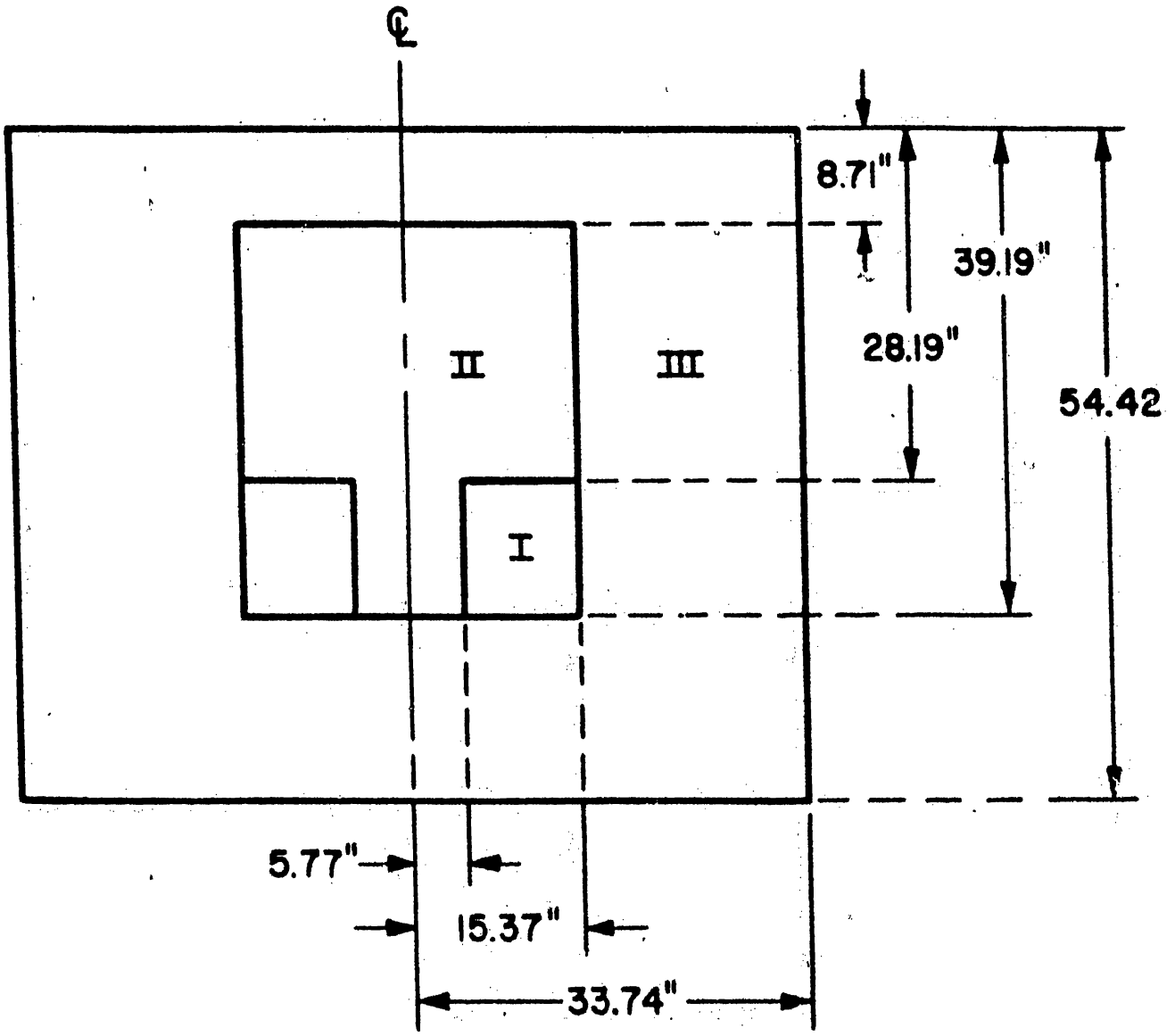

FIG. 8 DIMENSIONS OF CONFIGURATION B

TABLE X

COMPOSITIONS FOR CONFIGURATION B

	% Volume Composition					
	U-235	U-238	Stainless Steel	Al	Mo	Zr
Region I	14.5	42.34	13.9	0	15.5	5.1
Region II	0	0	9.32	4.22	0	0
Region III	0.11	48.7	21.0	13.47	0	0

From the Argonne measurements of power distribution and reactivity worth, we have made up the power distribution and reactivity per unit volume for the homogenized core material shown in Tables XI and XII.

TABLE XI

POWER DISTRIBUTION* FOR CONFIGURATION B

Region I

Axial Position Measured from Bottom (cm)	Radial Position Measured From the Axis (cm)				
	15.2	19.0	25.4	31.8	38.1
0	6.5	7.0	7.0	6.1	3.9
8.2	8.2	8.4	8.4	7.2	5.5
13.9	10.4	11.5	11.5	9.6	6.9
19.3	11.8	13.5	13.6	10.7	7.3
24.8	11.6	12.8	12.9	10.5	7.0
27.9	9.8	9.5	7.0	7.2	5.2

*The normalization is arbitrary

TABLE XII

REACTIVITY* PER UNIT VOLUME FOR CONFIGURATION B

Region I

Axial Position Measured from Bottom (cm)	Radial Position Measured From the Axis (cm)				
	15.2	20.3	26.7	33.0	39.4
0	5.7	4.2	3.6	2.4	1.4
8.3	5.4	4.8	4.4	2.9	1.7
13.8	5.1	6.0	6.2	4.1	2.5
19.3	5.5	6.8	7.2	5.8	3.3
24.8	4.4	5.6	5.9	4.8	3.3
27.9	4.7	4.5	4.4	4.0	2.2

*Reactivity expressed in units $10^{-6} \Delta k/cm^3$.
See the footnote on page 19.

We have already mentioned that in the two-dimensional calculations we have used the procedure employed in the M-B-T analysis of Chapter III, in which the excursion is broken into two phases. In the first phase one neglects reactivity feedback and determines the reactivity attained at the time the energy density at the position of maximum power reaches the threshold energy Q^* . Then the initial conditions for the start of the disassembly phase are Eqs. (18), (22), and $Q(t_1) = Q^*$ just as in Chapter III. We do not concern ourselves further here with Phase I.

To do the calculation it is necessary to specify the prompt neutron generation time ℓ, which we set equal to 10^{-7} sec, the core density, the equation of state parameters Q^* and $(\gamma-1)$, the initial reactivity, and which Model, a or c, is to be used for the surface movement approximation. Upon examination of the power distributions of Tables VIII and XI, we see that the power shape at any core-reflector interface has about the same character as it would have for an ordinary spherical core, i.e., it decreases as the surface is approached from the core side, and the slope is comparable to that which occurs at the surface of a spherical core. Therefore the considerations of surface treatment discussed in Chapter II and Appendix C apply as well here and for such surfaces we prefer Model c. At the surfaces between the fuel regions I and II of Configuration A and the low density region III there is negligible restraint to surface movement, so there we use Model a, the free surface approximation; similarly, for the boundary between Regions I and II in Configuration B. In Configuration A there are also the boundaries between the two core regions I and II. These we treat by the free surface approximation, Model a.*

---

*It is an interesting point that this is a good approximation. Because most of the reactivity and most of the mass in the two regions is due to the uranium, the contribution to the rate of reactivity reduction from a thin layer of material bracketing the interface is just proportional to the total momentum of the layer, and independent of how much of the momentum is from material in one region or the other. But this net momentum is calculated correctly if one simply assumes the free surface approximation for each region separately. When one region is treated,

The discussion of the treatment of surface movement is actually not of critical importance for the two configurations being analyzed here. We find that the surface movement contributes a negligible fraction of the reactivity decrease. When all the surfaces are treated by the more conservative Model c, we obtain a negligible difference in the energy release. However, this may not always be true, and one should check each particular problem so that, if the surface movement is important, he will know to what extent the approximations influence the results.

TREATMENT OF MATERIAL MIXTURES

In all of the calculations of the preceding sections, we were dealing with an idealized system in which the core was composed of pure uranium. Now for the first time we are considering a real system in which the core is composed of a mixture of materials. The fuel alloy itself in the Fermi Reactor is an alloy of uranium and molybdenum, rather than pure uranium. (Few reactors use pure uranium as a fuel.)* However, for our purpose, which is to study the effects of non-uniform fuel distribution and non-spherical configurations, we avoid the issue of the differences between pure uranium and a uranium-molybdenum alloy and treat the fuel as pure uranium.

---

the surface is calculated to be moving to the left; and when the other region is treated, the surface is calculated to be moving to the right. When the reactivity effect for the two regions is added, the net effect from the nearly discontinuous pressure drop across the interface is correctly calculated.

*See also the discussion on page 159.

In our studies, once the power distribution $N(\underline{r})$ and reactivity worth distribution $D(\underline{r})$ are specified, the core material plays the role of an inert hydrodynamic fluid. Its only properties of interest are its density and equation of state.* It is only in the estimate of the equation of state that we treat the fuel alloy as pure uranium. This is believed to be a reasonable approximation.**

It is not difficult to account for the presence of the other materials, which neither generate a significant amount of heat nor absorb a significant amount of heat from the fuel because of the short time duration of the power excursion. They do, however, add inertia to the core and occupy space in it. The result is that we now must consider three different material densities, the density that enters Eq. (6), the density for Eq. (8), and the density for Eq. (54). The density for Eq. (6), the hydrodynamic equation expressing essentially the force balance, is clearly just the total homogenized density of all the core materials since it represents the inertia effect. The density for Eq. (8), the equation of state is

$$\rho_{(8)} = \frac{v_u \rho_u}{1 - v_0} \quad , \tag{58}$$

where ρ_u is the density of uranium, 18.7 gm/cc, v_u is the fraction

---

*Thus U^{238} and U^{235} are very nearly identical in this analysis.

**See also the discussion on page 159

of the volume occupied by uranium (or, because we are treating the U-Mo alloy as pure uranium, we take v_u to be the fraction of the volume occupied by $U^{235} + U^{238} + Mo.$), and v_0 is the volume fraction of all other materials. Thus, the fuel is restricted to occupy a volume which is less than the total core volume, and for this reason a given energy generation causes a higher pressure than would be produced if the other materials were absent. We neglect the fact that the other materials will be compressed, to some extent, into a smaller volume when the uranium pressure becomes large.

Finally, the density for Eq. (54), the expression for the total energy generated, is clearly

$$\rho_{(54)} = v_u \rho_u \ , \tag{59}$$

where again v_u is the volume fraction of the $U^{235} + U^{238} + Mo.$

First consider Region II of Configuration A. Using the data of Table VII, we obtain:

$$\rho_{(6)} \approx 14 \text{ gm/cc} \ ;$$

$$\rho_{(8)} \approx 17 \text{ gm/cc} \ ;$$

$$\rho_{(54)} \approx 13.6 \text{ gm/cc} \ .$$

The quantity $\rho_{(8)} = 17$ gm/cc happens to be slightly greater than the density of liquid uranium (16.8 gm/cc) at the melting point. Then from our Table A. II in Appendix A we see that the threshold energy for Region II of Configuration A would be essentially zero. The same is

true in Region I of Configuration B. The energy release for such a case is quite small, and to be more conservative, as is appropriate to a safety analysis, we use the equation of state parameters from Table A. II for a density of 15 gm/cc, i.e., $\gamma - 1 = 1.62$ and $Q^* = 0.23 \times 10^{10}$ erg/gm. This corresponds to a situation where there is still about 10% void space mixed with the uranium. It would be somewhat optimistic to assume that the uranium would actually compact to full liquid density in a meltdown accident. Thus, for the equation of state for Region II of Configuration A and Region I of Configuration B, we use

$$\begin{aligned} P &= (1.62)(15)(E - 0.23 \times 10^{10}) \\ &= 24.3(E - 0.23 \times 10^{10}) \ , \end{aligned} \tag{60}$$

where P is expressed in dynes/cm^2 and E is in ergs/gm.

Next consider Region I of Configuration A. Using the same procedure as for Region II, we obtain

$$\rho_{(6)} \approx 7 \text{ gm/cc} \ ;$$

$$\rho_{(8)} \approx 6.7 \text{ gm/cc} ;$$

$$\rho_{(54)} \approx 5.3 \text{ gm/cc} .$$

Then the equation of state from Table A. II and a density 6.7 gm/cc is

$$\begin{aligned} P &= (.71)(6.7)(E - 1.3 \times 10^{10}) \\ &\approx 4.8\,(E - 1.3 \times 10^{10}) \ , \end{aligned}$$

where P is in dynes/cm^2 and E is in ergs/gm.

CALCULATIONS

Now notice that the threshold Q* in Region I of Configuration A is about 6 times as great as that in Region II. Furthermore, Table VIII shows that the maximum power density in Region I is only about 3/5 of that in Region II. Therefore, the threshold equation used to relate pressure to energy predicts that there will be no material movement in Region I until the energy generated exceeds the energy required to produce pressure in Region II by about an order of magnitude. In the calculations it was found that so large an energy was never attained and all of the material movement and associated reactivity effects came from Region II. This is important when we discuss an equivalent spherical model that can predict the energy release quite well.

Using the parameters and the method discussed above with the power and reactivity distributions given in Tables VIII through XII, we have calculated the energy release for Configurations A and B using initial reactivities above prompt critical for Phase II of 0.001, 0.002, and 0.004. The results are given in Table XIII.

TABLE XIII

ENERGY RELEASE FOR CONFIGURATIONS A AND B

Initial Reactivity ($k-1-\beta$)	Configuration A Energy Release (10^8 joules)	Configuration B Energy Release (10^8 joules)
0.001	4.3	5.8
0.002	6.6	8.8
0.004	13.1	17.0

AN EQUIVALENT SPHERICAL MODEL

Now it is interesting to try to compare the results of Table XIII with what would be calculated by the M-B-T method for some kind of equivalent spherical model. A possible equivalent model would be one in which all of the materials in Regions I, II and III of Configuration A, or I and II of B, are homogeneously distributed throughout a sphere of equal volume. However, this is also obviously a poor approximation because we have seen in Chapter III that the energy release calculations are quite sensitive to Q^*, the threshold energy, and this procedure would result in a much higher threshold than we have used in the two-dimensional calculations.

A much better spherical model is the following: First consider Configuration A. All of the material in Region II is put into a sphere having the volume of Region II. Region I is ignored for the time being, because it was found to contribute nothing to the reactivity reduction.

However, it does generate heat and, in fact, integration of the power distribution of Table VIII gives the result that 63% of the power is generated in Region I. The total energy release is then the energy calculated for Region II divided by the ratio of energy generated in Region II to the total energy, i.e. 1/0.37.

With the spherical model specified, we use the data of Tables IX and XII in the following way: We assume parabolic distributions for the power and reactivity which have about the same maximum and average as the distributions of Tables IX and XII. Thus we take for the power distribution

$$N(r) = 1 - 0.5\,\frac{r^2}{a^2}$$

and for the reactivity distribution

$$D(r) = 1.69 \times 10^{-5}\left(1 - 0.5\,\frac{r^2}{a^2}\right)$$

The volume of Region II is 30.5 liters so the equivalent spherical radius a is 19.4 cm. The parameter d for Eq. (25) in the Bethe-Tait calculation is:

$$d = 1.69 \times 10^{-5} \quad .$$

Table XIV summarizes the parameters for the equivalent spherical calculation for Configuration A.

TABLE XIV

PARAMETERS FOR M-B-T CALCULATION OF CONFIGURATION A

q	(Eq. (24))	0.5
d	(Eq. (25))	1.69×10^{-5}
a	(sphere radius)	19.4 cm
ρ	(density)	15 gm/cc
(γ-1)	(Eq. (17))	1.6
Q*	(Eq. (17))	0.23×10^{10} erg/gm
l	(prompt neutron generation time)	10^{-7} sec

By similar considerations we obtain the parameters for a spherical model for Configuration B.

TABLE XV

PARAMETERS FOR M-B-T CALCULATION OF CONFIGURATION B

q	(Eq. (24))	0.5
d	(Eq. (25))	8.6×10^{-6} cm^{-3}
a	(sphere radius)	30 cm
ρ	(density)	15 gm/cm^3
(γ-1)	(Eq. (17))	1.6
Q*	(Eq. (17))	0.23×10^{10} erg/gm
l	(prompt neutron generation time)	10^{-7} sec

It might at first sight appear that we have to do the two-dimensional energy release calculation first in order to obtain the information for our equivalent spherical model. This is of course not true. The only two-dimensional information we are using is the power and reactivity distributions, which are input to the energy release calculation and can be obtained for example from a two-dimensional multigroup diffusion theory calculation. In many cases it may even be possible first to postulate the spherical model and then also calculate the power and reactivity distributions in spherical geometry,although this is less reliable.

Using the parameters from Tables XIV and XV and the results given in Figure 1, we have calculated the energy release by the M-B-T method. The calculations are summarized in Tables XVI and XVII.

TABLE XVI

SUMMARY OF M-B-T CALCULATION FOR CONFIGURATION A

$k_1-1-\beta$	0.001	0.002	0.004
x	0.0058	0.046	0.37
y	1.35	2.45	5.4
Q(10^{10} erg/gm)	0.54	0.79	1.48
Energy Release for Region II (10^8 joules)	1.6	2.3	4.3
Total Energy Release (10^8 joules)	4.2	6.2	11.6
Energy Release From Table XIII (10^8 joules)	4.3	6.6	13.1

TABLE XVII

SUMMARY OF M-B-T CALCULATION FOR CONFIGURATION B

$k_1-1-\beta$	0.001	0.002	0.004
x	0.0074	0.059	0.47
y	1.45	2.7	6.0
Q(10^{10} erg/gm)	0.56	0.85	1.61
Total Energy Release (10^8 joules)	6.1	9.3	17.6
Energy Release From Table XIII (10^8 joules)	5.8	8.8	17.0

The parameter x is calculated from Eq. (3). Then y is read from Figure 1. Q is calculated from y by Eq. (31). The total energy for the region treated in the calculation is found from Eq. (54). Then as explained above, the total energy for both Regions I and II in Configuration A is obtained by multiplying by the ratio (1/0.37) of total energy to energy in Region II as calculated from the power distribution of Table VIII. In Configuration B there was only one fuel region.

The last two rows in Tables XVI and XVII give a comparison of results for the two-dimensional and spherical calculations. They show that we have had striking success in estimating the energy release for the very complicated two-dimensional situations by the simple spherical model. It seems likely that a satisfactory spherical model can be found for most situations that might be encountered, but perhaps not in every

case. If the power distributions and reactivity distributions are known for the two-dimensional configuration as was the case here, then one can be fairly confident about choosing the spherical model. If they are not known, then there is always the possibility that the unknown distributions have some unusual character, and there would be some doubt about the results.

It is also interesting to compare the results obtained here with those of Chapter IV for homogeneous spheres of density ~ 7.5 gm/cc. Those cases correspond to cores which were also originally similar to the Fermi Reactor core but which collapsed only slightly and uniformly. If we choose for comparison, cases from Table II which produced approximately the same value of the maximum reactivity attained above prompt critical $(k_1-1-\beta)$, we see that the energy release was ~ 3 times greater in the uniform spheres than in the cases treated in this chapter.

The two configurations, A and B, were quite drastic departures from the normal reactor core geometry, and yet we found that the power distribution and reactivity worth distribution followed one another rather closely. As long as this happens and as long as there are no really strange effects which we have not been able to imagine, it seems likely that any rearrangement of the fuel in a fast reactor from its normal uniform distribution will result in an energy release (for a given initial reactivity) that is either about the same as or, as happened here, less

than that which would be calculated for the original uniform distribution. If some significant fraction of the core material, e.g. 10 percent or more, collects into a compact nearly full density arrangement, then, as we found for Configuration A, both the power density and reactivity worth concentrate in that region. Because the high density implies a low threshold energy, this type of a configuration gives low energy release. However, we cannot quite conclude definitely that there is no rearrangement of fuel which would give a larger energy release. One possibility which can be imagined (although we do not see how it could actually arise) is a spherical core with a spherical hole in the center. Our methods would predict that such a configuration gives about the same energy as a sphere with no hole in it. But because of the large displacements of material into the hole, it is not clear that our methods are applicable. A very highly refined technique would be required to calculate the reactivity effects with confidence in such a case.

APPENDIX A

EQUATION OF STATE

The pressure of the material in the core of a reactor during the power excursion resulting from a hypothetical core meltdown accident is a function of the composition, density, and temperature of the material. The relationship among these quantities is called the equation of state. In our work what is actually needed is a relation between the pressure and the energy content,for particular compositions and densities. We have generally referred to this relation also as the equation of state, and clearly either of these "equations of state" can be obtained from the other if in addition the heat capacity relating energy to temperature is known. The basis of the equation of state used in the calculations of the main body of the dissertation is given in this appendix.

One of the topics under investigation is the influence on the energy release calculation, of the general form of the equation of state. Most fast reactor explosion studies[1, 14-17] have utilized a threshold type of equation of state, Eq. (17), in which the pressure is assumed to be zero until the energy density exceeds a given threshold energy Q^*. In reality there must always be some pressure (equal to the saturated vapor pressure) even at energies below

threshold. We should like to determine under what conditions it is permissible to neglect the pressure which actually exists before the energy exceeds Q^*, and how much error is introduced when this pressure below threshold is neglected. Therefore, in addition to presenting the basis for the usual threshold equation that we use in the calculations of Chapters III and IV, we also develop a slightly modified vapor pressure equation for Chapters IV and V and compare it to the threshold equation for a uranium density of 7.5 gm/cc.

In order to make sensible comparisons between the calculations for the threshold model and some model in which the pressure approaches zero asymptotically, it is necessary that the two models be consistent with one another in some sense. As a basis for consistency we have required that the models give very nearly the same pressure for energies equal to or greater than $1.5Q^*$. In addition, for the comparison to be sensible, the vapor pressure model should give pressures at energies below Q^* which are approximately correct. By making a slight alteration of the parameters in the standard formula for saturated vapor pressure we have been able to meet these requirements satisfactorily. What is important is that we have a reasonable general form for the expression and consistency with the threshold model. Whether or not the expression is quantitatively accurate is of secondary importance.

THE PRESENT STATE OF KNOWLEDGE

A considerable amount of theoretical work has been done on the equation of state of uranium for the range of temperature and density of interest to reactor explosion studies.[26, 45, 46] In this range there are almost no experimental data, the Los Alamos data all being at very high density or at temperature orders of magnitude higher than the highest temperatures of interest in this work. Before actually selecting parameters for Eqs. (17) and (47) we review the status of the knowledge about the true equation of state of uranium. This should give the reader some feeling for the sources of uncertainty in the parameters we choose (even though the uncertainties are not of great importance to this dissertation). Also, it should become evident that further research is required in this area before one can hope to calculate explosive energy release with high accuracy.

There is some information available relating to the equation of state. The saturated vapor pressure is known at temperatures not far above the melting point.[47] This is valuable information because within the saturation region, experience with other materials has shown that a simple two parameter formula will often give the vapor pressure accurately all the way from the melting point to the critical point.[48] The other piece of data that is well known is the heat capacity of liquid uranium just above the melting point.[49] This is not so helpful because it may change by as much as $\pm$ 50% at higher temperatures.

Finally, the pressure-temperature relation is known for uranium at the density of the solid state up to temperatures of about 5000°K.[46] From this meager data on uranium, and general knowledge about the behavior of gases and liquids, we must construct an equation of state covering the temperature range from the melting point and up to ~ 30,000°K and densities from the density of liquid uranium at the melting point down to ~ 1/2 that density or less.

At temperatures below the critical point and at low densities the saturated vapor pressure curve combined with some estimate of the heat capacity will serve our purposes. At temperatures above the critical point two basic approaches[26,45] have been used to estimate the equation of state for uranium. One is to assume that it obeys a Van der Waals equation and the other that it obeys the law of corresponding states, so that the empirical data on other materials can be applied. Robert D. Cowan[46] gave a brief review of two attempts at estimating the equation of state by these two methods. He says:

> "In much of the pressure-density range of interest, uranium doubtless exists as a mixture of liquid and vapor phases; the critical values (V_C, T_C, and P_C) are therefore of great interest. Brout[26] assumed Elrod's[45] estimated value T_C = 14,000°K = 1.206 volts, and used the empirical facts that for most substances V_C/V_{solid} = 3.11 and P_CV_C/RT_C = 0.3, thereby obtaining V_C = 40 cc/mol and P_C = 8650 atm. = .0088 Mb. He then simply made use of average empirical data for various inorganic and organic gases[30] expressed in terms of the reduced variables V^* = 0.6 and 0.8 and $T^* > 1$.
>
> Stratton[45] kept Brout's values T_C = 1.206V and V_C = 40 cc/mol but used in place of empirical data the van der Waal's equation

$$P^* = \frac{8T^*}{3V^*-1} - \frac{3}{V^{*2}} \qquad (1)$$

for which $P_cV_c/RT_c = 3/8 = 0.375$. He therefore had to use a critical pressure 25% greater than Brout's value: $P_c = 10,800$ atm = 0.0110 Mb. In the two-phase region the van der Waals equation is inadequate, and Stratton used the empirical vapor-pressure relation[47]

$$\log_{10} P = -0.292 - \frac{2.010}{T} \qquad (2)$$

where P is in Mb and T in volts. Although (2) is presumably valid only for low T (the experimental range is $T < 0.15$ volts), by a strange coincidence it gives at T_c precisely Stratton's value $P_c = 0.0110$ Mb; thus it can be used throughout the two-phase region without arithmetical inconsistency. The boundaries of the two-phase region (i.e. the saturated liquid and saturated vapor curves) are thus given by the intersections of (2) with the negative slope (on a PV plot) portions of (1).

"There are evidently appreciable differences between Brout's and Stratton's equations of state—a 25 percent difference in P_c for example. At first thought one might be inclined to favor Brout's, since it is based on empirical data whereas Stratton's is purely hypothetical. However, Brout was extrapolating to higher temperatures by more than a factor ten. Moreover, he was trying to obtain an equation of state for a metal from those for non-metals, and it is by no means certain that these are identical. (The author was unable to find any critical point data on metals such as sodium or mercury with which to make comparisons.) Hence the uncertainties in both Brout's and Stratton's results are probably as great as the differences between them, and there is probably not really any impelling reason for choosing one over the other.

"There is an obvious source of error in both equations of state, and that is the omission of any contribution of ionization to the pressure, energy, etc. For the materials (CO_2, NH_3, CH_4 etc.) on which Brout based his calculations, T_c is so low that ionization is negligible even for $T^* = 3$ or 4; but for uranium, $T_c = 1.2$ volts and ionization effects are very likely significant, if not at T_c then certainly at 3 or 4 times higher temperatures. Indeed, the calculations to be made below show that the electron pressure at the critical point may be more than twice Brout's value; thus Stratton's value of P_c may well be more accurate than Brout's."

Cowan investigated the contribution of electron pressure to the equation of state of uranium. As indicated above in his review of the previous work on the equation of state of uranium, Dr. Cowan's work has shown that at temperatures above the critical point, the electron pressure may be appreciable. His calculations[46] are subject to several simplifying assumptions which could introduce errors and in fact it does not seem likely that accurate theoretical calculations can be made with the available basic data.

In this dissertation the effects of ionization are ignored. It seems clear, however, that if one needs accurate estimates for explosive energy release then ionization must be considered. The situation is helped some by the fact that we require an equation of state relating pressure to energy density rather than to temperature. Ignoring ionization tends to cause an underestimate of the pressure at a given temperature. This is due to the fact that the ionization effectively increases the number of moles of "gas" contained in the given volume. However, the total internal energy of the system is also approximately proportional to the number of moles of "gas." For an ideal gas, these two effects cancel one another and give the result that the pressure is determined by the total energy contained in a given volume and for that amount of energy it is independent of the number of moles. Therefore, to a first approximation, the ionization does not affect the pressure-energy relationship.

Normally, a certain amount of energy is required to create an ion pair in a gas. However, Cowan[46] points out that at the densities we are concerned with, i.e. ~ half the normal liquid density, and greater, uranium, being a metal, is already ionized even at zero temperature. Therefore, no additional internal energy is required to produce the free electrons.

Our uranium-electron gas is not at all an ideal gas, because of the high density. However, we have examined Cowan's calculations[46] and find that for a given total energy, the calculated pressure is approximately the same, whether the electron contribution is included or not. We have therefore chosen to use Brout's[26] estimates without including the effects of ionization, and we believe that the inclusion of such refinements can not be justified until additional experimental information becomes available.

Ionization may be of some importance to an evaluation of the damage potential of a nuclear explosion of given energy release. Thus, if the expansion process is sufficiently rapid to leave the gas in an ionized condition when it is fully expanded, then the work available to do damage is reduced by the amount of energy corresponding to the ionization energy. This, however, is not pertinent to the present subject.

THRESHOLD EQUATION OF STATE

Once ionization has been ignored, then there is a choice between

using Brout's[26] or Stratton's[45] equation of state or developing a new one. As Cowan has said in the above review there is probably no impelling reason for choosing one over the other. Also, it appears that until some further experimental data becomes available there is no advantage to be gained from developing a new one. Therefore, as recommended by H. A. Bethe,[51] the author has elected to use what is basically the calculations of R. H. Brout.[26] Table A. I summarizes the equation of state for two particular values of the specific volume as taken from Brout's Tables VIII and IX.

TABLE A. I

BROUT'S CALCULATED EQUATION OF STATE

Density = 7.44 gm/cc			Density = 9.92 gm/cc		
T*	P*	E/RT_C	T*	P*	E/RT_C
0.99		2.7	0.96		2.0
1.10	1.85	2.95	1.05	2.0	2.1
1.23	3.0	3.25	1.11	3.0	2.2
1.50	5.0	3.95	1.21	5.0	2.5
1.76	7.0	4.5	1.33	7.0	2.8
2.3	10.0	5.35	1.6	10.0	3.4
2.9	15.0	6.3	1.9	15.0	4.0
3.4	20.0	7.1	2.4	20.0	5.0

Note:

$T = 14,000\ T^*$ (degrees Kelvin)
$P = 8,650\ P^*$ (atmospheres)
$T_C = 14,000$ K
R = gas constant

In the calculations of the energy release done in Chapters III and VI, an equation of state of the form

$$P = (\gamma - 1)\rho(E - Q^*) \qquad (A.1)$$

is required, where $(\gamma-1)$ and Q^* are parameters which can be chosen to fit the Brout calculated points. Rather than making some type of "best fit" to the points we have elected to draw a straight line which is slightly on the conservative side, i.e., which on the average gives less pressure for a given energy release than the Brout calculation and, therefore, will result in a slightly larger calculated energy release. A comparison between the straight line approximation and the calculated points is given in Figure A.1.

The Brout calculations were for uranium having a density of either 7.44 or 9.92 gm/cc, i.e., normal density uranium (18.75 gm/cc) mixed with 60% void and 47% void respectively. More dense configurations are also of interest in reactor meltdown accident studies and so it is necessary to have an estimate of the equation of state for the higher densities. An attempt was made to repeat the Brout calculations at higher densities. However, it was found that at high densities, the method involves the subtraction of numbers which are nearly equal and therefore does not yield reliable results.

The method used for very high desnities is based upon the fact that very little pressure is produced until there has been sufficient thermal expansion of the liquid uranium to fill the void spaces. Then

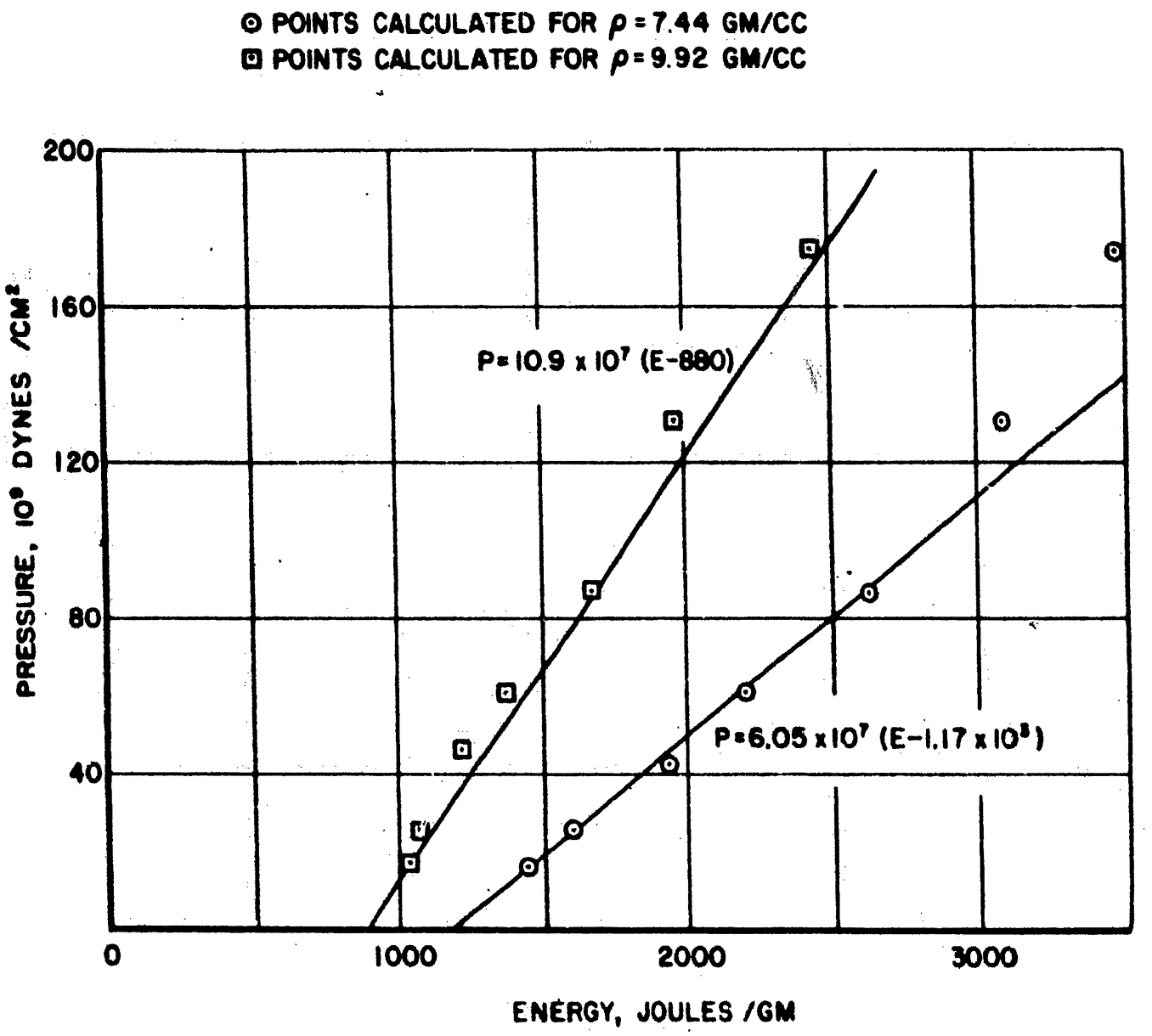

FIG. A.1 COMPARISON OF CALCULATED EQUATION OF STATE AND THRESHOLD EQUATION

the pressure increases approximately linearly with energy according to the relation[52]

$$\left(\frac{\partial P}{\partial E}\right)_V = \frac{1}{2\alpha T}\left\{-1+\sqrt{1+\frac{4c^2\alpha^2 T}{C_V}}\right\}, \qquad (A.2)$$

where α is the coefficient of thermal expansion and c is the velocity of sound.

For the fully dense liquid at 1500 degrees Kelvin, and using the value of c for mercury (it is not known for liquid uraniun), Downs[52] estimated $\left(\frac{\partial P}{\partial E}\right)_V = 1.13$. He used $C_V = 14 \times 10^5$ erg/gram°K and $\alpha = 8 \times 10^{-5} \cdot K^{-1}$. It is quite possible that c for uranium is higher, the value for solid uranium being 3×10^5 cm/sec.[59] If c were taken equal to 2×10^5 cm/sec for the liquid, Eq. (A. 2)would give $\left(\frac{\partial P}{\partial E}\right)_V = 2$. Thus, since c is not known for liquid uranium, estimation of $\left(\frac{\partial P}{\partial E}\right)_V$ from Eq.(A. 2) is somewhat risky, the error in $\left(\frac{\partial P}{\partial E}\right)_V$ being nearly proportional to the error in c^2.

In Reference 46, Figure 1, Cowan gives experimental results on the pressure as a function of temperature for uranium at the density of the solid state that are valid at relatively low temperatures, i.e., $T < 100°C$. The P-T relationship up to a temperature of 0.1 ev is nearly a straight line with an average slope $\left(\frac{\partial P}{\partial T}\right)_V = 0.84$, where P is in megabars and T is in volts. The slope then decreases and the average up to a temperature of 0.5 volts is $\left(\frac{\partial P}{\partial T}\right)_V = 0.7$. Cowan also

did some high temperature theoretical calculations by the Thomas-Fermi-Dirac model. The theoretical and experimental curves did not meet smoothly, and so in the intermediate temperature range Cowan fared in a smooth curve which approaches the experimental curve at low temperature and the theoretical curve at high temperature. The quantity $\left(\frac{\partial P}{\partial T}\right)_V$ can be converted to $\left(\frac{\partial P}{\partial E}\right)_V$ by dividing the specific heat:

$$\left(\frac{\partial P}{\partial E}\right)_V = \frac{1}{C_V}\left(\frac{\partial P}{\partial T}\right)_V . \qquad (A.3)$$

Now there has been considerable disagreement about the average C_V for uranium. The value just above the melting point is known[49] to be 9 cal/gm mole. Brout[26] argues that it should quickly drop with increasing temperature to about 6 cal/gm mole and then decrease further. Stratton[45] has assumed it is constant at 9 cal/gm mole. Some recent calculations[53] seem to indicate that it may even increase slightly with temperature. If the value 6 cal/gm mole is selected then $\frac{1}{\rho}\left(\frac{\partial P}{\partial E}\right)_V$ would be 3.2. A specific heat of 9 cal/gm mole gives 2.1. Cowans interpolated P-T curve with the higher specific heat gives 1.4. It appears that there is no way of accurately pinning down the value of $\frac{1}{\rho}\left(\frac{\partial P}{\partial E}\right)_V$ with existing experimental information. We select the value

$$\frac{1}{\rho}\left(\frac{\partial P}{\partial E}\right)_V = 2 \qquad (A.4)$$

for uranium at the normal density of the solid state.

We do no calculations at quite so high a density. The accidents

are always assumed to have come from meltdown of a reactor core so the highest density of interest is the density of the liquid at the melting point. That is approximately 16.8 gm/cm^3. To obtain values for $\gamma-1$ at intermediate densities between the solid density and the densities of the Brout calculations we assume that $\gamma-1$ is a linear function of the density. Q^* is taken to be zero for the density of the liquid at the melting point and a linear function of the density for densities intermediate between the melting point density and the density of the Brout calculations. This at least assures that our results are a smooth function of the density. It has been found in the calculations that the results are not very sensitive to $\gamma-1$ but are quite dependent upon the value of Q^*.

Table A.II summarizes the values of $\gamma-1$ and Q^* that are used in the calculations.

TABLE A.II

EQUATION OF STATE OF URANIUM

ρ gm/cm^3	$\gamma-1$	$Q^*(10^{10}$ erg/gm)
7.5	0.82	1.16
8.3	0.93	1.03
10	1.11	0.87
12.5	1.37	0.55
15	1.62	0.23
16.8	1.80	0
18.7	2	-

One must remember that the values of Q* listed in Table A. II are predicated upon the assumption that the liquid is initially at its normal melting point. If calculations are to be performed starting with the fuel at some other temperature, then the value of Q* must be adjusted to account for the difference in heat content between that temperature and the normal melting point.

The parameters in Table A. II for the threshold type equation of state have been chosen in such a way that the pressure is approximately correct when the energy density is appreciably above the threshold Q* . For energy densities very near Q* the equation underestimates the pressure and for energies less than Q* it is completely meaningless. In calculations using this equation the pressure is set identically equal to zero until the energy exceeds Q*. It is easy to see the qualitative nature of the error which is introduced by using an equation of state of this form. If it is used in a calculation which gives an energy release a few times larger than Q*, then the approximation is quite good. But if it is used in a calculation in which the energy release is calculated to be only a little larger than Q*, the energy may be greatly overestimated. In fact, no matter how weak the accident is, this equation of state will always yield an energy release at least equal to Q* since it is the pressure which disassembles the core and stops the power generation.

SATURATED VAPOR PRESSURE

Previously, no one has investigated quantitatively how much error may be introduced in the calculated energy release due to the neglect of pressure which exists prior to Q^* . To do this, we must perform the calculations with an equation of state which follows the threshold equation fairly closely for $E > Q^*$ but then comes into zero asymptotically as the energy goes to zero. Also, we would like the equation to be a good approximation to the actual behavior of uranium, or the comparison would be rather meaningless. A simple physical picture of the threshold energy, which is most sensible in fairly high density situations, helps to point out a reasonable form for the equation of state we are seeking. We start with liquid uranium just above the melting point and interspersed uniformly with void spaces. As the temperature rises the liquid expands, partially filling the internal voids. As the temperature increases further the voids are finally completely filled by the expanded liquid and then the pressure begins to rise. The threshold energy is essentially the energy required to produce the amount of thermal expansion of the liquid to fill the voids. The main effect we are neglecting is the saturated vapor pressure which exists even below the threshold.

A standard form for the saturated vapor pressure is[48]

$$P = Be^{-\frac{A}{T}} \qquad (A.5)$$

where A and B are constants. Experimentally it has been observed[48]

that many substances have a vapor pressure which follows this expression over many decades of pressure, all the way from the melting point to near the critical pressure. From measurements at very low pressure the constants have been determined[47] for uranium to be

$$B = 53,700°K \ ;$$

$$A = 5 \times 10^{5} \text{ Atm.}$$

What we need of course is an expression relating pressure to energy rather than to temperature. As mentioned earlier, the specific heat of uranium is not known as a function of temperature, so we have to choose values arbitrarily. Under these conditions there is no longer any reason to precisely preserve the values of the constants A and B. What we have done is to assume that the specific heat is a constant and pick a value for it and values for B and A such that our pressure curve passes through the normal boiling point and then follows our straight line threshold equation of state for a density of 7.5 gm/cc from $E = 1.5\ Q^*$ to $E = 6\ Q^*$. The comparison is shown in Figure A.2. The exponential form follows the straight line within 5% over this range. We believe that this procedure produces an exponential curve which departs from the straight line at low energy in a way which makes some physical sense. It clearly still contains some arbitrariness but that cannot be avoided since the true equation of state just is not known. Our final expression which is used in the calculations is:

$$P = 7.6 \times 10^{11} \exp\left[\frac{5880}{150 + E}\right] \text{dynes/cm}^2;\ E \text{ in joules/gm.} \quad (A.6)$$

The total amount of adjustment of the constants A and B to force the curve to follow the threshold equation was not great. Table A. III compares the altered P-T curve to the original one for selected points between the atmospheric boiling point and a temperature of 10,000°K, which corresponds to an energy near Q*. The specific heat used was 6.06 cal/gm. Others[54] have previously proposed a similar alteration of the vapor pressure curve to force it to pass through the predicted critical point.

TABLE A. III

COMPARISON OF EXPERIMENTAL AND ALTERED SATURATION CURVES

T(Kelvin)	P_a (atm)	P_b (atm)
4,080	0.98	0.98
5,000	10.7	11.8
6,000	63.	75
7,000	230.	280
8,000	600.	750
10,000	2300.	3000

Note: P_a is the experimental pressure extrapolated from low pressure. P_b is our curve with the constants A and B in Eq. (A.5) altered—see the text above.

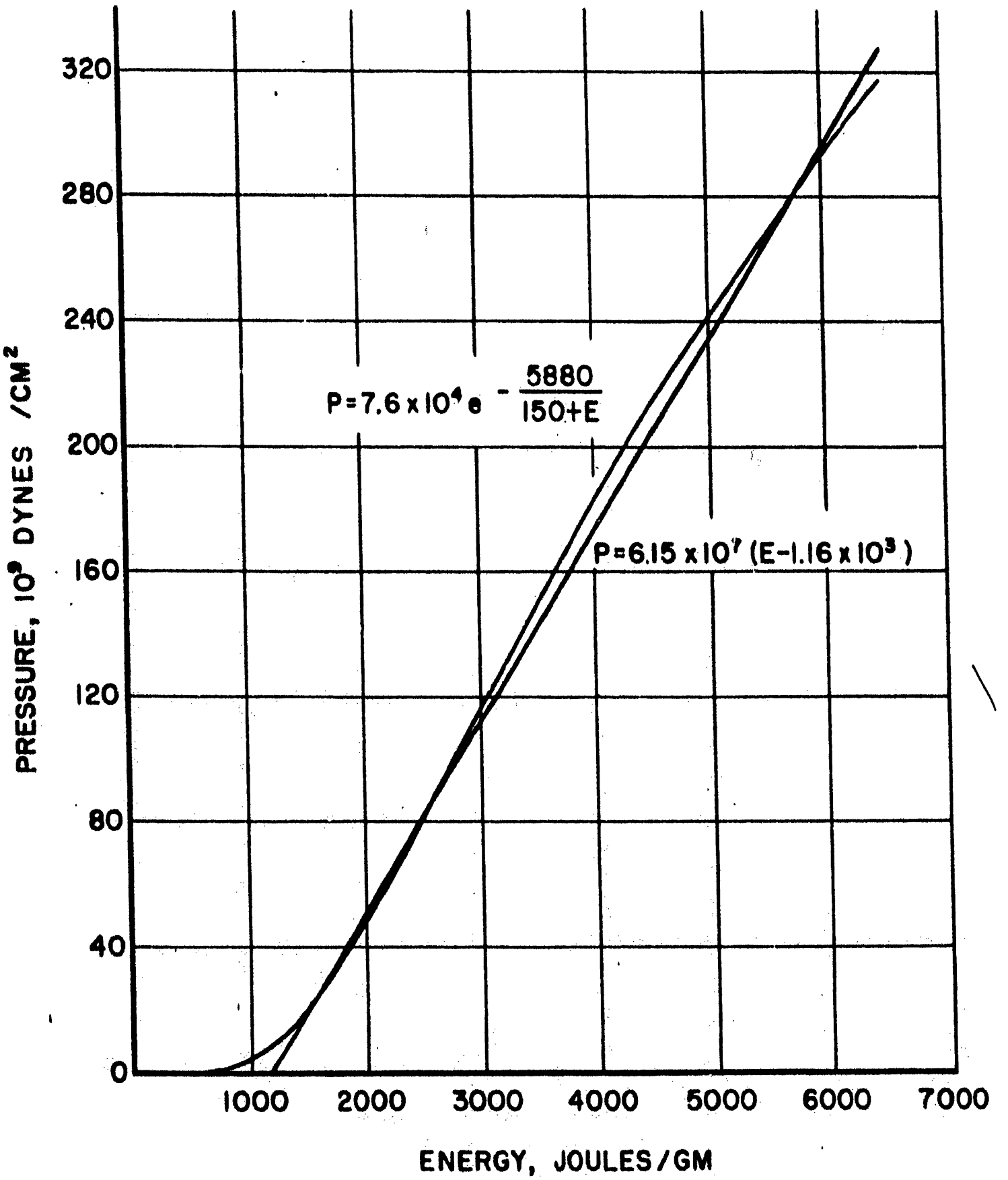

FIG. A.2 A COMPARISON OF TWO EQUATIONS OF STATE

APPENDIX B

MATERIAL MOVEMENT AND DENSITY CHANGES

A major assumption upon which all of our work has been based is that during the power excursion the pressure at a given point in the core is independent of the density changes which occur due to material movement; hence the pressure is specified entirely by the initial material density and the energy density at that point. The reason that this is expected to be a good approximation is that the total amount of uniform expansion which would be required to terminate an excursion is of the order 1 to 2 percent or less for most accidents which are studied. For the most severe case, only about 4 percent uniform expansion is required. However, under the explosive conditions encountered, the expansion is sometimes quite non-uniform, and we must investigate the possibility that substantially larger density changes would occur in some parts of the core. In this Appendix we calculate the material movement and density changes in two of the cases presented in Chapter IV, a fairly mild case initiated by a reactivity insertion rate $\alpha = 0.06\ \text{sec}^{-1}$ and the most severe case studied, $\alpha = 6.4\ \text{sec}^{-1}$. It is shown that it is a good approximation to neglect the effect of density changes on pressure for the cases studied.

Equation (6) becomes, for spherical symmetry

$$\frac{d^2 u(r,t)}{dt^2} = -\frac{1}{\rho}\frac{dP(r,t)}{dr} \quad . \tag{B.1}$$

The initial conditions are

$$u(r,0) = 0 \quad , \quad \frac{du(r,0)}{dt} = 0 \quad . \tag{B.2}$$

The continuity equation relates the density to the displacement:

$$\frac{\partial \rho(r,t)}{\partial t} = -\operatorname{div}\left(\rho \frac{du(r,t)}{dt}\right) \quad . \tag{B.3}$$

In our spherically symmetric geometry, Eq. (B.3) reduces to

$$\frac{\partial \rho(r,t)}{\partial t} = -\frac{1}{r^2}\frac{d}{dr} r^2 \rho \frac{du(r,t)}{dt} \quad . \tag{B.4}$$

This can be differentiated with respect to time and combined with Eq. (B.1) to give

$$\frac{\partial^2 \rho(r,t)}{\partial t^2} = +\frac{1}{r^2}\frac{d}{dr} r^2 \frac{dP(r,t)}{dr} \quad . \tag{B.5}$$

In the time differentiation the term involving $\frac{\partial \rho}{\partial t}$ on the right hand side was neglected as second order.

We take the form for the pressure that was used in Chapter V:

$$P = Be^{\frac{-A}{E(r,t) + E_0}} \quad , \tag{B.6}$$

where

$$E(r) = Q(t) \cdot N(r) \quad ; \tag{B.7}$$

then

$$\frac{dP}{dr} = \frac{ABQ(t)}{[E(r,t) + E_0]^2} e^{\frac{-A}{E(r,t) + E_0}} \frac{dN(r)}{dr} \quad . \tag{B.8}$$

Our calculations in this Appendix are limited to parabolic power distributions:

$$N(r) = 1 - q\frac{r^2}{a^2} \quad , \tag{B.9}$$

$$\frac{dN(r)}{dr} = -\frac{2qr}{a^2} \quad . \tag{B.10}$$

Equation (B.10) is substituted into Eq. (B.8) to give

$$\frac{dP}{dr} = -\frac{2ABqQ(t)}{a^2}\,\frac{re^{-\frac{A}{E(r,t)+E_0}}}{[E(r,t)+E_0]^2} \quad , \tag{B.11}$$

and then Eq. (B.11) is combined with Eq. (B.1):

$$\frac{d^2u(r,t)}{dt^2} = \frac{2ABq}{\rho a^2}\,Q(t)\,\frac{re^{-\frac{A}{E(r,t)+E_0}}}{[E(r,t)+E_0]^2} \quad . \tag{B.12}$$

The computer program written for the method of Chapter V calculates $Q(t)$. Thus every factor on the right hand side of Eq. (B.12) is known, and the displacement u at any position r can be obtained by integrating twice with respect to time. It is immediately evident from the form of Eq. (B.12) that the displacement is proportional to r for small r, since $N(r)$ is constant for small r. Then, if the exponential factor is strong enough, the displacement passes through a maximum at some point and decreases towards the edge of the core.

The change in density with time has quite a different behavior. To obtain the density from Eq. (B.5) we need

$$-\frac{1}{r^2}\frac{d}{dr}r^2\frac{dP(r,t)}{dr} = -\frac{2ABqQ(t)}{r^2a^2}\frac{d}{dr}\frac{r^3e^{-\frac{A}{E(r,t)+E_0}}}{(E(r,t)+E_0)^2} \quad . \tag{B.13}$$

When the indicated differentiation is performed the result is

$$\frac{d^2\rho}{dt^2} = -\frac{6ABqQ(t)}{a^2}\,\frac{e^{\dfrac{-A}{E_0 + E(r,t)}}}{(E(r,t) + E_0)^2}\left\{1 + \right.$$

$$\left. -\frac{2}{3}\,\frac{E(r,t)\,q}{[E(r,t) + E_0]^2}\,\frac{r^2}{a^2}\left[\frac{A}{E(r,t) + E_0} - 2\right]\right\} . \qquad (B.14)$$

It can be seen that this gives rise to a density which is a minimum at $r = 0$, increases to a maximum which can be higher than the initial density at some position, and then decreases again toward the edge of the core.

We are also interested in determining the position at which material motion has the greatest effect on the reactivity reduction. Referring to Eq. (45) we see that this will be at about the position where $r^2 \frac{dP}{dr}$ is a maximum. That is not quite correct because the expression also contains $\frac{dD(r)}{dr}$. Referring to Table D. I, we see that $\frac{dD(r)}{dr}$ does not vary a great deal over most of the range for a typical fast reactor core, and we ignore its variation. The maximum occurs where

$$\frac{d}{dr} r^2 \frac{dP}{dr} = 0 . \qquad (B.15)$$

We have already done this differentiation to obtain Eq. (B.14) and see that the position of the maximum is given by the solution of

$$1 - \frac{2}{3}\,\frac{E(r,t)\,q}{[E(r,t) + E_0]}\,\frac{r^2}{a^2}\left[\frac{A}{E(r,t)} - 2\right] = 0 . \qquad (B.16)$$

This equation does not necessarily have a solution, i.e., the expression $r^2 \frac{dP}{dr}$ could increase monotonically between $r = 0$ and $r = a$. That is actually the case for a sufficiently large value of $Q(t)$.

DENSITY CHANGES

Consider first the density changes predicted by Eq. (B.14) for two cases which have been calculated, one a moderate power excursion produced by a reactivity insertion rate of 0.06 sec^{-1} and the other a strong one from a 6.4 sec^{-1} reactivity insertion rate. The excursions were calculated by a digital computer using the method of Chapter IV. The calculated value of Q as a function of t is presented in Table B.I. The time scale has arbitrarily been shifted so that the first entry in the table is at $t = 0$. Also included is an $\alpha = 1.9$ sec^{-1} case to be used in Appendix C.

TABLE B.I

THREE SELECTED POWER EXCURSIONS

1. $\alpha = 0.06$ sec^{-1} - $Q_{final} = 1.0 \times 10^4$ joules/cm^3

t (μ-sec)	0	40	80	120	160	200	240
Q (10^4 joules/cm^3)	0.31	0.37	0.45	0.53	0.64	0.75	0.86

2. $\alpha = 1.9$ sec^{-1} - $Q_{final} = 3.7 \times 10^4$ joules/cm^3

t (μ-sec)	0	8	16	24	32	40
Q (10^4 joules/cm^3)	1.20	1.52	1.92	2.40	2.90	3.33

3. $\alpha = 6.4$ sec^{-1} - $Q_{final} = 8.4 \times 10^4$ joules/cm^3

t (μ-sec)	0	6	12	18	24	30	36
Q (10^4 joules/cm^3)	1.51	2.22	2.97	4.08	5.40	6.70	7.68

The other quantities required for the calculation of density ρ from Eq. (B. 14) are given in Table B. II.

TABLE B. II

CONSTANTS FOR DENSITY CALCULATION

$A = 4.41 \times 10^{4}$ joules/cm^{3}

$B = 4.6 \times 10^{11}$ dynes/cm^{2}

$q = 0.6$

$a = 40$ cm

$E_0 = 1120$ joules/cm^{3}

Equation (B. 14) is easily integrated numerically. The results are shown in Figure B. 1 where the ratio of density at time t to initial density (7.5 gm/cc) is plotted as a function of the ratio of energy $Q(t)$ to the final asymptotic energy release Q_{final}. This is more meaningful than a plot versus time, since it shows explicitly how much of the energy release comes after there has been any given density change. Thus in the $\alpha = 0.06$ sec^{-1} case shown in Figure B. 1, it can be seen that 90 percent of the energy has been generated before the density at the center has decreased 3. 3 percent. In the $\alpha = 6.4$ sec^{-1} case shown in Figure B. 2, 90% of the energy has been generated before the density at the center has decreased 5%. At all other locations the change in density is less. At the position $r/a = 3/4$, the case shown in Figure B. 2 gives a slight increase in

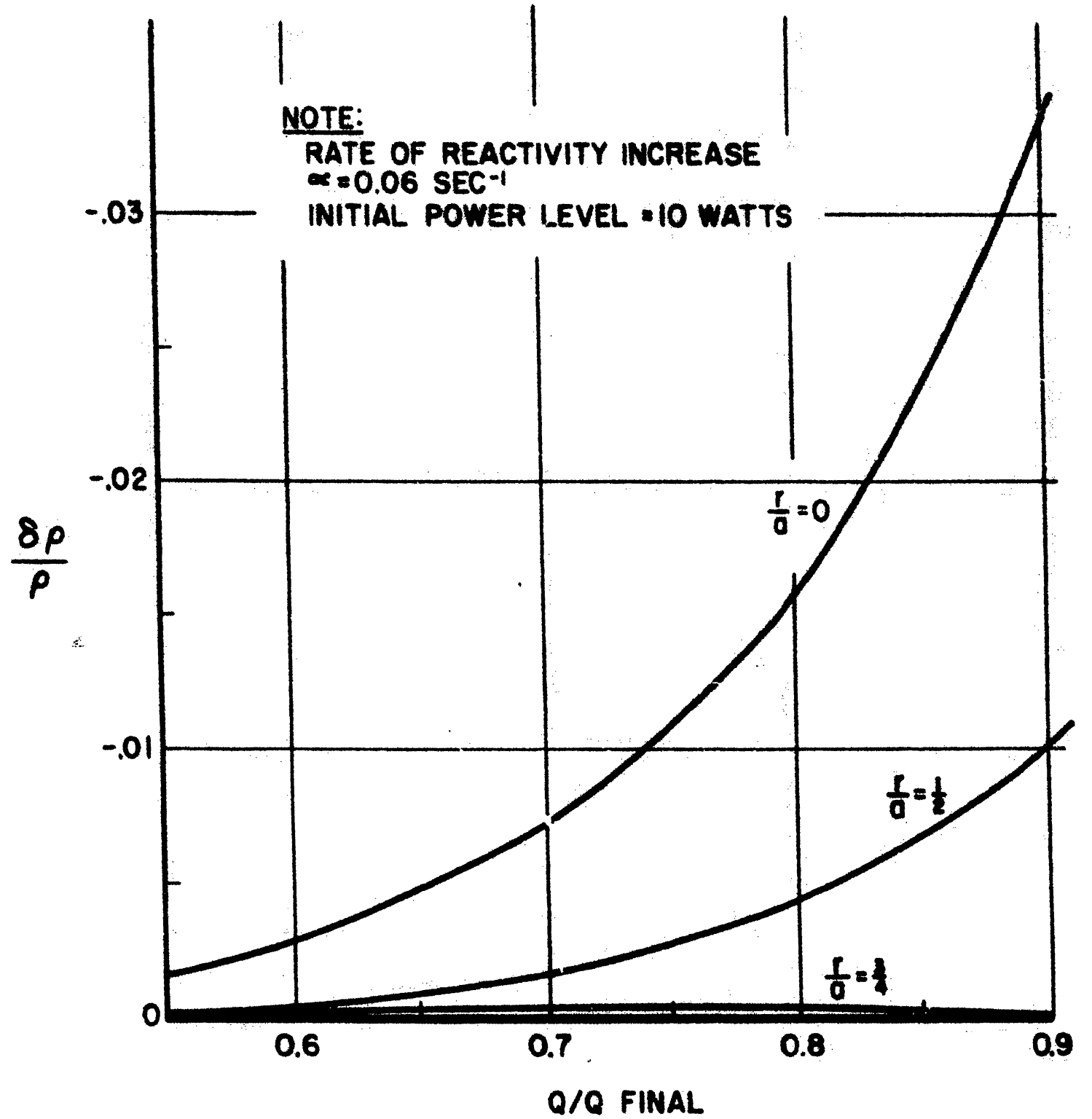

FIG. B.1 DENSITY CHANGES DURING A WEAK POWER EXCURSION

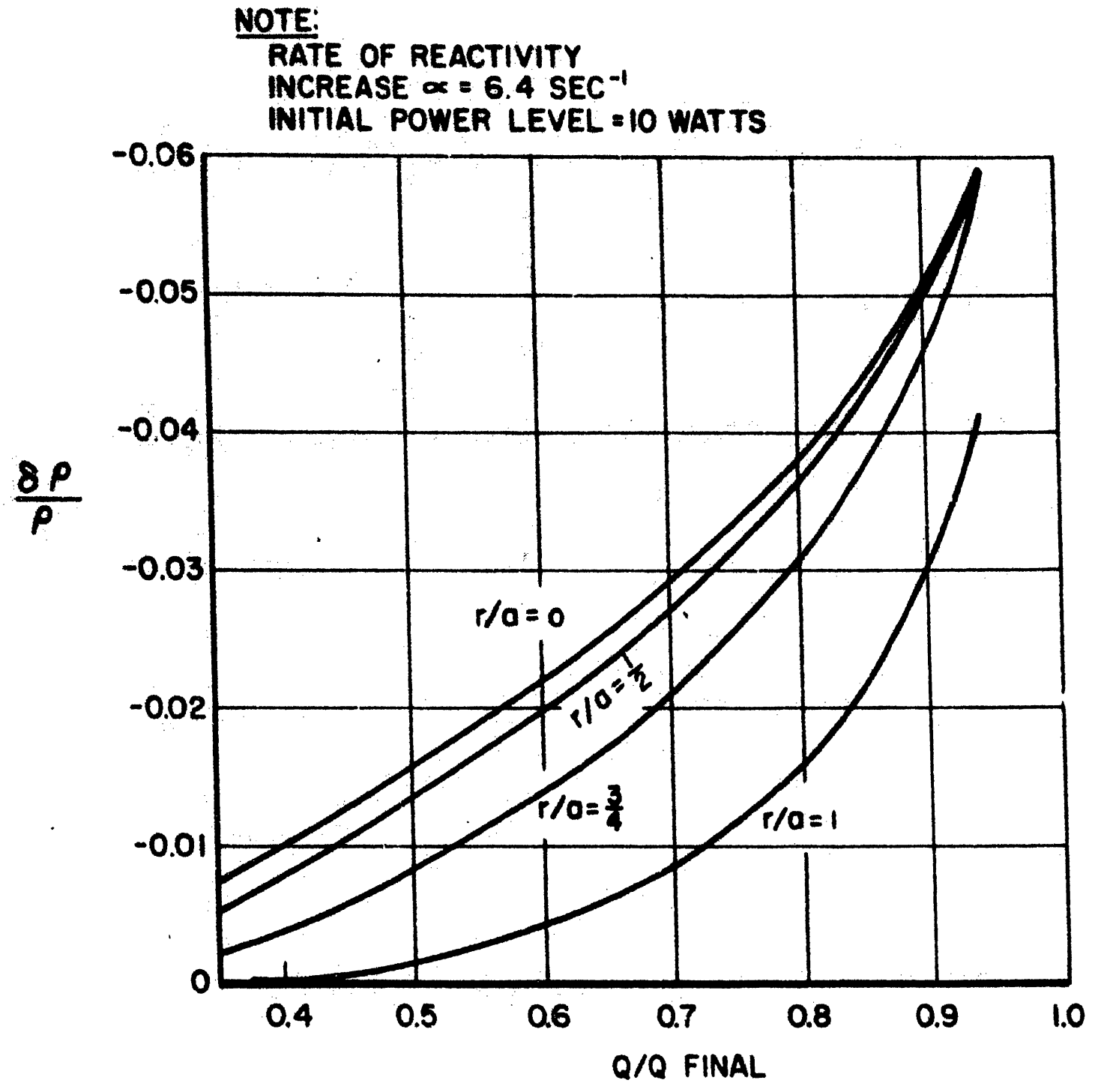

FIG. B.2 DENSITY CHANGES DURING A STRONG POWER EXCURSION

density near the end of the power excursion but the change is too small to be seen on the graph.

PRESSURE CHANGES

What is the significance of these density changes? Clearly they are small enough so that the perturbation theory used to calculate reactivity changes is accurate. How about the validity of the assumption that pressure is unaffected by the change in density? For the particular cases calculated the assumption is quite accurate.

For sufficiently small density changes, the relationship between density and pressure can be written:

$$\frac{dP}{P} = \gamma \frac{d\rho}{\rho} \qquad (B.17)$$

or

$$\frac{P}{P_0} = \left(\frac{\rho}{\rho_0} \right)^{\gamma} \qquad (B.18)$$

In explosion analysis the density changes are too rapid for heat transfer to occur, so the expansions are adiabatic. In the ideal gas approximation, the quantity γ is the ratio of specific heats, 1.67 for a monatomic gas and 1.4 for a diatomic gas. Our gas is not by any means ideal, but the effective value* of γ is not a great deal larger than 1.67. Brout[26] has calculated adiabats for expanding uranium vapor and examination of his work indicates that $\gamma_{eff} = 3$ is a reasonable approximation for a

---

*We define the effective value of γ by Eq. (B.17), i.e. $\gamma_{eff} = \frac{\rho}{P} \frac{dP}{d\rho}$.

uranium density of 7.5 gm/cc; and for $\rho = 10$ gm/cc $\gamma_{eff} \approx 4$. Thus, in the most severe case studied the error in the pressure at the core center due to ignoring the effect of density changes is always less than about 15 percent until after the excursion is 90 percent complete. By direct calculation, we have found that an error in pressure of this magnitude throughout the entire core and for the entire power excursion makes an error of about 7 percent in the calculated energy release. However, the error in pressure is not so great over the entire core, and for the entire power excursion. In the most severe case, shown in Figure B. 2, it appears that we should consider on the average a density reduction of $\sim 2\%$ and hence an error in pressure of $\sim 6\%$, and an error in energy release of $\sim$ 3%. In all our other calculations, with the exception of those in Chapter VI where higher fuel densities are used, the error in pressure and in the calculated energy release is even less. The higher density cases are examined next.

PRESSURE CHANGES FOR THE HIGH DENSITY SYSTEM

While our work is mainly intended to apply to situations in which the uranium density is not too high, i.e. 10 gm/cc and less, we have included some calculations in Chapter VI for a core having a density of 15 gm/cc. Brout did not calculate the adiabats for systems having a density greater than 10 gm/cc. However, we can calculate the change in pressure for an adiabatic expansion from the pressure-density-energy relationship, Eq. (17), which has been used to approximate the true

behavior:

$$P = (\gamma-1)\rho(E-Q^*) \quad . \tag{B.19}$$

The quantities $(\gamma-1)$ and Q^* depend upon the density ρ . They have been estimatec and con be found in Appendix A.

We differentiate the pressure with respect to density

$$\frac{dP}{d\rho} = \frac{\partial P}{\partial \rho} + \frac{\partial P}{\partial(\gamma-1)} \cdot \frac{d(\gamma-1)}{d\rho} + \frac{\partial P}{\partial Q^*} \frac{dQ^*}{d\rho} + \frac{\partial P}{\partial E} \frac{dE}{d\rho} \tag{B.20}$$

The individual contributions are easily obtained from Eq. (B.19):

$$\frac{\partial P}{\partial \rho} = (\gamma-1)(E-Q^*) = \frac{P}{\rho} \quad ; \tag{B.21}$$

$$\frac{\partial P}{\partial(\gamma-1)} = \rho(E-Q^*) = \frac{P}{\gamma-1} \quad ; \tag{B.22}$$

$$\frac{\partial P}{\partial Q^*} = -(\gamma-1)\rho = -\frac{P}{(E-Q^*)} \quad ; \tag{B.23}$$

$$\frac{\partial P}{\partial E} = (\gamma-1)\rho = \frac{P}{(E-Q^*)} \quad . \tag{B.24}$$

In preparing Table A. II we assumed that $(\gamma-1)$ and Q^* were linear functions of the density for densities greater than 10 gm/cm^3. Then we obtain directly from Table A. II

$$\frac{d(\gamma-1)}{d\rho} = \frac{2 -).11}{18.7 - 10} = 0.1 \text{ cm}^3/\text{gm} \quad ; \tag{B.25}$$

and

$$\frac{dQ^*}{d\rho} = \frac{0 - .87 \times 10^{10}}{16.8 - 10} = -0.13 \times 10^{10} \text{ cm}^5/\text{gm sec}^2 \; . \tag{B.26}$$

Finally, from the first law of thermodynamics, we have, for an adiabatic expansion,

$$\frac{dE}{d\rho} = -\frac{1}{\rho^2}\frac{dE}{dV} = \frac{P}{\rho^2} \quad . \tag{B.27}$$

Now we insert Eqs. (B.21)-(B.27) into Eq. (B.20), multiply by ρ, and divide by P, and obtain

$$\gamma_{eff} = \frac{\rho}{P}\frac{dP}{d\rho} = \gamma + \frac{0.1\rho}{\gamma-1} + \frac{0.13\times 10^{10}\rho}{E - Q^*} \quad , \tag{B.28}$$

where ρ is expressed in gm/cm^3 and $E - Q^*$ is in erg/gm. Thus we see that our pressure-density-energy relation leads to an expression similar to Eq. (B.17) for an ideal gas, except that there are two extra terms and the γ in Eq. (B.28) is larger than that for an ideal gas. The second term on the right hand side, $\frac{0.1\rho}{\gamma-1}$, can be seen from Table A.II to be nearly independent of ρ and equal to ~ 0.9. The last term on the right is not so well behaved. It diverges as $E \to Q^*$. This is of course not a real effect and is due to our choosing a threshold equation for the pressure, when there really is no threshold. However, the formula does make good sense as long as E is $\sim 2Q^*$ or greater. We have calculated $\frac{\rho}{P}\frac{dP}{d\rho}$ as a function of density ρ and energy E from Eq. (B.28) and displayed the results in Table B.III. The parameters $(\gamma-1)$ and Q^* are taken from Table A.II.

Notice in Table B.III that the values of $\frac{\rho}{P}\frac{dP}{d\rho}$ for 10 gm/cm^3 are larger than 4, the value quoted above as calculated from Brout's adiabats. The high values, as we have mentioned already, are due to the fictitious threshold. The high values near threshold for the higher densities, e.g., 15 gm/cc, are more realistic, since the threshold model

TABLE B. III

$\frac{\rho}{P}\frac{dP}{d\rho}$ FROM THE THRESHOLD EQUATION

$(10^{10}$ E erg/gm)	ρ (gm/cc)			
	10	12.5	15	16.8
0.4	--	--	14.5	8.8
0.8	--	9.5	6.4	5.7
1.2	6.9	5.5	5.0	4.8
1.6	4.8	4.5	4.4	4.4
2.0	4.2	4.1	4.1	4.1
2.4	3.9	3.9	3.9	3.9

is a better approximation at high density. But the important point to be made about Table B. III is that the values of $\frac{\rho}{P}\frac{dP}{d\rho}$ are not excessively large even at high density, as long as the energy density is at least about 0.3×10^{10} erg/gm or more above the threshold.

Consider the problems treated in Chapter VI, which involved a uranium density of 15 gm/cc. The final energy density Q at the core center is given for those problems in Table XVI . It varied from 0.54×10^{10} erg/gm to 1.61×10^{10} erg/gm depending upon the initial reactivity assumed. The density decrease at the core center was comparable in these calculations to the density decrease shown in Figures B. 1 and B. 2, i. e., $\sim$ 4% at the time the energy generation is 90% complete. Thus, referring to Table B. II, we see that the

pressure at the core center has actually decreased due to expansion by a factor of about $(1.04)^{10} \approx 1.5$ for the weakest excursion treated; and by a factor of about $(1.04)^{4.4} \approx 1.2$ for the strongest explosion. At earlier times the error in pressure is always less than this.

We can determine an upper limit to the error produced in the calculated energy release due to this error in the pressure by assuming as before that the pressure is in error by these amounts throughout the entire core for the entire power excursion. This is equivalent to reducing $(\gamma-1)$ by that factor. The parameter x of Eq. (30) is inversely proportional to $(\gamma-1)$. Therefore, referring to Figure 1 and Table XVI we find that the value of y for the weakest excursion treated might be increased from 1.35 up to 1.5, giving an increase in Q of ~6%. For the strongest excursion y would be increased from 5.4 to 5.9, which corresponds to an increase in Q of ~7%. But here again the pressure is not in error by so large an amount over the entire core for the entire power excursion, and we estimate that the actual error in the energy release calculation is ~ 3%.

THE POSITION OF MAXIMUM REACTIVITY REDUCTION

In Figures B.1 and B.2 we showed that the density reduction due to material displacement during the power excursion is mainly confined to a region near the core center, for weak excursions, and is fairly

uniform for the strongest explosion studied, but even in that case the density reduction is greatest at the core center. Thus the errors in pressure at points away from the core center are less than those calculated above for the central position. We now show that most of the reactivity reduction comes from material movement at positions $r/a > \frac{1}{2}$, so that at least in the weaker excursions the error in pressure at the core center is of little consequence to the energy release calculation.

In Table B. IV we have shown the approximate spatial distribution of the integrand of d^2k/dt^2, Eq. (45), as calculated from $r^2 \frac{dP}{dr}$, Eq. (B.11) multiplied by r^2. We have tabulated this quantity at four selected time points spanning the power excursion, and it can be seen that for the $\alpha = 0.06$ sec^{-1} case the integrand peaks for all these times in the neighborhood of $r/a = 5/8$ to $3/4$. Also, we see that the contribution from all points inside the region $r/a < \frac{1}{2}$ is only about 15 percent of the total. Thus even if the pressure were substantially in error at the core center, that error would not have a major influence on the energy release calculation.

Table (B. IV) also shows the spatial distribution of the reactivity feedback for the $\alpha = 6.4$ sec^{-1} case. There the distribution is shifted farther outward yet, and is, in fact, maximum at the outer edge of the core. This again helps in justifying the neglect of density decrease, which is maximum at the core center. However, it is not so helpful

TABLE B. IV

DISTRIBUTION* OF THE REACTIVITY FEEDBACK AS CALCULATED FROM EQUATION (B. 11) TIMES r^2

$\alpha = 0.06\ \text{sec}^{-1}$ case

Q/Q_{final}	position (r/a)					
	0	1/4	1/2	5/8	3/4	7/8
0.46	0	0.2	0.89	1.0	0.70	0.27
0.56	0	0.16	0.86	1.0	0.82	0.36
0.66	0	0.14	0.82	1.0	0.91	0.48
0.78	0	0.12	0.74	1.0	1.3	0.86

$\alpha = 6.4\ \text{sec}^{-1}$ case

Q/Q_{final}	position (r/a)					
	0	1/2	5/8	3/4	7/8	1
0.44	0	0.12	0.25	0.46	0.74	1.0
0.54	0	0.10	0.21	0.39	0.68	1.0
0.65	0	0.08	0.17	0.33	0.62	1.0
0.75	0	0.07	0.15	0.31	0.57	1.0

*arbitrarily normalized

in the more severe accidents, since there is also some appreciable density reduction at positions well away from the center as shown in Figure B. 2. However, it raises the new question of whether or not the conditions at the core surface might become very important for the more severe accidents. One might think that the results would depend strongly upon whether the core were immediately

surrounded by a reflector or if instead there were a small gap between core and reflector, thus allowing the surface to move freely. This question is studied in some detail in Appendix C. We show that the results are not greatly sensitive to the conditions at the core surface.

To summarize the results of this appendix, we have found that the assumption that the pressure is independent of the small expansion which occurs to terminate the power excursion, is a completely satisfactory one for a determination of the total energy release, for all of the cases treated. The error introduced by this approximation is about 3% or less. The pressure at the core center may be overestimated by as much as a factor 1.5 for the weaker excursions studied having a uranium density of 15 gm/cm^3. At the lower density of 7.5 gm/cm^3 the pressure is in error by at most 15% at the core center. These errors occur when the energy generation is 90% complete, and are less at earlier times. They are also less at points away from the core center. While the error in pressure at the core center is sometimes large, it results in a much smaller error in the energy release, which is estimated to be $\sim$ 3% or less in all cases studied.

APPENDIX C

MATERIAL MOTION NEAR THE CORE SURFACE

In Table B. IV of Appendix B it was shown that for severe accidents a large fraction of the reactivity feedback is contributed by material within several centimeters of the edge of the core. Then we need to ask how important is the nature of the restraint imposed at the surface? Will the movement of material interior to the surface be substantially different for a free surface from what it would be if the surface pushes against a reflector? We have found that for typical fast power reactor reflectors, or blankets as they are usually called, the results are not strongly sensitive to the nature of the reflector.

SURFACE MOTION IN CHAPTER IV

Before setting up a simple model to investigate the differences between various assumptions on the surface boundary condition, it is instructive to see how much movement occurs near the surface as calculated by the method which was selected for approximating the boundary effect in the calculations of Chapter IV. Recall that in this method we have in a sense ignored the surface by assuming the pressure gradient to be continuous across the surface. We have calculated the material movement for the two cases presented in Table B.I of Appendix B labeled $\alpha = 1.92$ sec^{-1} and $\alpha = 6.4$ sec^{-1}.

The displacement u of an element of material from its initial position is obtained by integrating Eq. (B. 12) twice with respect to time, using the values of Q(t) from Table B. I and the constants from Table B. II. This has been done for an element of material at the core surface and the results are shown in Table C. I where the displacement is tabulated as a function of the ratio of energy generated Q(t) to the final asymptotic value of the energy. There it can be seen that at the time the energy generation is 90 percent complete, the displacement of material at the surface is calculated to be 5 mm for the $\alpha = 6.4\ \text{sec}^{-1}$ case and only 1.8 mm for the $\alpha = 1.92\ \text{sec}^{-1}$ case. For less severe accidents the material at the surface scarcely moves at all until after the power excursion has been terminated.

The calculated surface movement is impressively small. One should keep in mind that this work is aimed at predicting the results of a reactor accident which is usually assumed to be initiated by core meltdown, which is inherently a rather disorderly process. Even if there were a fairly massive blanket surrounding the core there probably would not be a sharply defined boundary separating the melting core and the blanket, and probably the blanket would not really offer much restraint to the movement until the displacements become larger than the values we are calculating here. However, it is shown below that the material displacement at the surface which would be predicted by a free surface assumption is several times greater, and so in reality the reflector would be expected to offer some restraint.

TABLE C. I

DISPLACEMENT NEAR THE CORE SURFACE

$\alpha = 6.4\ \text{sec}^{-1}$ case		$\alpha = 1.92\ \text{sec}^{-1}$ case	
Q/Q_{final}	u(cm)	Q/Q_{final}	u(cm)
0.44	0.037	0.46	0.004
0.54	0.08	0.58	0.016
0.65	0.15	0.70	0.05
0.75	0.25	0.78	0.08
0.84	0.39	0.83	0.12
0.92	0.56	0.89	0.18

We have therefore carried out a calculation of the motion of material near a core-reflector interface in the acoustic approximation, including the effect of the inertial restraint offered by the reflector. We also calculate the surface motion for a free surface (Model a) and for our fictitious Model c which simply ignores the existence of the surface.

A SIMPLE MODEL WITH THE ACOUSTIC APPROXIMATION

In order to work with a simple problem which can be treated analytically, we replace the spherical core-reflector interface by an infinite plane boundary and the core region by a semi-infinite region of material having the same properties as the core. The reflector is then simulated by a homogeneous slab of thickness a. This type of model can of course be a good representation only within a few centimeters distance from the boundary, and then only if the distribution of material displacement achieves its asymptotic value within that distance, i.e., if the distance that a pressure signal can propagate in the time available

is a few centimeters or less. It will be shown that this is the case and that the geometrical model chosen is therefore a reasonable one. If this were not true the spherical geometry would influence the results, and the problem could not be studied in one dimension.

The pressure can be separated into two parts:

$$P(x, t) = P_V(x, t) + \Pi(x, t) \quad , \qquad (C.1)$$

where P_V is the pressure which would exist if there were no material movement, i.e., the constant volume pressure build-up due to a given energy input. Then Π is the difference between the actual pressure P and P_V, and represents the acoustic excess pressure which is related to the adiabatic compressibility $1/\rho c^2$ * by

$$\Pi(x, t) = -\rho c^2 \frac{\partial u(x, t)}{\partial x} \quad , \qquad (C.2)$$

where ρ and c are the density and acoustic velocity (assumed to be constant). Actually the compressibility may change appreciably as the material is heated, so this is a fairly crude approximation. However, we are only seeking a qualitative result, and believe that the approximation is suitable for this purpose. This belief is supported by showing that the main result is not sensitive to the value of c.

The constant volume pressure $P_V(r, t)$ is directly determined by

---

*The quantity $\frac{\partial u(x, t)}{\partial x}$ is the fractional amount of expansion (or compression if it is negative) of an element of material at position x and time t. The acoustic velocity c is defined by[56] $c = \sqrt{1/\rho\kappa}$ where κ is the adiabatic compressibility. Therefore, ρc^2 is $1/\kappa$ and Π is the pressure difference due to the fractional expansion $\partial u/\partial x$.

the energy generation $E(r,t)$. The relationship we have used to connect the two for this analysis is Eq. (47). With the constants from Table B. II and the calculated $Q(t)$ from the case labeled $\alpha = 1.92\ \text{sec}^{-1}$ in Table B. I we have calculated $P_V(r,t)$ at three points near the edge of the core. The values are given in Table C. II.

TABLE C. II

$P_V(r,t)$ IN KILOBARS FOR THE $\alpha = 1.92\ \text{sec}^{-1}$ CASE

	r(cm)		
t (μ-sec)	34.4	37.2	40.0
0	2.6	1.25	.45
8	7.5	4.0	1.7
16	18.2	10.6	5.2
24	35.7	23.2	12.5
32	59.3	40.3	23.9

In order to solve the simple problem analytically it is necessary to approximate $P_V(r,t)$ by some simple function which can be used as the inhomogeneous term in the equation of motion. For this purpose we have selected an exponential time dependence and a linear space dependence

$$P_V(r,t) \approx K\left(1 - \frac{X}{L}\right)e^{\lambda t} \quad . \tag{C.3}$$

Choosing values to fit the data of Table C. I we find

$$P_V(r,t) = 0.6\left(1 - \frac{X}{3}\right)e^{1.1 \times 10^5 t} \tag{C.4}$$

where

t is in seconds

P_V is in kilobars

x is the distance (negative) from the edge of the core in cm, i.e., $x = r - 40$

Comparison of Eq. (C. 3) with Table C. II shows that it gives a good qualitative representation of the pressure as a function of space and time.

The hydrodynamic equation of motion in the acoustic approximation[55] is simply

$$\frac{\partial^2 u(x,t)}{\partial t^2} = -\frac{1}{\rho}\frac{\partial P(x,t)}{\partial x} \quad . \tag{C.5}$$

When Eqs. (C. 1), (C. 2) and (C. 3) are substituted into Eq. (C. 5) the result is

$$\frac{\partial^2 u_1(x,t)}{\partial x^2} - \frac{1}{c_1^2}\frac{\partial^2 u_1(x,t)}{\partial t^2} + \frac{Ke^{\lambda t}}{L\rho_1 c_1^2} = 0 \quad , \tag{C.6}$$

where the subscript 1 has been introduced to indicate the core region. In the reflector P_V is assumed to be zero, and so the corresponding equation for the reflector is

$$\frac{\partial^2 u_2(x,t)}{\partial x^2} - \frac{1}{c_2^2}\frac{\partial^2 u_2(x,t)}{\partial t^2} = 0 \tag{C.7}$$

The boundary conditions at the interface between core and reflector are continuity of total pressure P and continuity of displacement:

$$\begin{aligned} P_V(0,t) + \Pi_1(0,t) &= \Pi_2(0,t) \quad ; \\ u_1(0,t) &= u_2(0,t) \quad . \end{aligned} \tag{C.8}$$

The boundary condition at the outer surface of the reflector is

$$\Pi_2(a, t) = 0 \quad . \tag{C.9}$$

We shall seek only the asymptotic solutions:

$$u_1(x, t) = f(x)\, e^{\lambda t} \quad . \tag{C.10}$$

Substitution of this into Eq. (C.6) gives an equation in $f(x)$:

$$\frac{\partial^2 f(x)}{\partial x^2} - \frac{\lambda^2}{c_1^2} f(x) = -\frac{K}{L\rho_1 c_1^2} \quad . \tag{C.11}$$

The solution of the homogeneous equation is

$$f_h(x) = e^{\pm \frac{\lambda x}{c_1}} \quad . \tag{C.12}$$

The negative sign in the exponent is excluded because that would give a term which diverges exponentially as $x \to -\infty$. A particular solution is

$$f_p(x) = \frac{K}{L\rho_1 \lambda^2} \quad . \tag{C.13}$$

Therefore, the complete asymptotic solution for the core region is

$$u_1(x, t) = e^{\lambda t}\left(A e^{\frac{\lambda x}{c_1}} + \frac{K}{L\rho_1 \lambda^2}\right) \quad . \tag{C.14}$$

The solution in the reflector is

$$u_2(x, t) = e^{\lambda t}\left(B e^{\frac{\lambda x}{c_2}} + C\, e^{-\frac{\lambda x}{c_2}}\right) \quad . \tag{C.15}$$

The boundary condition (C.9) at $x = a$ gives

$$-\rho_2 c_2^2 \left(\frac{B\lambda}{c_2} e^{\frac{\lambda a}{c_2}} - \frac{C\lambda}{c_2} e^{-\frac{\lambda a}{c_2}}\right) = 0 \quad , \tag{C.16}$$

$$C = B e^{\frac{2\lambda a}{c_2}} \quad ;$$

$$u_2(x,t) = Be^{\lambda t}\left[e^{\frac{\lambda a}{c_2}} + e^{-\frac{\lambda x}{c_2}} e^{\frac{2\lambda a}{c_2}}\right] . \qquad (C.17)$$

From continuity of $u(x,t)$ at $x = 0$ there results

$$B\left[1 + e^{\frac{2\lambda a}{c_2}}\right] = A + \frac{K}{L\rho_1\lambda^2} . \qquad (C.18)$$

From continuity of pressure

$$-\rho_1 c_1^2 \frac{\lambda}{c_1} A + K = -\rho_2 c_2^2 \frac{\lambda B}{c_2}\left[1 - e^{\frac{2\lambda a}{c_2}}\right] . \qquad (C.19)$$

Equations (C.18) and (C.19) can be solved simultaneously to give for A

$$A = \frac{K\left(1 - \frac{\rho_2 c_2 R}{L\rho_1\lambda}\right)}{\rho_1 c_1 \lambda\left(1 + \frac{\rho_2 c_2 R}{\rho_1 c_1}\right)} , \qquad (C.20)$$

where

$$R = \frac{\left[e^{\frac{2\lambda a}{c_2}} - 1\right]}{\left[e^{\frac{2\lambda a}{c_2}} + 1\right]} , \qquad (C.21)$$

contains the effect of reflector thickness. R varies monotonically from 0 to 1 as a goes from 0 to ∞ . Then the complete solution for motion of the core material is

$$u_1(x,t) = \frac{K}{\lambda} e^{\lambda t}\left[\frac{1}{L\rho_1\lambda} + \frac{\left(1 - \frac{\rho_2 c_2 R}{L\rho_1\lambda}\right) e^{\frac{\lambda x}{c_1}}}{\left(1 + \frac{\rho_2 c_2 R}{\rho_1 c_1}\right)\rho_1 c_1}\right] . \qquad (C.22)$$

In the limits $a \to \infty$ and $a \to 0$ this reduces to

$$u_1(x,t) = \frac{Ke^{\lambda t}}{\lambda}\left[\frac{1}{L\rho_1\lambda} + \frac{(1-\frac{\rho_2 c_2}{L\rho_1\lambda})e^{\frac{\lambda x}{c_1}}}{(1+\frac{\rho_2 c_2}{\rho_1 c_1})\rho_1 c_1}\right]; \quad a \to \infty \qquad (C.23)$$

$$u_1(x,t) = \frac{Ke^{\lambda t}}{\lambda}\left[\frac{1}{L\rho_1\lambda} + \frac{e^{\frac{\lambda x}{c_1}}}{\rho_1 c_1}\right] \qquad a \to 0 \ . \qquad (C.24)$$

Equation (C.24) is the approximation of a free surface, Model a, and the first term of Eq. (C.22) corresponds to the approximation of Model c. For a reflector which is sufficiently thin that $\frac{2a\lambda}{c_2} \ll 1$, R can be expanded

$$R \sim \frac{2a\lambda}{c_2} \qquad \frac{2a\lambda}{c_2} \ll 1 \ , \qquad (C.25)$$

and u_1 is, asymptotically,

$$u_1(x,t) \sim \frac{Ke^{\lambda t}}{\lambda}\left[\frac{1}{L\rho_1\lambda} + \frac{(1-\frac{2\rho_2 a}{\rho_1 L})}{(1+\frac{2\rho_2 a\lambda}{\rho_1 c_1})}\frac{e^{\frac{\lambda x}{c_1}}}{\rho_1 c_1}\right] \qquad \frac{2a\lambda}{c_2} \ll 1 . \qquad (C.26)$$

SOME EXAMPLES

Now if the core is in contact with a reflector composed of rods or plates of metal separated by a liquid coolant, and these pieces are relatively thin, i.e., about one cm, and if the pressure wave has time to propagate a few centimeters, then the motion of material in the core would be about the same as if the reflector were a homogeneous mixture having an "average" density and an "average" compressibility. The reflector would normally be of the order of one foot thick, and so, if

λ is large, Eq. (C. 23) for an infinite reflector can be applied.

Alternatively, the core might be in contact with the same reflector but with coolant drained out leaving void spaces. Then the pressure signal would not be easily transmitted into the reflector, and it is better to approximate the reflector by a layer of metal about equal the thickness of a single rod or plate. (Recall that the total movement to terminate the excursion is only about 1/2 cm or less.) In this case Eq. (C. 22) should be used, or (C. 26) if the layer is sufficiently thin.

Some numerical examples are evaluated for illustrative purposes. It should be remembered, however, that wide variations in reflector properties are possible, so that each situation needs to be evaluated separately. The first example is a reflector composed of 50 percent by volume of uranium and 50 percent by volume of liquid sodium. The core is assumed to be composed of uranium gas at a density of 7. 5 gm/cc. The acoustic velocity for the core can be estimated from the expression for an ideal gas[57]

$$c_1 \approx \sqrt{\frac{\gamma P}{\rho}} \qquad \text{(C. 27)}$$

where γ is the usual ratio of specific heats. For an average pressure near the core edge of 10 kilobars the result is $c_1 \approx 4 \times 10^4$ cm/sec. This estimate is apt to be a little low since high density uranium gas is less compressible than an ideal gas. Also note that as the pressure changes by a factor of ten the velocity of sound changes by about a

factor of three so the assumption of a constant value for c_1 is only suitable for a qualitative study of the behavior.

The acoustic velocity in the homogenized blanket is calculated from the formula for liquids and isotropic solids.[56]

$$c_2 = \sqrt{\frac{1}{\rho\kappa}} \qquad (C.28)$$

where κ is the compressibility. For sodium[58] $\kappa \approx 2.5 \times 10^{-11}$ $cm^2/dyne$. For uranium κ is expected* to be about 10^{-12} $cm^2/dyne$, so for the mixture $\kappa \approx 1.3 \times 10^{-11}$ $cm^2/dyne$. The mixed density is 9.7 gm/cc so $c_2 \approx 9 \times 10^4$ cm/sec. These constants can be inserted in Eq. (C.22) and give for an infinite reflector.

$$u_1(x,t) = \frac{Ke^{\lambda t}}{\lambda}\left\{ \frac{1}{2.5\times10^6} + \frac{\left[1 - \frac{(9.7)(9\times10^4)}{2.5\times10^6}\right]}{\left[1 + \frac{(9.7)(9\times10^4)}{3\times10^5}\right]} \frac{e^{2.75x}}{3\times10^5} \right\}$$

$$\approx \frac{Ke^{\lambda t}}{L\rho_1\lambda^2}\left\{ 1 + 1.4\, e^{2.75x} \right\} \qquad \text{(Reflected)}$$

The free surface assumption, Eq. (C.24), gives

$$u_1(x,t) \approx \frac{Ke^{\lambda t}}{L\rho_1\lambda^2}\left\{1 + 8.3e^{2.75x}\right\}; \qquad \text{(Model a)}$$

whereas Model c, which simply drops the second term, gives

$$u_1(x,t) = \frac{Ke^{\lambda t}}{L\rho_1\lambda^2} \qquad \text{(Model c)}$$

For the particular example treated it can be seen that there is a

*This is based upon an acoustic velocity for uranium $c \sim 2\times10^5$ cm/sec.[59]

great difference in the calculated movement of material close to the core surface, depending upon whether the surface is tamped by a reflector or completely free. Our Model c predicts less movement than both the free surface model and the tamped model. It corresponds to a situation in which there is a slightly more effective tamper than was chosen. It is a more conservative model in the sense that it slightly underestimates the reactivity reduction in an excursion, and therefore tends to overestimate the energy release. However, while there is a large difference in the calculated movement close to the surface, the difference is confined to a layer about 1 or 2 cm thick because of the factor $e^{2.75x}$ in the expression for u. All three models agree for points more than 2 cm into the core. We therefore do not expect the surface treatment to have a major influence on the calculated energy release.

The surface movement calculated above was for a particular situation and was based upon an assumed constant value for the acoustic velocity c_1. A value three times greater gives

$$u_1(x,t) = \frac{Ke^{\lambda t}}{L\rho_1\lambda^2}\{1 + .91\, e^{.92x}\} \qquad \text{(Reflected)}$$

$$u_1(x,t) = \frac{Ke^{\lambda t}}{L\rho_1\lambda^2}\{1 + 2.6e^{.92x}\} \qquad \text{(Model a)}$$

$$u_1(x,t) = \frac{Ke^{\lambda t}}{L\rho_1\lambda^2} \qquad \text{(Model c)}$$

In this case there is less discrepancy between the three results close to the surface, but the surface effect propagates farther into the core. The same conclusion is still reached, however. The difference between the three methods applies only to a thin region near the surface and is not expected to have a large effect on the energy release calculation.

For an acoustic velocity three times smaller, i.e., $c_1 = 1.3 \times 10^4$ cm/sec we get

$$u_1 = \frac{Ke^{\lambda t}}{L\rho_1 \lambda^2}\left[1 + 1.65\, e^{8.25x}\right] \qquad \text{(Reflected)}$$

$$u_1 = \frac{Ke^{\lambda t}}{L\rho_1 \lambda^2}\left[1 + 25\, e^{8.25x}\right] \qquad \text{(Model a)}$$

$$u_1 = \frac{Ke^{\lambda t}}{L\rho_1 \lambda^2} \qquad \text{(Model c)}$$

Notice that the lower value of c_1 makes a much larger difference in the displacement at the surface, and the layer thickness becomes correspondingly thinner. It is significant that the difference between displacements calculated from Models a and c, integrated over volume, is exactly the same for all three values of c_1 used above. In Chapter II we argued from basic principles that this would happen and that if the presence of the surface were felt in only a thin layer near the surface, then an approximate treatment could be used for the movement of material near a free surface. Our calculations here show that the approximation is a reasonable one.

We now consider the other example of a reflector mentioned above, one in which it is presumed that the coolant has drained out leaving nothing to transmit the pressure waves into the reflector beyond the first row of rods. This situation is simulated by assuming the reflector to be a layer of solid uranium metal one centimeter thick. The acoustic velocity in solid uranium is $\sim 2 \times 10^5$ cm/sec.[59] Then

$$\frac{2\lambda a}{c_2} \approx 1.1$$

and neither the infinite reflector Eq. (C.23) nor the asymptotically thin approximation Eq. (C.26) is suitable. From Eq. (C.21)

$$R = \frac{e^{1.1} - 1}{e^{1.1} + 1} = 0.5$$

and from Eq. (C.22)

$$u_1(x,t) = \frac{Ke^{\lambda t}}{L\rho_1\lambda^2}\left\{1 + \frac{\left[1 - \frac{(18.7)(2\times10^5)(.5)}{2.5\times10^6}\right]}{\left[1 + \frac{(18.7)(2\times10^5)(.5)}{(7.5)(4\times10^4)}\right]} \frac{e^{2.75x}(1.25\times10^6)}{(7.5)(4\times10^4)}\right\}$$

$$= \frac{Ke^{\lambda t}}{L\rho_1\lambda^2}\{1 + 0.3\, e^{2.75x}\}$$

As in the previous example we again find that the surface movement is not very important. It is interesting that a one centimeter layer of solid metal taken here to simulate the reflector gives more restraint to surface movement than the infinite reflector composed of a mixture of uranium and sodium. This is because the pressure wave did not

really move far enough into the reflector to justify the homogeneous model for the sodium uranium mixture, and we should regard this last calculation as more nearly correct for the sodium uranium mixture also. The homogeneous model would be better for a slower rate of pressure increase, i.e., a smaller value for λ .

These calculations have shown that for the conditions encountered here, the manner in which the surface movement is treated is not terribly important, but also it has been found in the above examples that the method of Model c is conservative; it predicts slightly smaller material movements and hence smaller reactivity feedback than would be calculated from an exact treatment. This is not a completely general result. It can be seen from Eq. (C.22) that a set of parameters ρ_2 , c_2 , L , ρ , λ could be chosen such that the second term becomes negative, and then Model c, which drops that term, predicts more surface movement. This is the case for the weaker accidents because L and λ are smaller. However this is not disturbing because the surface movement is negligible in the weak excursions.

To see directly the difference between the energy release with a free surface and with a reflected surface (approximated by our Model c), we have calculated it with both assumptions in Chapter III, and have compared the results in Figure 1 (of that Chapter). There was no difference for weak and moderate excursions, and a difference of $\sim$ 15% for the most severe case studied.

APPENDIX D

THE REACTOR MODEL

The calculations of Chapter IV and V required a choice of some particular reactor model with which to work. Since we are primarily concerned with studying a method of analysis rather than attempting to do a safety study for some real reactor, it seemed appropriate to choose as simple a model as possible. On the other hand, the main features of the system should bear some resemblence to a real reactor. Since the author is most familiar with the Enrico Fermi Reactor, the reactor model chosen is similar to the Fermi Reactor, but it is a much more simple system. In this appendix we describe the model and make some comparisons to the Fermi Reactor.[60]

The model chosen is a spherical homogeneous reactor, 40 cm in radius and containing only uranium at a density of 7.5 gm/cm^3. In the explosion analysis it is not necessary to specify the uranium enrichment or the nature of the reflector. These characteristics only enter through the influence they have on the power distribution, reactivity worth distribution, and prompt neutron generation time. Instead of calculating these quantities for the specified model, we choose them arbitrarily, emphasizing that our methods give one the freedom of obtaining such quantities in any convenient way such as a multigroup diffusion theory calculation, transport theory calculation, or even from

critical experiment measurements.

For the power distribution, we have used

$$N(r) = 1 - q\frac{r^2}{a^2} , \qquad (D.1)$$

with $q = 0.6$. This is very nearly the distribution calculated for a spherical model of the Fermi Reactor. The power distribution in ERB-II[1] is better fit by equation (D.1) with $q = 0.48$.

In most of our calculations we have also used a parabolic form for the distribution of reactivity worth per unit volume. A parabola is not usually a very good representation for the distribution of reactivity worth. Nevertheless, we have used it because the usual Bethe-Tait calculation involves a parabolic shape for the reactivity worth, and we make comparisons between the results of a modified Bethe-Tait calculation and our method. The calculations require only the gradient of the distribution. In most of the calculations we have used

$$\frac{dD(r)}{dr} = -d\frac{r}{a^2} , \qquad (D.2)$$

with $d = 6.4 \times 10^{-6}$ cm^{-3}. To show how this compares with the distribution in a real fast reactor, we have calculated the distribution for a variation of the Fermi Reactor in which the core was collapsed to a radius of 40.17 cm so that the volume would be about the same as in our model. The calculation was done by first order perturbation theory using the fluxes and adjoints from an AIM multigroup diffusion theory calculation. Table D.I compares the calculated distribution with the integral of our assumed distribution (D.2). The two were set equal at $r = 0$. The

table also compares the power distributions.

Notice that the shape of the assumed parabolic power distribution deviates from the calculated power distribution for the collapsed core of the Fermi Reactor. However, the deviation is rather smooth and the slopes of the two curves never differ by more than about 30%. The parabolic reactivity distribution also follows that for the collapsed core of the Fermi Reactor except near the edge of the core where the slope of the parabola is a maximum whereas the calculated distribution flattens appreciably. The slopes at the core edge differ by a factor of 2.

TABLE D. I

A COMPARISON OF POWER DISTRIBUTIONS AND REACTIVITY WORTH DISTRIBUTIONS

	Power Distributions		Reactivity Worth Distributions $\Delta k/k/cm^3 \times 10^5$	
r/a	Collapsed Fermi Reactor	$1-0.6\frac{r^2}{a^2}$	Collapsed Fermi Reactor	$0.384 - 0.32\frac{r^2}{a^2}$
0	1	1	0.384	0.384
0.094	0.991	0.994	0.379	0.381
0.188	0.970	0.977	0.369	0.372
0.283	0.933	0.950	0.350	0.357
0.377	0.886	0.910	0.326	0.336
0.471	0.826	0.860	0.298	0.309
0.566	0.757	0.797	0.267	0.276
0.659	0.679	0.724	0.233	0.245
0.762	0.590	0.652	0.197	0.198
0.878	0.486	0.539	0.157	0.139
1.000	0.380	0.400	0.121	0.064

To see how important the distribution of reactivity worth is to the energy release calculation, we have compared the results for a parabolic distribution to the results for two other different distributions.

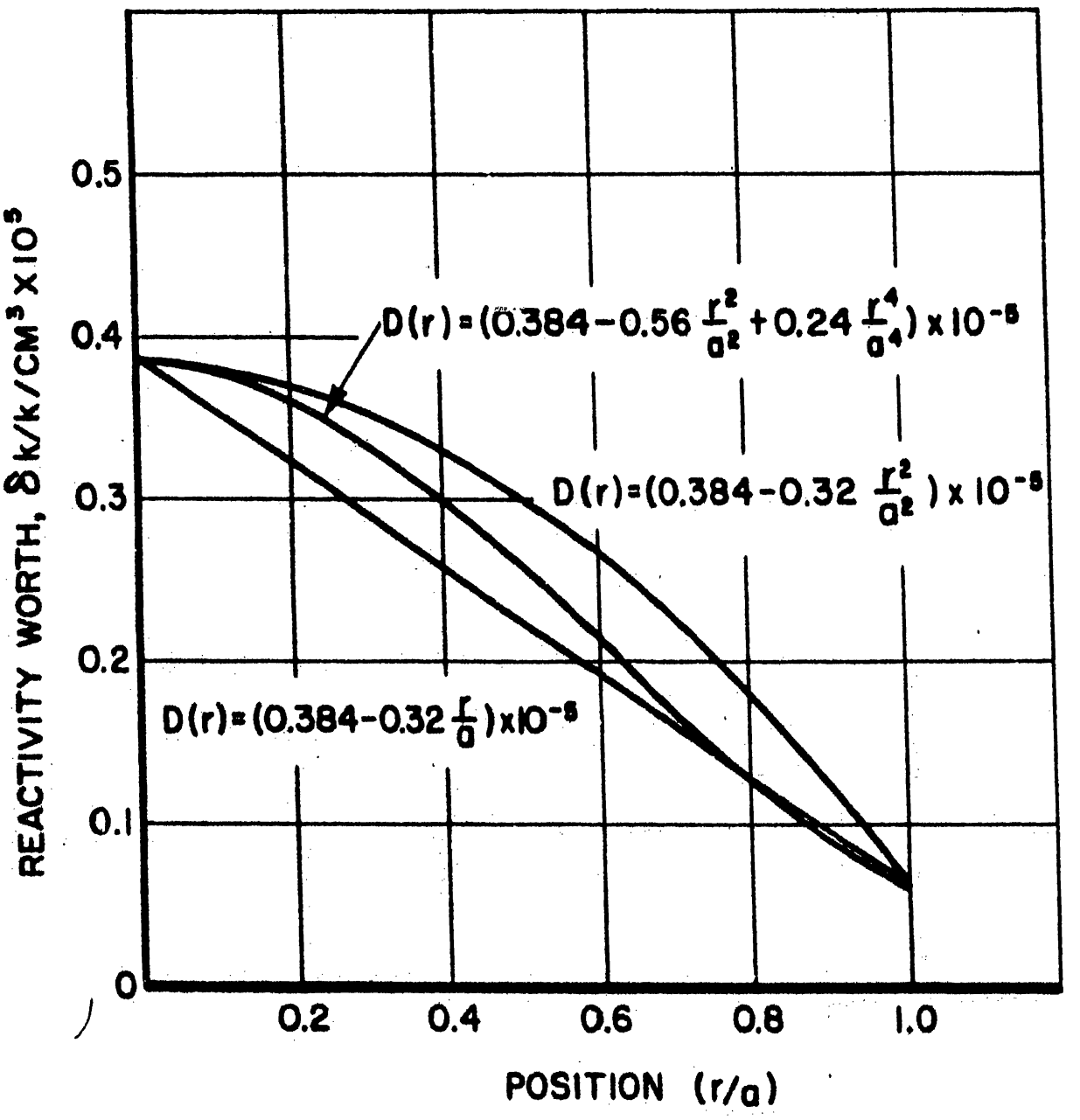

FIG. D.1 COMPARISON OF THREE REACTIVITY DISTRIBUTIONS

They are

$$D(r) = (0.384 - 0.32 \frac{r}{a}) \times 10^{-5} , \qquad (D.3)$$

and

$$D(r) = (0.384 - 0.56 \frac{r^2}{a^2} + 0.24 \frac{r^4}{a^4}) \times 10^{-5} . \qquad (D.4)$$

The distributions have been plotted in Figure D.1. The quantity held constant in the three cases is the decrease in reactivity from the center to the edge of the core. The effect that the shape of the distribution has on energy release is discussed in Chapter IV. The maximum difference in calculated energy release was 25%, indicating that the shape should be properly treated, but that the results are not extremely sensitive to it. These, after all, were extremely differing distributions.

The parameters of the reactor model have been summarized in Table I of Chapter IV with the exception of the variations in reactivity worth mentioned above. The lifetime of 10^{-7} seconds is comparable to the lifetime in the Fermi Reactor, which is calculated[60] to be 1.5×10^{-7} seconds when the reactor is in its normal state, but which would be a little smaller if the sodium were boiled out of the core, and the core was melted and collapsed into a smaller volume (as is usually assumed in explosion studies). The core radius of 40 cm is a little smaller than the radius of the Fermi Reactor core, which would have about a 45 cm radius if it were assumed spherical. The density is about the same as the density of the Fermi Reactor.

The delayed neutron fractions and precursor decay constants used

in our calculations are those reported by Keepin et al[61] and are shown in Table D. II.

TABLE D. II

DELAYED NEUTRON DATA

i	β_i	λ_i (sec^{-1})
1	0.00021	0.01244
2	0.0014	0.0305
3	0.00125	0.1114
4	0.00253	0.3014
5	0.00074	1.113
6	0.00027	3.014

The major difference between our simple model and a real reactor is the composition of the core. We have idealized the problem by choosing a core composed of pure uranium. The core of a real power reactor is always composed of a mixture of several materials. In some thermal reactors the uranium occupies only a small fraction of the volume of the core, but in fast reactors a large fraction of the core is taken up by the fuel material and the coolant. Since the coolant is usually assumed missing from the core in a meltdown accident, either because it has drained out or has boiled out, the materials present during the explosion are the fuel material and whatever structural material is required. The time width of the power excursion in even the weakest of the excursions we have treated is a few milliseconds. There is, therefore, no time for any significant heat transfer to the structural material. This material only occupies space and increases the amount of inertia that is resisting

the expansion. It can easily be accounted for in the analysis of a real reactor by including the added inertia in Eq. (6), the hydrodynamics equation. This is usually a moderate effect since the total mass of structural material is usually smaller than the mass of fuel.

When the fuel heats and begins to expand, the pressure rises faster because of the space occupied by the structural material. In the threshold model, Eq. (17), for the equation of state, the threshold energy Q^* is reduced and $\gamma-1$ is increased. This effect can also easily be accounted for. It is important if the density is high, i.e., $\rho > 10$ gm/cc. It is not so important at lower densities where the pressure is given by the saturated vapor pressure, i.e., where there really is no very noticeable threshold.

Finally, there is another rather important difference between our model and most real reactors. Even the fuel material itself is usually not pure uranium. The fuel in the Fermi Reactor is uranium alloyed with 10 weight percent of molybdenum. There are also alloying additions to the EBR-II fuel. Some of the fast reactors under consideration are fueled with uranium oxide or uranium carbide. One proposed core loading for the Fermi reactor is a cermet of UO_2 in a stainless steel matrix.

We wish to stress that it is only in the equation of state and in the constants for the Doppler effect that the type of material of which the core is composed is of any major importance to our calculations of energy release. The core material for our purposes is merely an inert,

hydrodynamic fluid which is characterized by a density, equation of state, and reactivity worth distribution. The latter is normally about the same for all the various possible reactor fuel types.

We expect that our model of a core composed of pure uranium is actually a reasonably good approximation (except for the core size chosen) to both the Fermi Reactor and the EBR-I and EBR-II Reactors, as well as other fast reactors which might be considered,as long as they are fueled with metalic uranium alloys. The differences in the equation of state are not expected to be terribly great. For example, the Fermi Reactor fuel, uranium metal alloyed with 10 percent molybdenum is expected to have approximately the same equation of state as pure uranium because the total amount of alloy addition is not excessively large,and the critical constants[54] are of the same order of magnitude for uranium and molybdenum. However, for reactor types utilizing fuels like uranium oxide or carbide, for example, it is necessary to make new estimates for the equation of state.

APPENDIX E

THE DOPPLER EFFECT

In Chapter V we have investigated the influence of the Doppler effect upon the calculation of the energy release. To do this we required some knowledge of the temperature dependence of the Doppler temperature coefficient of reactivity. In this Appendix we show that under certain conditions the temperature coefficient of reactivity is inversely proportional to the three halves power of the absolute temperature. This is not a new result, since it was demonstrated in 1955 by Goertzel et al.[36] We sketch a derivation presented by the author in a separate publication.[24] The purpose is to clarify the conditions under which the assumed temperature dependence is valid, and then to point out the nature of the temperature dependence under other conditions.

From first order multigroup perturbation theory, the change in reactivity with temperature due to Doppler effect can be written

$$T\frac{\partial k}{\partial T} = \sum_{E_j} T\frac{\partial k_E}{\partial T} \tag{E.1}$$

$$T\frac{\partial k_E}{\partial T} = \phi_E \left\{ [\nu W_H - W(E)]\, T\frac{\partial \tilde{\mu}_f(E)}{\partial T} - W(E)\, T\frac{\partial \tilde{\mu}_\gamma}{\partial T} \right\} \tag{E.2}$$

where the summation is over the energy groups into which the neutron energy spectrum has been divided. Here spatial effects have been

neglected or alternatively the flux ϕ_E and adjoints W_H and $W(E)$ are averaged over the reactor volume. W_H is the suitably normalized adjoint function, averaged over the fission neutron energy spectrum, $W(E)$ is the adjoint at the energy E_j, and $\tilde{\mu}_f$ and $\tilde{\mu}_\gamma$ are the effective fission and capture cross sections of the material for which we are calculating the Doppler effect. Next we invoke the narrow resonance approximation, which states that the effective cross section for the process x can be approximated by

$$\tilde{\mu}_x(E) = \frac{\int_E \frac{\mu_x(\epsilon)}{\mu_t(\epsilon)}\, d\epsilon}{\int_E \frac{1}{\mu_t(\epsilon)}\, d\epsilon}\,, \qquad \text{(E. 3)}$$

the integral extending over a narrow energy band about E. Here μ_t is the total cross section due to the mixture of all materials of the core.

In the neutron energy range which contributes most of the Doppler effect to a reactor like EBR-II or the Enrico Fermi Reactor, i.e., the 10 kev to 50 kev range, the total cross section $\mu_t(\epsilon)$ fluctuates only slightly about its average. The peaks of the resonances are not very high. Then in this energy range we can write

$$\begin{aligned} \frac{1}{\mu_t(\epsilon)} &= \frac{1}{\langle\mu_t\rangle + [\mu_t(\epsilon) - \langle\mu_t\rangle]} \\ &\approx \frac{1}{\langle\mu_t\rangle} \cdot \left[1 - \frac{\mu_t(\epsilon) - \langle\mu_t\rangle}{\langle\mu_t\rangle}\right] \end{aligned} \qquad \text{(E. 4)}$$

where the bracket < > indicates the average over a narrow energy range. This is a very fundamental approximation, and the assumed temperature dependence of the Doppler effect is only valid in situations in which this approximation is justified. There is one other approximation in which part of the temperature dependence is dropped, but that is a relatively minor one. When the approximation (E.4) is made, the derivative of the effective cross sections with respect to temperature can be written

$$T \frac{\partial \tilde{\mu}_x}{\partial T} - \frac{T}{\langle \mu_t \rangle} \frac{\partial \langle \mu_x \mu_t \rangle}{\partial T}$$

To evaluate the average $\langle \mu_x \mu_t \rangle$ one has to specify the detailed shape of μ_x and μ_t as a function of energy. This is not known experimentally at neutron energies above 1 kev for U-238 or above 36 ev for U-235. The procedure used in lieu of the experimental information has been to estimate the average resonance parameters and then average over assumed statistical distributions for these parameters. This has been done in Reference 24 and the final result for the Doppler temperature coefficient was found to be

$$T^{3/2} \frac{\partial k_E}{\partial T} = \frac{W(E)\phi_E}{\sqrt{8\pi}\sqrt{\frac{4KE}{A}}\langle \mu_t \rangle} \sum_s \rho^2 \cos 2\delta_l \langle \sigma_c \rangle_s \langle \sigma_f + \sigma_\gamma \rangle_s \langle S \rangle_s P^{(s)} \qquad (E.6)$$

Where K is the Boltzman constant, A the atomic weight, δ_l the

phase shift for neutrons of orbital angular momentum ℓ , σ_c the cross section for formation of the compound nucleus, $\langle S \rangle$ the average spacing of resonances and ρ the atomic density. P is a function of the resonance parameters and the index s refers to a sequence of levels corresponding to a given orbital and total angular momentum. There is no temperature dependence on the right hand side except in the quantity $P^{(s)}$. P contains the temperature in a very complicated way, but we have estimated in Reference 24 that P is very nearly constant, leaving only the $T^{3/2}$ effect on the left hand side of Eq. (E.6).

The approximation (E.4) is a good one for fast reactors like EBR-II and the Enrico Fermi Reactor. For reactors with a lower neutron energy spectrum, such as a large uranium oxide fast reactor, it is not so good. Some studies[25] done for large oxide systems indicate that the effect decreases less rapidly with temperature. However, it is true that as the temperature increases and the cross section resonances broaden, assumption (E.4) becomes better; at sufficiently high temperature the Doppler effect in the oxide reactor will also have a $T^{-3/2}$ temperature dependence. Of course, if one is doing an explosion analysis for a particular fast reactor, and if the Doppler coefficient is known as a function of temperature, it is easy to include that temperature dependence in the computer program which solves the energy release calculation.

APPENDIX F

THE DAMAGE POTENTIAL OF A GIVEN ENERGY RELEASE

In this appendix we briefly discuss some of the aspects of the problem of determining whether or not a given energy release can be contained within the reactor building. This is not intended to be a comprehensive review of the problem and is only included to help the reader assess the significance of the energy release calculations.

The damage potential of a given energy release is not simply proportional to the magnitude of the energy release. As an extreme example we cite the accidental energy burst in Godiva (a small fast critical assembly at Los Alamos) which Stratton[17] et al have analyzed. They show that only a very small fraction of the energy liberated in the excursion was available to do damage; the major fraction of the energy was used in raising the temperature of the assembly, which remained in the solid state.

Generally, the greater the energy density achieved in the excursion, the larger is the fraction of energy which is available to do damage. One possible measure of damage potential for cases in which the uranium is actually vaporized (as in the case in our calculations in contrast to the Godiva accident) is the total amount of adiabatic work which the gaseous uranium can do by expanding from the high

pressure which exists at the end of the power excursion, down to some lower pressure such as one atmosphere. Brout[26] has calculated this as a function of energy density for two uranium densities. For the more severe cases treated in this dissertation Brout's work indicates that slightly over half of the energy appears as work in the adiabatic expansion and the rest remains as internal energy of the uranium, which is still partially vaporized at the end of the expansion process. In the weaker excursions the available energy is less.

One can attempt to calculate the effects of the energy release in a straightforward manner: by setting up a theoretical model for the materials and structural members surrounding the core of the reactor, and then calculating the response of these materials as the uranium vapor expands and pushes on them. The application of this method generally requires many simplifying assumptions which, however, can usually be chosen in such a way that the results obtained are conservative.

Another approach which has been used[19] is to construct an actual physical model of the reactor vessel and materials contained in and around it and simulate the energy release by detonating a chemical explosive. This has the advantage that the very complicated effects which are associated with real structures, which have to be simplified in a theoretical study, can at least in principle be included in the experiments. But the interpretation of the experiment is still subject

to the uncertainties involved in relating the damage potential of the nuclear energy release to that of the chemical explosive. A logical basis for relating the two is the amount of work which can be done in an adiabatic expansion. Using this procedure, Bethe and Tait[14] estimated that the energy release in their calculations was equivalent to the detonation of three hundred pounds of TNT. Other studies[12] of hypothetical fast reactor meltdown accidents have also yielded an energy release equivalent to a few hundred pounds of TNT. This is probably a reasonable procedure for most purposes provided that the maximum pressure attained in the nuclear excursion is of the order of 100 kilobars, which is approximately the pressure attained in a TNT explosion.[33] However, there would still be some differences in the dissipation of the energy because of differences in the detailed shape of the pressure as a function of expansion for the two materials.

Whatever be the basis for determining the effects of the nuclear energy release, the evaluation of the effects can be completely separated from the calculation of the energy release. The nuclear power excursion is completely terminated before there has been any significant expansion of the high pressure uranium gas, and therefore the terminal conditions of the energy release calculation can be used as the initial conditions for a determination of the effects.

BIBLIOGRAPHY

Reference

1. W. J. McCarthy, Jr., R. B. Nicholson, D. Okrent and V. Z. Jankus, Studies of Nuclear Accidents in Fast Power Reactors, Paper P/2165, Proceedings of the Second International Conference on the Peaceful Uses of Atomic Energy (Geneva, 1958).

2. APDA-133, Fast Reactor Core Design Parameter Study, Report by Atomic Power Development Associates, Inc. (1960); also see Reference 38.

3. F. W. Thalgott, et al., Stability Studies on EBR-I, Paper P/1845, Proceedings of the Second International Conference on the Peaceful Uses of Atomic Energy (Geneva, 1958).

4. R. O. Brittan, Analysis of the EBR-I Meltdown, Paper P/2156, Proceedings of the Second International Conference on the Peaceful Uses of Atomic Energy (Geneva, 1958).

5. R. R. Smith, et al., A Mechanism Explaining the Instability of EBR-I, Mark-II, Report by the Argonne National Laboratory, ANL-6266 (1960).

6. See, for example, the Hazards Summary Reports for any of the power reactors now in operation.

7. F. Storrer, Temperature Response to Power, Inlet Cooland Temperature, and Flow Transients in Solid Fuel Reactors, Report by Atomic Power Development Associates, Inc., APDA-132 (1959); also see References 5 and 27.

8. W. E. Nyer and S. G. Forbes, SPERT Program Review, Report by Phillips Petroleum, IDO-16634 (1960).

9. J. H. Kittel, M. Novick and R. F. Buchanan, The EBR-I Meltdown - Physical and Metallurgical Changes in the Core, Report by the Argonne National Laboratory, ANL-5731 (1957).

10. J. J. Pickett, A. R. Kaufmann and J. E. Roman, Jr., Progress Report on Single-Pin Meltdown Tests for PRDC During the Period February, 1957 through June, 1957, Report by Nuclear Metals, Inc., NMI-4402 (1958); also see A. R. Kaufman, J. J. Pickett and J. E. Roman, Jr., Pouring of Molten U-10 w/o Mo alloy over Prototype of PRDC Fuel Pin Support and Lower Axial Blanket Rods, Terminal Report, Report by Nuclear Metals, Inc., NMI-4411 (1959); also see D. G. Freas, A. F. Leatherman, J. E. Gates, Meltdown Studies of Irradiated Uranium-10 w/o Molybdenum Fuel Pins, Report by Battelle Memorial Institute, BMI-PRDC-656 (1960).

11. H. G. Elrod, Jr., Freezing and Remelting of Radioactive Material on Cold Vertical Pins, Report by Nuclear Development Corporation of America, NDA-14-181 (1957).

12. Technical Information and Hazards Summary Report, Report by Power Reactor Development Company, Volume VII, Part B, of Revised License Application as Amended (AEC Docket No. 50-16) (1962).

13. G. A. Freund, et al., Design Summary Report on the Transient Reactor Test Facility TREAT, Report by the Argonne National Laboratory, ANL-6034 (1960); also see C. E. Dickerman, D. Okrent and E. Sowa, The Fast Reactor Safety Programme in TREAT, Paper SM-18143, Proceedings of the Seminar on the Physics of Fast and Intermediate Reactors (Vienna, 1961).

14. H. A. Bethe and J. H. Tait, An Estimate of the Order of Magnitude of the Explosion when the Core of a Fast Reactor Collapses, UKAEA-RHM (56)/113 (1956).

15. J. H. Tait, A Review of Calculations of the Consequences of the Collapse of a Fast Reactor Core, UKAEA AERE T/M 167.

16. V. Z. Jankus, A Theoretical Study of Destructive Nuclear Bursts in Fast Power Reactors, Report by Argonne National Laboratory, ANL-6512 (1962); also see Chapter IV. 4, Safety Problems, Volume III of Physics of Fast and Intermediate Reactors, Proceedings of the Seminar on the Physics of Fast and Intermediate Reactors (Vienna, 1962).

17. W. R. Stratton, et al., Analysis of Prompt Excursions in Simple Systems and Idealized Fast Reactors, Paper P/431, Proceedings of the Second International Conference on the Peaceful Uses of Atomic Energy (Geneva, 1958).

18. D. Okrent, et al., Ax-1, A Computing Program for Coupled Neutronics-Hydrodynamics Calculations on the IBM-704, Report by Argonne National Laboratory, ANL-5977 (1959); also see Reference 16.

19. W. R. Wise, Jr., Possible Jump of Rotating Shield Plug for the Enrico Fermi Atomic Power Plant, Naval Ordnance Laboratory Reactor Vessel Containment Program (NOL-285) for the Division of Reactor Development, U. S. Atomic Energy Commission (May 15, 1962).

20. R. O. Brittan, Reactor Containment, Argonne National Laboratory Report ANL-5948 (1959).

21. F. B. Porzel, Design Evaluation of BER in Regard to Internal Explosions, Argonne National Laboratory Report ANL-5651 (1957).

22. R. Daane, R. Mela, J. DeFelice, Progress Report on the Study of Low Probability, High Hazard, Fast Reactor Accidents, Report by Nuclear Development Corporation of America, NDA-14-107 (1955).

23. D. C. Menzies, UKAEA, personal communication.

24. R. B. Nicholson, The Doppler Effect in Fast Neutron Reactors, Report by Atomic Power Development Associates, Inc., APDA-139 (1960).

25. P. Greebler and B. A. Hutchins, The Doppler Effect in a Large Fast Oxide Reactor - Its Calculation and Significance for Reactor Safety, Chapter IV.3, Doppler Effect, Volume III of the Proceedings of the Seminar on the Physics of Fast and Intermediate Reactors (Vienna, 1962).

26. R. H. Brout, Equation of State and Heat Content of Uranium, Report by Atomic Power Development Associates, Inc., APDA-118 (1957).

27. H. A. Bethe, Reactor Safety and Oscillator Tests, Report by Atomic Power Development Associates, Inc., APDA-117 (1956); also see H. Hurwitz, Jr., Derivation and Integration of the Pile-Kinetic Equations, Nucleonics 5, 61-67 (1949).

28. A. Sommerfeld, "Mechanics of Deformable Bodies", Page 94, Academic Press, Inc., New York, 1950.

29. J. E. Wilkins, Jr., The Behavior of a Reactor at Prompt Critical when the Reactivity is a Linear Function of Time, Nuclear Sci. and Eng. 5, 207 (1959); also see Reference 27.

30. W. Lash Miller and A. R. Gordon, J. of Phys. Chem., 35, 2785 (1931).

31. V. Z. Jankus, personal communication.

32. J. W. Stephenson, Jr., R. B. Nicholson, Weak Explosion Program, ASTRA 417-6.0 (1961).

33. M. A. Cook, "The Science of High Explosives", Rheinhold, New York, 1958.

34. A. M. Weinberg and E. P. Wigner, "The Physical Theory of Neutron Chain Reactors", Univ. of Chicago Press, Chicago, 1958.

35. L. Dresner, "Resonance Absorption in Nuclear Reactors", International Series of Monographs in Nuclear Energy, Pergamon Press, New York, 1960.

36. H. A. Bethe, On the Doppler Effect in Fast Reactors, Report by Atomic Power Development Associates, Inc., APDA-119 (1957); also see G. Goertzel, et al., Paper 613, International Conference on the Peaceful Uses of Atomic Energy (Geneva, 1955).

37. A. R. Baker, T. A. J. Jaques, A Measurement of the Contribution of the Doppler Effect to the Temperature Coefficient of Reactivity in a Fast Reactor, UKAEA Report AERE R/M 168.

38. W. B. Loewenstein an D. Okrent, The Physics of Fast Power Reactors; A Status Report, Paper P/637, Second International Conference on the Peaceful Uses of Atomic Energy (Geneva, 1958); also see Reference 2.

39. D. C. Menzies, personal communication.

40. J. W. Stephenson, R. B. Nicholson, Reactor Explosion Program, ASTRA 417-3.0 (1960).

41. A. L. Hess, W. Gemmell, J. K. Long, and R. L. McVean, Critical Studies of a 450-Liter Uranium Oxide Fast Reactor Core, Report by Argonne National Laboratory, ANL-6336 (1960).

42. W. Gemmell, Studies of Two Fast Reactor Critical Assemblies Based on Meltdown Configurations, Transactions of the American Nuclear Society, 1960 Winter Meeting.

43. F. W. Thalgott, J. K. Long and W. Gemmell, Personal communication.

44. D. M. O'Shea, D. Okrent and J. M. Chaumont, Some Calculations Pertaining to Fast Reactor Safety, Report by Argonne National Laboratory, ANL-6501 (1962).

45. H. Elrod, Estimation of the Critical Temperature and Pressure of Uranium, Report by Nuclear Development Corporation of America, NDA-14-122 (1956); also see H. Elrod, Revisions and Extensions of Estimated Saturation Properties of Uranium, NDA-14-139 (1956); also see W. R. Stratton, et al., Reference 17.

46. R. D. Cowan, On the Equation of State of Uranium at Low Densities and Temperatures, Los Alamos Scientific Laboratory, unpublished.

47. E. G. Rauh and R. J. Thorn, The Vapor Pressure of Uranium, J. of Chem. Phys. 22, 1414 (1954).

48. Guggenheim, "Thermodynamics", Page 144, Interscience Publishers, New York, 1950.

49. J. J. Katz and E. Rabinowitch, "The Chemistry of Uranium", Part 1, Page 146, McGraw Hill, New York (1951); also see Reference 26.

50. Houghen and Watson, "Chemical Process Principles", John Wiley and Sons, New York, 1947.

51. H. A. Bethe, personal communication.

52. B. W. Downs and H. A. Bethe, Power Surges in a Pool of Molten Core Material, Report by Atomic Power Development Associates, Inc., APDA-125, (1958).

53. G. Koppel and J. DeFelice, The Specific Heat of Liquid Uranium in the Region $T_r = .313$ to $T_r = .70$, Report by Nuclear Technology Corporation, unpublished (1962).

54. P. Marnell, J. DeFelice and J. Barker, Some Thermodynamics Properties of Uranium, Molybdenum, Iron and Zirconium at High Temperatures and Pressures, Nuclear Technology Corporation, February 10, 1962.

55. See Reference 28.

56. A. Sommerfeld, "Mechanics of Deformable Bodies", Pages 99-100, Academic Press, New York, 1950.

57. See Reference 56.

58. G. W. Thomson and E. Garelis, Physical and Thermodynamic Properties of Sodium, A Critical Review, Report by Ethyl Corporation Research Laboratories, Detroit, Michigan (1955).

59. S. J. Rothman and E. S. Fisher, A Note on the Elastic Constants of Uranium, Nuclear Sci. and Eng. 5, 195 (1959).

60. APDA-124, Enrico Fermi Atomic Power Plant, Report by Atomic Power Development Associates, Inc. (1959); also see Reference 12, Volume I.

61. G. R. Keepin, et al., Delayed Neutrons from Fissionable Isotopes of Uranium, Plutonium, and Thorium, Report by the Los Alamos Scientific Laboratory, LA-2118 (1957).